Table과 Figure

성균관대학교 의과대학 삼성서울병원 내과 이준행

Writing Tables and Figures for Medical Journals

Sung-Tae Hong, MD

President, KAMJE

Editor, Journal of Korean Medical Science

Seoul National University, Korea

hst@snu.ac.kr

Table과 Figure

- 본론에 들어가기에 앞서
- Table
- Figure
  - 해상도란 무엇인가?
  - Vector image란 무엇인가?
  - 논문제출을 위한 적절한 해상도는?
  - Powerpoint file을 TIFF로 바꾸기

본론에 들어가기에 앞서...

성균관대학교 의과대학 삼성서울병원 내과 이준행

어디에 문제가 있습니까?

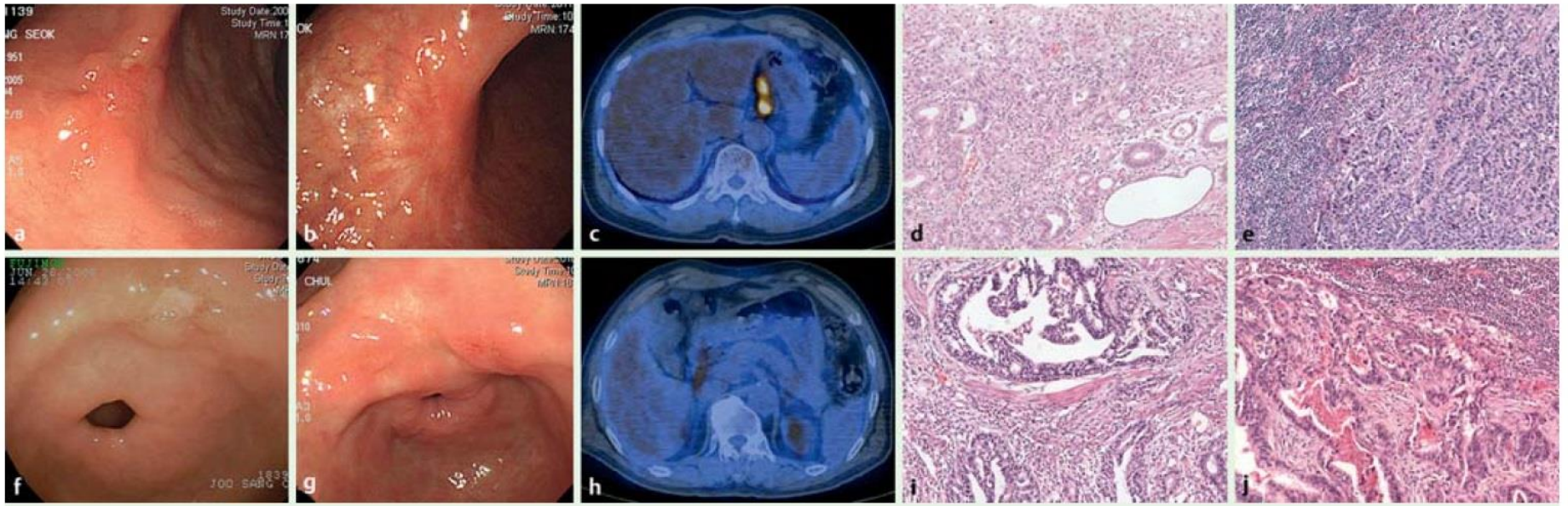

Fig. 4 Two cases of extragastric recurrence after curative endoscopic submucosal dissection (ESD) for early gastric cancer. **a – e** Patient #1 in **Table 3** (Present study): the cancer met the absolute indication and was treated with curative ESD, and was located at the angle. **a** Esophagogastroduodenoscopy (EGD) appearance of lesion before ESD. **b** EGD view 61 months after ESD. **c** 18^{F}-fluorodeoxyglucose (FDG) positron emission tomography-computed tomography (PET-CT) image 61 months after ESD; hypermetabolic lesions are seen in perigastric lymph nodes. **d** Histological appearance of ESD specimen (hematoxylin and eosin [H&E], × 200). **e** Histological appearance of lymph node with cancer cell infiltration (H&E, × 200). **f – j** Patient #2 in **Table 3** (Present study): the cancer met the expanded indication and was treated with curative ESD, and was located at the antrum. **f** EGD appearance of lesion before ESD. **g** EGD view 48 months after ESD. **h** 18^{F}-FDG PET-CT image 48 months after ESD; hypermetabolic lesions are seen in lymph nodes around the common hepatic artery. **i** Histological appearance of ESD specimen (H&E, × 200). **j** Histological appearance of lymph node with cancer cell infiltration (H&E, × 200).

Endoscopy 2015

어디에 문제가 있습니까?

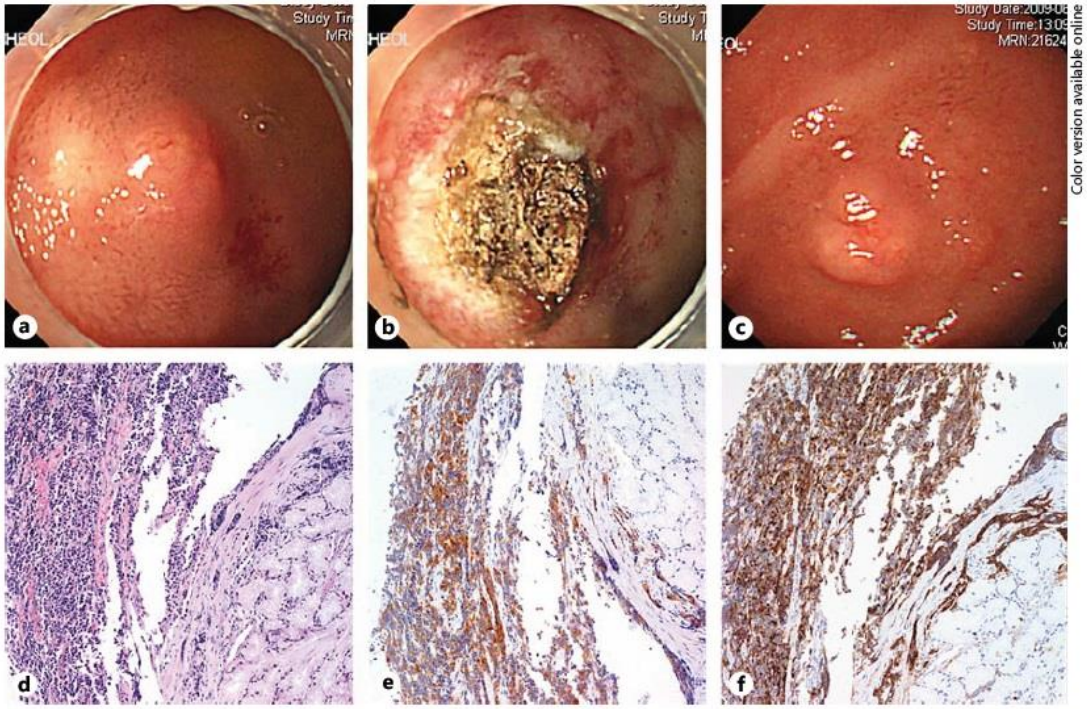

Fig. 2. Endoscopic images before and after APC and initial histologic findings of patients with local recurrence. **a** Endoscopy image before APC showing 8-mm sized round elevated lesion in the bulb. **b** Corresponding view of tumor immediately after APC. **c** Endoscopy image of recurred tumor in 6-month follow-up endoscopy. **d–f** Initial histologic findings before APC: (**d**) tumor cells composed of small ovoid nuclei with indistinct nucleoli (HE, ×200); (**e**) immunohistochemistry for synaptophysin showing diffuse weak positive staining in tumor cells (×200), and (**f**) immunohistochemistry for chromogranin showing diffuse strong positive staining in tumor cells (×200).

Digestion 2013;87

Annotation 지우기

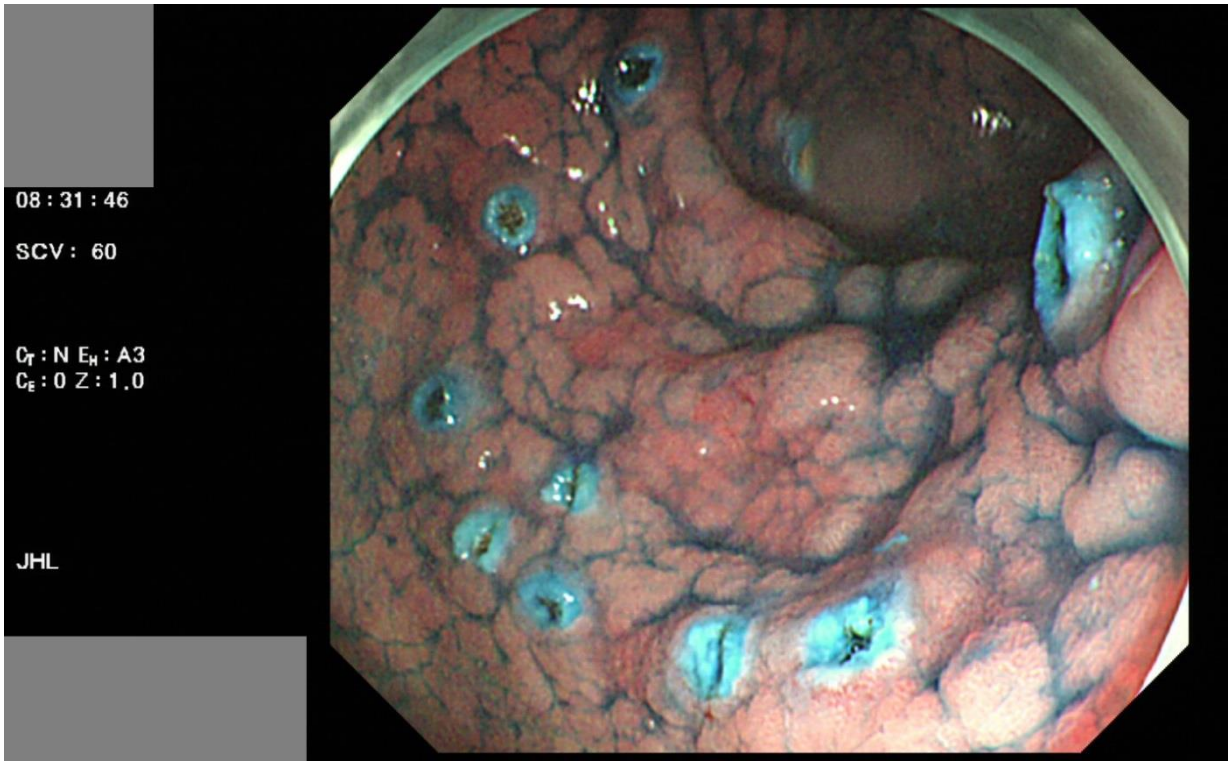

어디에 문제가 있습니까?

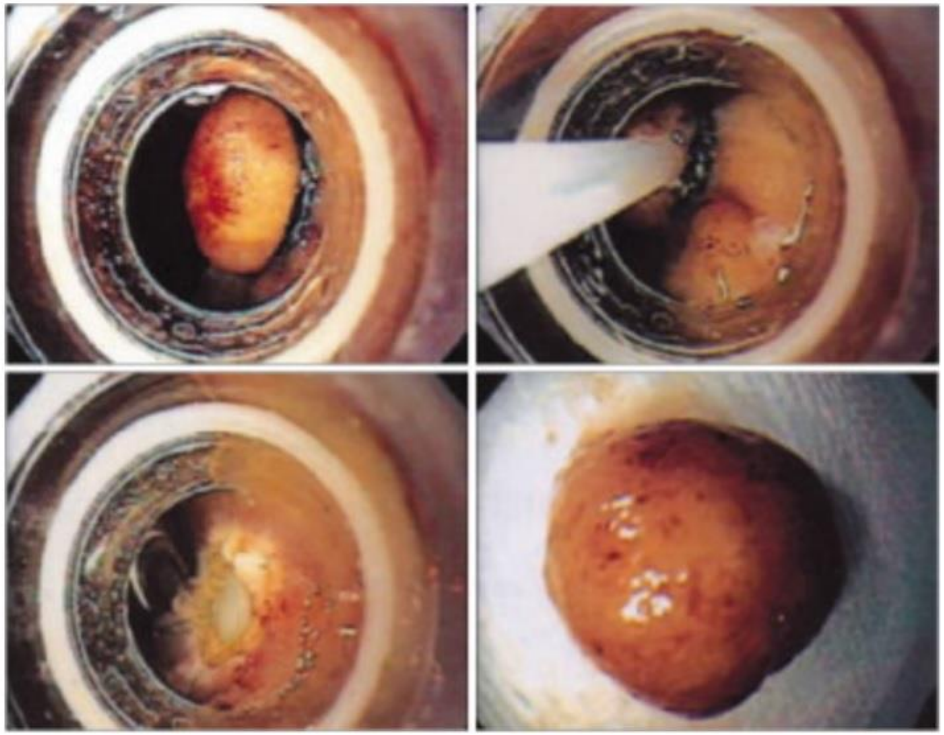

Figure 3. Endoscopic resection of the tumor. The solid mass was successfully removed by endoscopic resection, which measures about 8×6 mm in the longest diameter.

가로 세로 비율

대한소화기내시경학회지 2005

Original image의 문제일 수도 있다!

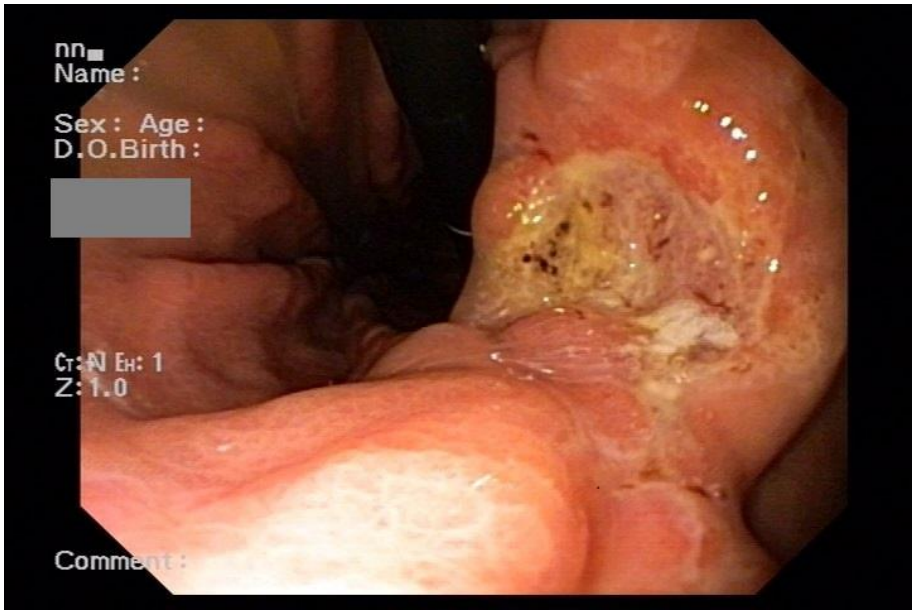

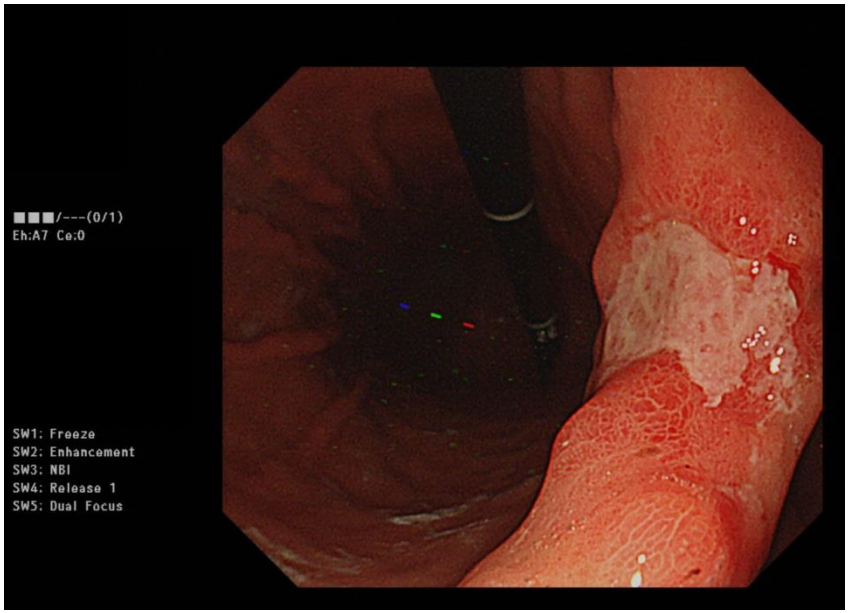

가로 세로 비율

어디에 문제가 있습니까?

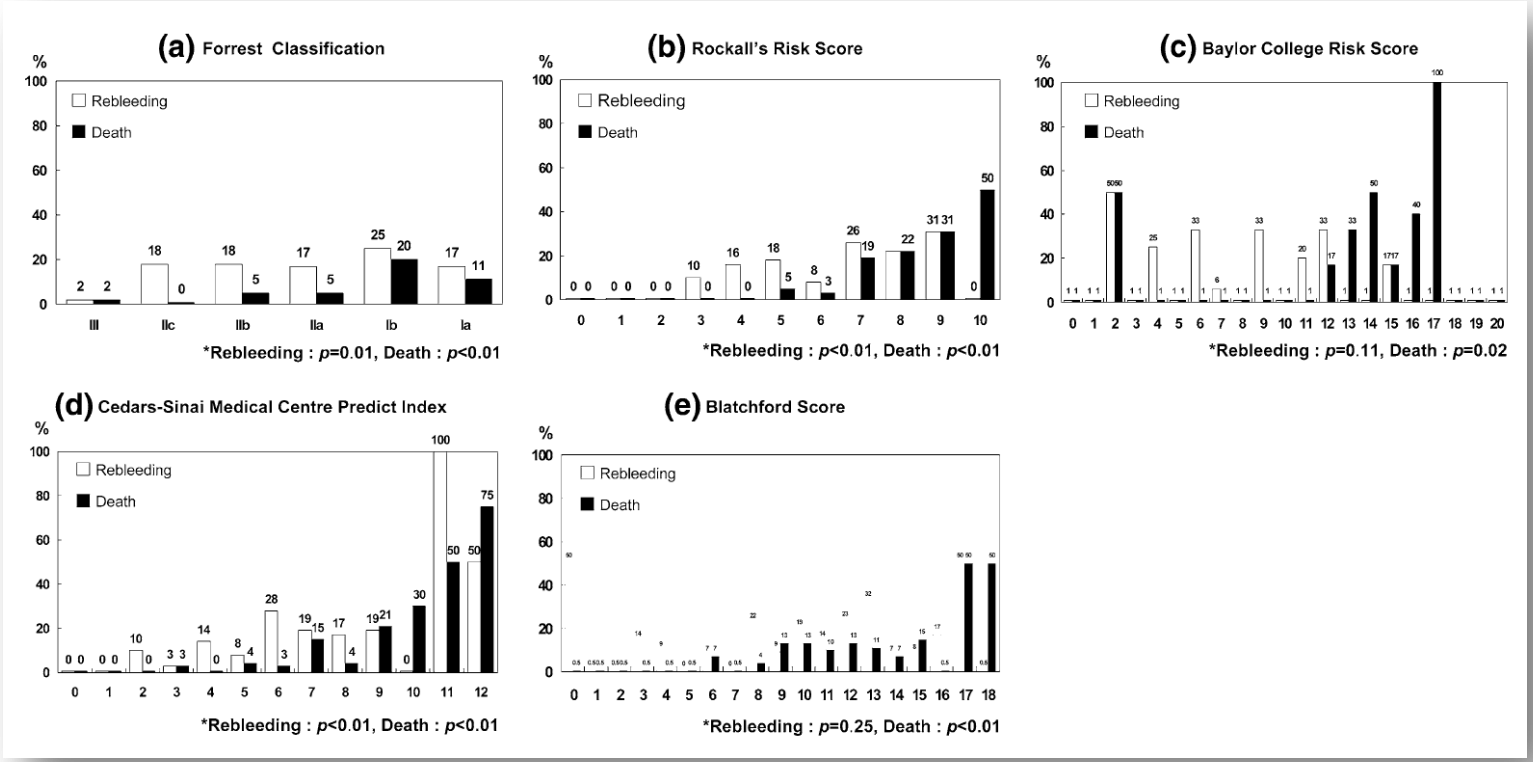

Arrows, numbers

Kim BJ. Dig Dis Sci 2009

중간정리 – 문제들이 보이십니까?

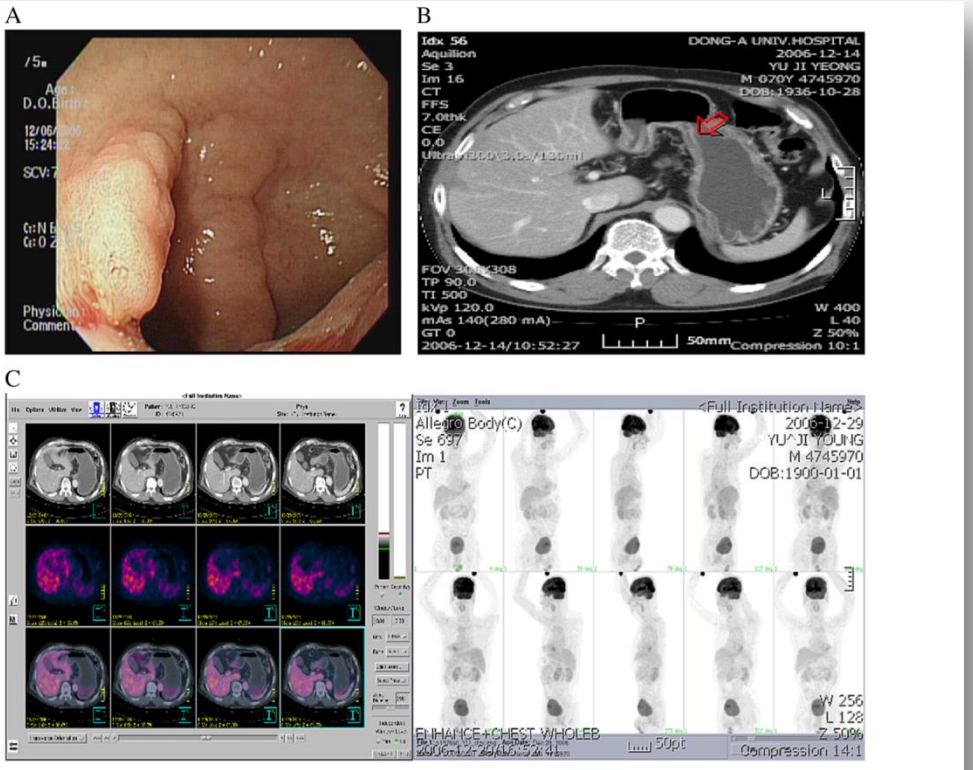

Figure 1. A. Endoscopic finding. Well-demarcated, elevated nodular lesion can be seen at anterior wall of antrum. B. Conventional CT finding. Focal irregular wall thickness can be seen at anterior wall of antrum, but shows no lymph node or distant metastasis. C. Representative FDG-PET image of a patient with early gastric cancer without lymph node metastasis or distant metastasis. Transversal slices of respectively PET-CT fusion and FDG-PET show no highlighting pathological FDG-PET uptake in the gastric wall. No lymph node or distant metastases can be observed. Coronal slice of total body FDG-PET examination with physiological FDG-PET shows no uptake in the gastric wall. Again, no lymph node or distant metastasis is observed.

- 개인정보보호
- Annotation
- 가로-세로 비율
- Presenting Multiple images
- Arrows, numbers

Scand J Gastroenterol 2009

어디에 문제가 있습니까?

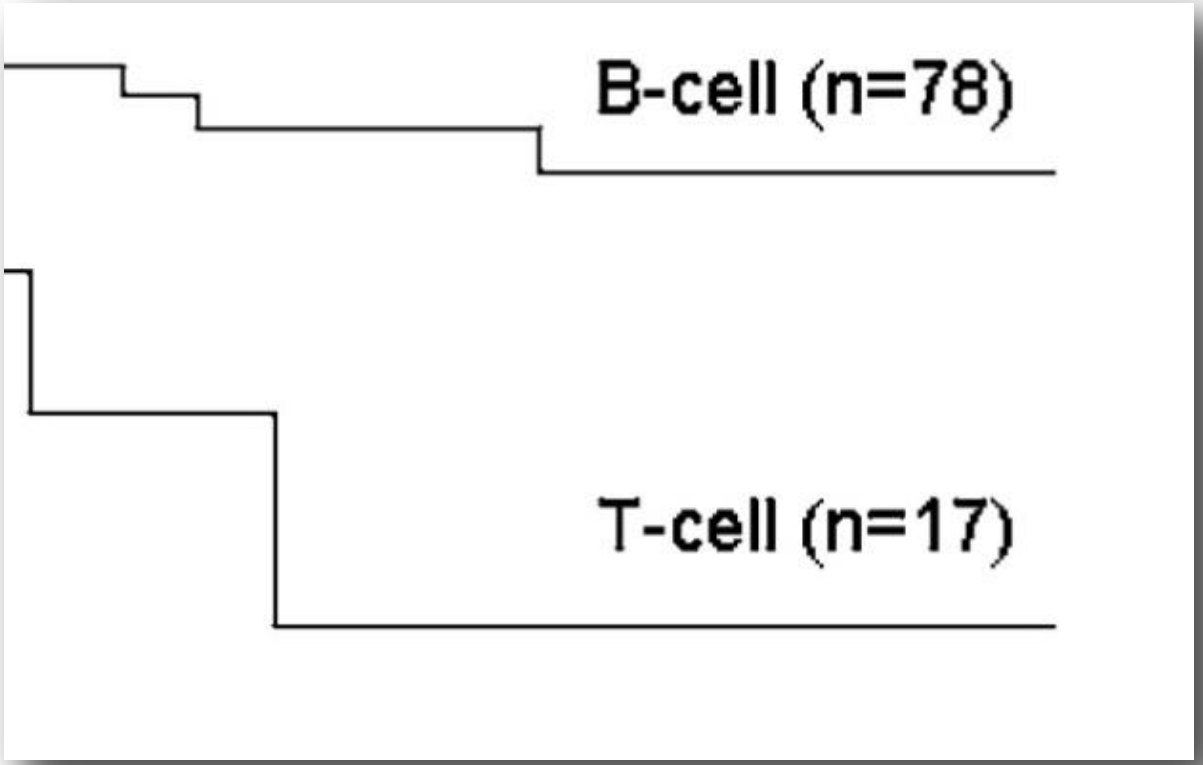

Kim YH. Dig Dis Sci 2005

어디에 문제가 있습니까?

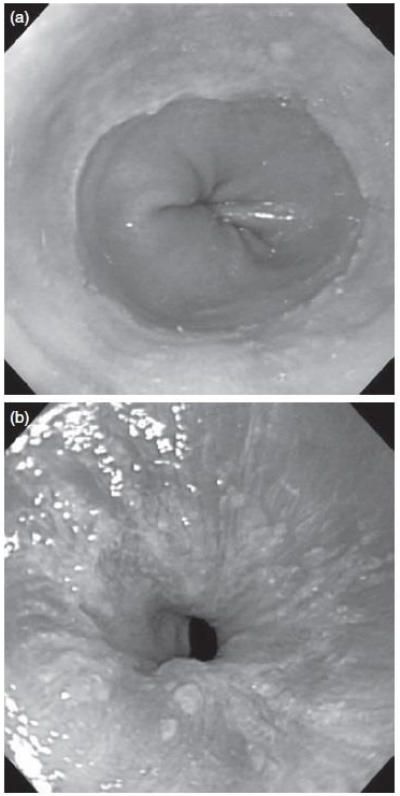

Figure 1 Sample pictures of minimal changes of the lower esophagus. (a) White turbid discoloration, (b) Z-line blurring.

Table 2 Comparison of symptoms of 22 923 individuals with or without minimal changes

	Normal (n = 19 896)	Minimal changes (n = 3027)	P-value
History of GERD	1355 (6.8%)	321 (10.6%)	< 0.01
Any seven† symptoms	9950 (50.0%)	1662 (54.9%)	< 0.001
Heartburn	4891 (24.6%)	812 (26.8%)	0.02
Acid regurgitation	7034 (35.4%)	1164 (38.5%)	< 0.01
Chest pain	2870 (14.4%)	458 (15.1%)	0.25
Hoarseness	1914 (9.6%)	313 (10.3%)	0.18
Globus sensation	2363 (11.9%)	450 (14.9%)	< 0.01
Cough	1434 (7.2%)	203 (6.7%)	0.39
Epigastric soreness	4680 (23.5%)	788 (26.0%)	< 0.01

†Seven symptoms: heartburn, acid regurgitation, chest pain, hoarseness, globus sensation, cough and epigastric soreness.
GERD, gastroesophageal reflux disease.

Table 3 Odds ratio for the presence of minimal changes in persons with or without individual symptom(s)

Symptom	Odds ratio	95% CI	P-value
Heartburn	1.123	0.982–1.285	0.906
Acid regurgitation	1.040	0.901–1.201	0.591
Chest pain	0.981	0.817–1.178	0.838
Hoarseness	0.974	0.765–1.242	0.834
Globus sensation	1.320	1.158–1.505	< 0.001
Cough	0.881	0.683–1.136	0.329
Epigastric soreness	1.162	1.034–1.305	0.012

Table 4 Risk factors for minimal changes (n = 23 341)

Risk factor	Odds ratio	95% CI	P-value
Male gender	1.339	1.237–1.449	< 0.0001
Smoking	1.269	1.165–1.383	< 0.0001
Alcohol	0.937	0.824–1.065	0.3180
Diabetes mellitus	0.970	0.822–1.145	0.7175
History of *H. pylori* eradication	1.222	1.075–1.395	0.0030
Stooping posture during work	1.235	1.122–1.358	< 0.0001
Hiatal hernia	4.444	3.759–5.263	< 0.0001
Atrophic or metaplastic gastritis	1.679	1.446–1.991	< 0.0001

CI, confidence interval.

Lee JH. J Gastroenterol Hepatol 2008

이 느낌이 나야 하는 사진이었습니다.

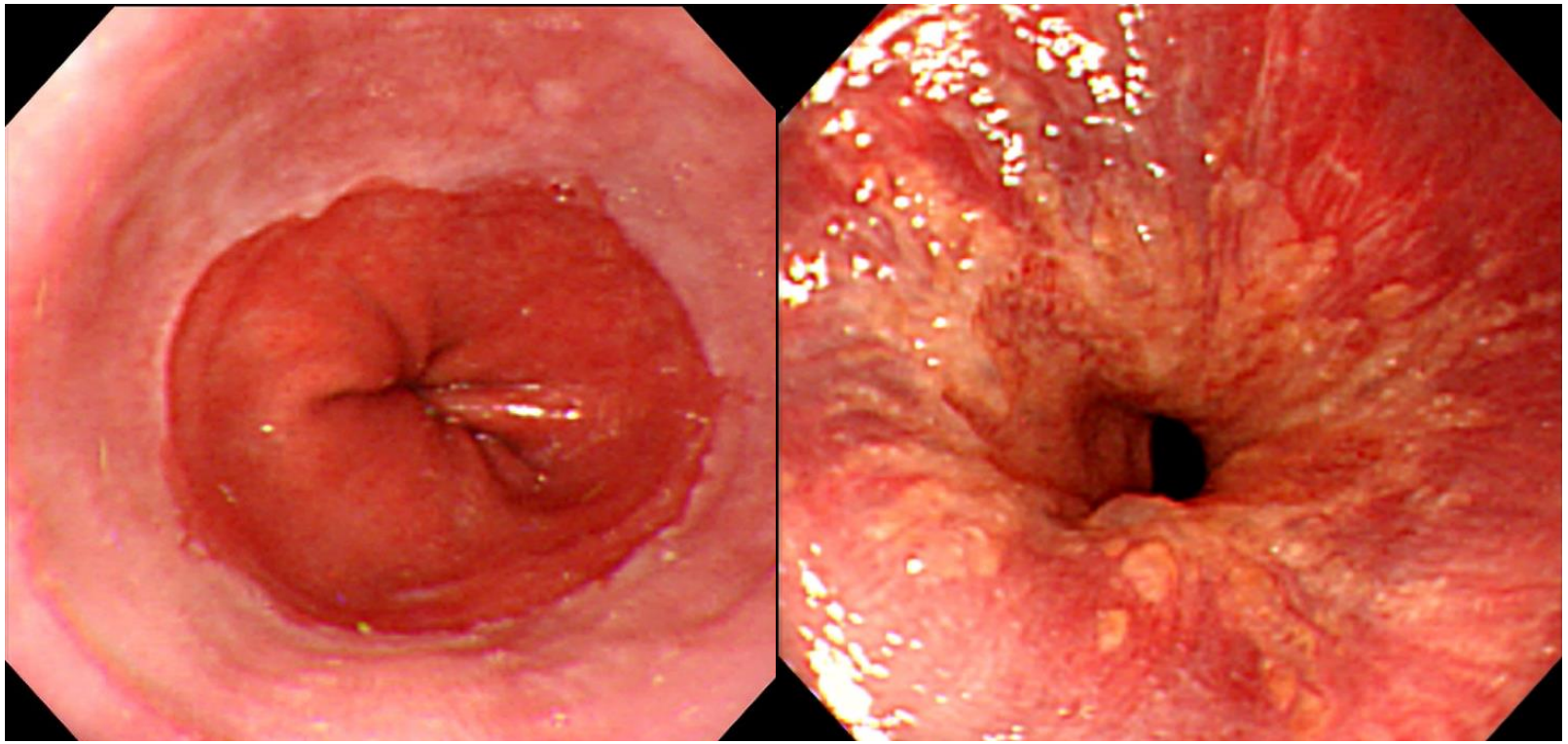

어디에 문제가 있습니까?

Case report/series S75

Feasibility and efficacy of argon plasma coagulation for early esophageal squamous cell neoplasia *

Authors: B.-H. Min, E. R. Kim, J. H. Lee, K. J. Kang, P.-L. Rhee, J. J. Kim, J. C. Rhee

Institution: Department of Medicine, Samsung Medical Center, Sungkyunkwan University School of Medicine, Seoul, Korea

submitted 19. August 2012
accepted after revision 5. February 2013

Bibliography
DOI http://dx.doi.org/10.1055/s-0033-1344225
Endoscopy 2013; 45: 575–578
© Georg Thieme Verlag KG Stuttgart · New York
ISSN 0013-726X

Corresponding author
J. H. Lee, MD
Department of Medicine
Samsung Medical Center
Sungkyunkwan University School of Medicine
Irwon-dong
Gangnam-gu
Seoul
135-710 Korea
Fax: +822-3410-6983
stomach@gmail.com

We present 19 cases in which argon plasma coagulation (APC) was used as curative initial treatment for 5 low-grade esophageal squamous intraepithelial neoplasias (ESINs), 12 high-grade ESINs, and 2 early esophageal squamous cell carcinomas (ESCCs). Complete response was defined as the absence of tumor from any biopsy taken from the ablated lesion. At follow-up endoscopy 2–4 months after APC, 94.7 % of patients had achieved complete response in a single treatment session. Only one patient with high-grade ESIN showed local recurrence. This patient underwent additional APC and showed complete response at 12 months after initial APC. At the 12-month follow-up endoscopy, again 94.7 % had a complete response. The exception was one patient with local recurrence, who underwent additional APC. After the 12-month follow-up endoscopy, no patient showed local recurrence during a median follow-up of 22 months. No stricture requiring endoscopic dilation occurred after the procedure. This study suggests that APC is a feasible and effective treatment modality for ESIN and early ESCC.

Introduction

Esophageal squamous cell carcinoma (ESCC), which accounts for most cases (90 %) of esophageal cancer in Asian countries, has a very poor prognosis when at an advanced stage [1, 2]. It is therefore important to detect and treat early-stage ESCC or its precursor lesion, esophageal squamous intraepithelial neoplasia (ESIN, squamous dysplasia). ESIN is a feasible target for endoscopic eradication [3]. Endoscopic treatment can also be performed for ESCCs confined within the lamina propria, as the risk for lymph node metastasis of these lesions is less than 5 % [4–6] and radical esophagectomy carries relatively high morbidity and mortality rates [7, 8].

Existing endoscopic treatment methods for ESIN and early ESCC include endoscopic mucosal resection (EMR), endoscopic submucosal dissection (ESD), and endoscopic ablation. Among these treatment modalities, endoscopic ablation therapy, particularly radiofrequency ablation (RFA), is currently widely used for the treatment of early esophageal adenocarcinoma and its precursor lesion, Barrett's esophagus with dysplasia [9]. Recently, a few small studies reported promising outcomes for RFA in endoscopic eradication of ESIN and early ESCC [10–12].

Argon plasma coagulation (APC) is a noncontact thermal technique using ionized argon gas to deliver a monopolar high-frequency current, which effectively coagulates, desiccates, and destroys tissue [13, 14]. The advantages of APC are ease of use, coagulation over a wide range with few adverse events, familiarity to endoscopists, and availability in most endoscopy units [13, 14]. To date, there have been few reports on the outcomes and safety of APC as a curative treatment modality for ESIN and early ESCC [15].

The aim of this study was to report our experiences with APC as a curative treatment and to evaluate the efficacy and safety of APC for ESIN and early ESCC.

Case series

Patients

At Samsung Medical Center, APC was regarded as the indicated treatment for early esophageal squamous cell neoplasia that either were low-grade (LGN) or high-grade squamous intraepithelial neoplasia (HGIN) diagnosed on the basis of forceps biopsy specimens, or were early ESCC confined within the mucosal layer, identified by endoscopic ultrasonography (EUS), if patients refused to undergo ESD or esophagectomy. In the case of patients with HGIN or ESCC, there had to be no evidence of lymph node or distant metastasis on chest and abdominal computed tomography (CT). A total of 19 APC procedures were performed in 19 patients with early esophageal squamous cell neoplasia (5 LGINs, 12 HGINs, and 2 early ESCCs) from January 2008 to September 2011. In principle, our institution recommends ESD or esophagectomy instead of ablation therapy (APC or RFA) for early mucosal ESCC identified by EUS, as EUS has limited accuracy for distinguishing between the mucosal and submucosal layers [16]. For ESCC invading the submucosal layer, esophagectomy is recommended. In fact, 10 cases of early ESCC and 2 of HGIN under high suspicion of cancer based on endoscopic appearance were removed by ESD in the study period. In this study, however, one patient with early ESCC chose APC instead of ESD or esophagectomy on the basis of personal preference, despite the doctor's recommendation. The other patient with early ESCC had severe ischemic heart failure which made him an inappropriate candidate for aggressive treatment; he underwent APC after providing informed consent. Among the 19 patients enrolled, no endoscopic or surgical treatment or radiation therapy was performed for any of the lesions before APC. All cases were collected consecutively from our database and the data were reviewed retrospectively. All patients signed an informed consent form.

endoscopic ultrasonography (EUS), if patients refused to undergo ESD or esophagectomy. In the case of patients with HGIN or ESCC, there had to be no evidence of lymph node or distant metastasis on chest and abdominal computed tomography (CT). A total of 19 APC procedures were performed in 19 patients with early esophageal squamous cell neoplasia (5 LGINs, 12 HGINs, and 2 early ESCCs) from January 2008 to September 2011. In principle, our institution recommends ESD or esophagectomy instead of ablation therapy (APC or RFA) for early mucosal ESCC identified by EUS, as EUS has limited accuracy for distinguishing between the mucosal and submucosal layers [16]. For ESCC invading the submucosal layer, esophagectomy is recommended. In fact, 10 cases of early ESCC and 2 of HGIN under high suspicion of cancer based on endoscopic appearance were removed by ESD in the study period. In this study, however, one patient with early ESCC chose APC instead of ESD or esophagectomy on the basis of personal preference, despite the doctor's recommendation. The other patient with early ESCC had severe ischemic heart failure which made him an inappropriate candidate for aggressive treatment; he underwent APC after providing informed consent. Among the 19 patients enrolled, no endoscopic or surgical treatment or radiation therapy was performed for any of the lesions before APC. All cases were collected consecutively from our database and the data were reviewed retrospectively. All patients signed an informed consent form.

Argon plasma coagulation

Patients underwent baseline high-resolution white-light endoscopy, narrow-band imaging, and chromoendoscopy with Lugol's solution (1.5–3 % iodine) to identify lesions. The location and size of each lesion were recorded and targeted biopsies were obtained. Patients with HGIN or ESCC also underwent a CT scan of the thorax and abdomen.

APC equipment included an axial APC probe (diameter 2.3 mm), an argon gas source, and a high-frequency electrosurgical generator (VIO 300D with APC2, Erbe Elektromedizin, Tübingen, Germany). All APC procedures were performed by two expert endoscopists (B.H.M. and J.H.L.) with the patient under sedation with midazolam and pethidine. The APC mode selected was according to endoscopist's preference (B.H.M.: forced mode; J.H.L.: pulsed mode). The argon gas flow was set at 1.0 L/min and the power of the electric current was set at 30–50 W. With this setting, APC was applied in 1- to 2-second bursts. After identifying lesions by chromoendoscopy, marking dots were made circumferentially at approximately 5–7 mm lateral to the margin of the lesion using APC. After marking, glycerin solution mixed with epinephrine was injected into the submucosal layer beneath the lesion to make a submucosal cushion. The lesion and neighboring mucosa including the marked sites were evenly ablated with APC until the lesion was completely coagulated. Bleeding during and after the procedure was controlled with APC. After APC treatment, patients were closely observed for at least 4 hours, and then allowed to drink water and semisolid food after chest radiographs were checked. One day after the procedure, patients were discharged with specific care instructions. Patients were provided with a standard dose of proton pump inhibitor for 14 days.

Outcome measures

The primary outcome parameter was complete response at 12 months after initial APC, defined as the absence of LGIN, HGIN, or ESCC from any biopsy taken from the ablated lesion. Secondary outcome parameters were (1) complete response at 2–4 months after initial APC, (2) the number of APC treatment sessions required to reach a complete response; and (3) any complications of APC, such as bleeding, perforation, or esophageal luminal stricture. Recurrence was diagnosed on the basis of clinical, endoscopic, ultrasonographic, or radiological signs of disease. Local recurrence was diagnosed when ESIN was detected adjacent to an endoscopic ablation area. If new ESIN was detected within 12 months, it was defined as a synchronous lesion; if it was detected after 12 months, it was defined as a metachronous lesion.

Table 1 Patient characteristics and clinical data in 19 cases of esophageal squamous intraepithelial neoplasia or early esophageal squamous cell carcinoma treated with argon plasma coagulation.

Patient no.	Sex	Age, years	Risk factors for ESCN	Histology	Size, mm	Circumferential extent	Endoscopic morphology	APC mode	Power, W
1	M	58		LGIN	3	Below 50 %	IIb	Pulsed	40
2	F	77		LGIN	5	Below 50 %	IIb	Pulsed	40
3	M	45	Ex-smoker	LGIN	5	Below 50 %	IIa	Forced	30
4	M	66	Smoker	LGIN	20	Below 50 %	IIb	Forced	30
5	M	62	Smoker	LGIN	20	Below 50 %	IIb	Forced	30
6	M	70	Smoker	HGIN	4	Below 50 %	IIc	Pulsed	40
7	M	63	Smoker	HGIN	5	Below 50 %	IIc	Pulsed	40
8	M	70	Ex-smoker	HGIN	5	Below 50 %	IIb	Pulsed	40
9	M	69	Smoker	HGIN	10	Below 50 %	IIb	Pulsed	40
10	M	68	Smoker	HGIN	10	Below 50 %	IIb	Forced	40
11	M	66	Smoker	HGIN	10	Below 50 %	IIb	Forced	40
12	F	68		HGIN	12	Below 50 %	IIb	Pulsed	40
13	M	74	Smoker	HGIN	20	Below 50 %	IIb	Pulsed	40
14	M	74	Ex-smoker	HGIN	20	Below 50 %	IIb	Pulsed	40
15	M	64		HGIN	30	Below 50 %	IIb	Pulsed	40
16	M	59		HGIN	50	Below 50 %	IIb	Pulsed	40
17	M	76	Smoker	HGIN	50	Below 50 %	IIb	Pulsed	40
18	M	74	Ex-smoker	ESCC	10	Below 50 %	IIb	Pulsed	50
19	M	58	Smoker	ESCC	30	Below 50 %	IIb	Pulsed	50
Overall	M/F = 17:2	68 (45–77)*		5 LGIN, 12 HGIN, 2 ESCC	10 (5–50)*		1 IIa, 16 IIb, 2 IIc		

ESCN, esophageal squamous cell neoplasia; APC, argon plasma coagulation; LGIN, low-grade squamous intraepithelial neoplasia; HGIN, high-grade squamous intraepithelial neoplasia; ESCC, esophageal squamous cell carcinoma; IIb, flat; IIa, slightly elevated; IIc, slightly depressed.
* Mean (range).

Table 2 Outcomes after argon plasma coagulation in 19 patients with esophageal squamous intraepithelial neoplasia or early esophageal squamous cell carcinomas.

Outcome parameters	Patients
Complete response 2–4 months after APC, n/N (%)	18/19 (94.7)
Complete response 12 months after APC, n/N (%)	18/19 (94.7)
APC session required to reach a complete response, n/N (%)	
1 session	17/19 (89.5)
2 sessions	2/19 (10.5)
Complications during and after APC, n/N (%)	
Bleeding	0/19 (0.0)
Perforation	0/19 (0.0)
Stricture	0/19 (0.0)
Median duration of follow-up, months	22 (range 12–38)

APC, argon plasma coagulation

Results

A total of 19 patients were included in this study: 5 had a baseline diagnosis of LGIN, 12 had HGIN, and 2 had ESCC confined within the mucosal layer identified by EUS. Median tumor size was 10 mm (range, 3–50 mm) and the circumferential extent of all lesions was below 50 %. The majority of lesions (16/19) were flat in endoscopic appearance. However, one lesion was slightly elevated and two lesions were slightly depressed. Patient characteristics and clinical data are shown in ▶ **Table 1**. ▶ **Table 2** summarizes the outcomes after APC.

At 2–4 months after initial APC, 18 of 19 patients (94.7 %) had a complete response. Only one patient (patient 17 in ▶ **Table 1**) with HGIN showed local recurrence. This patient underwent additional APC for local recurrence. At the 6-month follow-up endoscopy after the second APC, there was no evidence of local recurrence. However, metachronous recurrence (HGIN) was found, and this lesion was ablated with a third APC. At the 6-month follow-up endoscopy after the third APC, another metachronous recurrence was detected (HGIN) and this lesion was ablated with a fourth APC. At the 6-month follow-up endoscopy after the fourth APC, no local or metachronous recurrence was found in this patient.

No patient showed local recurrence after 12-month follow-up endoscopy. Median duration of follow-up after the initial APC was 22 months (range, 12–38 months).

No significant bleeding (a decrease in hemoglobin by more than 2 g/dL or need for transfusion) or perforation occurred during or after the APC procedure. No patient complained of dysphagia or showed esophageal luminal stricture requiring dilation during the follow-up period after APC.

Discussion

Recently, a few small studies reported on the promising outcomes of RFA for endoscopic eradication of ESIN and early ESCC [10–12]. In one study including 29 Chinese patients with ESIN or early ESCC [10], the complete response rate at the 12-month follow-up endoscopy was over 80 % with a mean of 1.7 sessions of RFA. Only flat (type 0-IIb) lesions were included and no EMR was performed before RFA. In this study, 4 cases (13.7 %) of strictures were reported and all 4 cases required endoscopic dilation. In another study of 13 Dutch patients with HGIN or early ESCC [11], a complete response was achieved in all patients after a median of 2 sessions (range, 1–4 sessions) of RFA. Nine patients (69.2 %) underwent EMR prior to RFA to remove nonflat lesions. In this study, 3 cases (23.1 %) of strictures were reported and all 3 cases required endoscopic dilation. These studies suggest that RFA is a feasible and effective treatment modality for ESIN or early ESCC. However, as shown in the above-mentioned studies, RFA has several disadvantages: (1) limited availability and the need for a special system; (2) the necessity of preceding endoscopic resection in cases of nonflat lesions to render the mucosa flat because of the limited ablation depth of RFA (0.5–1.0 mm) [11, 12]; (3) the need for repeated RFA sessions for complete eradication of the tumor; and (4) the relatively high risk (13.7 %–23.1 %) of luminal strictures which require endoscopic dilation [10, 11].

In contrast to RFA, APC can completely ablate slightly elevated or slightly depressed lesions without the assistance of EMR, since APC can destroy tissue to a depth of approximately 2–3 mm [17]. In the present study of the outcomes of APC for ESIN and mucosal ESCC, complete response for neoplasia was achieved in 94.7 % of patients, and in only one treatment session in the majority of these cases. No stricture requiring endoscopic dilation occurred after the APC procedure in the present study. These differences between APC and RFA might be caused by discrepancies in the size and extent of the lesions included in the respective studies. In our study, median tumor size was 10 mm (range, 3–50 mm) and the circumferential extent of all lesions was less than 50 %. In the Dutch study [11], on the other hand, median tumor size was 50 mm (range, 10–100 mm) and the circumferential extent of lesions was a median of 50 %. Differences in the extent of ablation between APC and RFA might be another cause; an 360° circumferential ablation was usually performed with RFA, in contrast to the targeted ablation of APC.

In the present study, a second-generation APC device (VIO 300D with APC2) was used. Compared to the first-generation device (APC 300 (ICC 200), the VIO/APC2 has several advantages. First, the overall efficiency of the device has been improved by 30 % to 50 %. In an in vitro study using porcine liver, Manner et al. [18] showed the VIO/APC2 could achieve a maximum coagulation depth of 6 mm. Second, three different modes are available on the device – forced, pulsed, and precise. In contrast to forced APC, which provides a continuous output, pulsed APC provides intermittent current with a homogenous, superficial, "spray-like" effect which is restricted to a depth of 2–3 mm. Therefore, pulsed APC can be a useful option for the ablation of larger and superficial lesions [13]. In the present study, pulsed mode on a low-power setting (30–50 W) was used in the majority of cases (14/19, 73.7 %) as the target lesions were superficial and the esophageal wall is thin [14]. Based on the high treatment efficacy with a low complication rate shown in the present study, pulsed APC at the low-power setting might be regarded favorably as an APC mode for the treatment of ESIN and early ESCC.

In conclusion, we found that APC achieved a high rate of complete response (94.7 %) without any significant complication for the treatment of ESIN and early ESCC. The majority of cases required only one treatment session to reach a complete response. Given the relatively small number of patients enrolled in this study, further large prospective studies are necessary to asses whether our promising results are applicable to a wider patient population with ESIN and early ESCC.

Competing interests: None

References

1 Kleinberg L, Forastiere AA. Chemoradiation in the management of esophageal cancer. J Clin Oncol 2007; 25: 4100–4117
2 Muriette C, Pinson G, Thibeault JP. Therapeutic strategies in oesophageal carcinoma: role of surgery and other modalities. Lancet Oncol 2007; 8: 545–553
3 Shimizu M, Nagaishi K, Yamaguchi H et al. Squamous intraepithelial neoplasia of the esophagus: past, present, and future. J Gastroenterol 2009; 44: 108–112
4 Araki K, Ohno S, Egashira A et al. Pathologic features of superficial esophageal squamous cell carcinoma with lymph node and distal metastasis. Cancer 2002; 94: 570–575
5 Choi JY, Park YS, Jung HY et al. Feasibility of endoscopic resection in superficial esophageal squamous carcinoma. Gastrointest Endosc 2011; 73: 880–889, 889.e881–882
6 Kim DU, Lee JH, Min BH et al. Risk factors of lymph node metastasis in T1 esophageal squamous cell carcinoma. J Gastroenterol Hepatol 2008; 23: 619–625
7 Birkmeyer JD, Siewers AE, Finlayson EVet al. Hospital volume and surgical mortality in the United States. N Engl J Med 2002; 346: 1128–1137
8 Chang AC, Ji H, Birkmeyer NJ et al. Outcomes after transhiatal and transthoracic esophagectomy for cancer. Ann Thorac Surg 2008; 85: 424–429
9 Shaheen NJ, Sharma P, Overholt BF et al. Radiofrequency ablation in Barrett's esophagus with dysplasia. N Engl J Med 2009; 360: 2277–2288
10 Bergman JJ, Zhang YM, He S et al. Outcomes from a prospective trial of endoscopic radiofrequency ablation of early squamous cell neoplasia of the esophagus. Gastrointest Endosc 2011; 74: 1181–1190
11 van Vilsteren FG, Alvarez Herrero L, Pouw RE et al. Radiofrequency ablation for the endoscopic eradication of esophageal squamous high grade intraepithelial neoplasia and mucosal squamous cell carcinoma. Endoscopy 2011; 43: 282–290
12 Zhang YM, Bergman JJ, Wouters Bet al. Radiofrequency ablation for early esophageal squamous cell neoplasia. Endoscopy 2010; 42: 327–333
13 Dumot JA, Greenwald BD. Argon plasma coagulation, bipolar cautery, and cryotherapy: ABCs of ablative techniques. Endoscopy 2008; 40: 1026–1032
14 Miyamoto N, Okamoto K, Kimura T et al. Endoscopic ablation therapy for gastrointestinal superficial neoplasia. Dig Endosc 2012; 24: 139–149
15 Nomura T, Miyashita M, Makino H et al. Argon plasma coagulation for the treatment of superficial esophageal carcinoma. J Nihon Med Sch 2007; 74: 183–187
16 Poh CI, May A, Rabenstein T et al. Endoscopic resection of early oesophageal cancer. Gut 2007; 56: 1625–1634
17 Eickhoff A, Jakobs R, Schilling D et al. Prospective nonrandomized comparison of two modes of argon beamer (APC) tumor desiccation: effectiveness of the new pulsed APC versus forced APC. Endoscopy 2007; 39: 457–462
18 Manner H, May A, Faerber M et al. The tissue effect of second generation argon plasma coagulation (VIO APC) in comparison to standard APC and PACPAC later in vitro. Acta Gastroenterol Belg 2007; 70: 352–356

Endoscopy 2013

Endoscopy report without endoscopic pictures

- Natural course of non-curative resection without additional treatment


Natural course of noncurative endoscopic resection of differentiated early gastric cancer

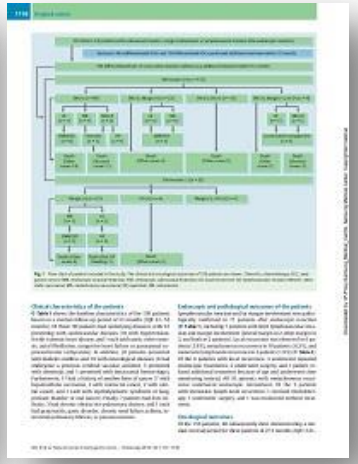

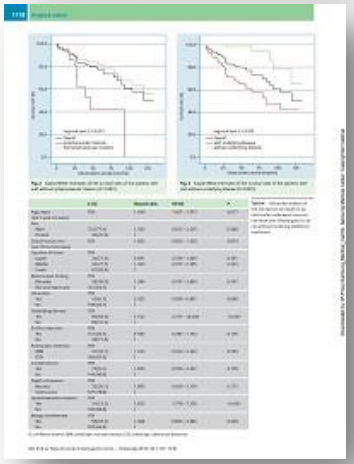

Endoscopy 2012

딱 3장이면 충분했는데...

Table 3 Data from three patients who died from progression of early gastric cancer.

	Patient number		
	1	**2**	**3**
Sex	M	M	F
Age, years	87	72	73
En bloc resection	–	+	+
Size, mm	45	31	34
Gross ulceration	–	–	–
Submucosal invasion	+	+	+
Margin involvement	+	+	–
Lymphovascular invasion	+	+	–
Survival period, months	93	17	64
Recurrence	Local	LNM	LNM
Duration of recurrence, months	36	17	6
Treatment	Conservative management	Conservative management	Chemo-therapy

Endoscopy 2012

Is surgery necessary for mucosal cancer with lymphovascular invasion?

Table 3. Lymph node metastasis rate according to criteria in EGC patients with lymphovascular invasion

Depth of invasion	Ulceration	Differentiated (%)		Undifferentiated (%)	
Mucosa	Ulcer (−)	≤ 2 cm	> 2 cm	≤ 2 cm	> 2 cm
		0/28 (0)	3/24 (12.5)	4/16 (25.0)	
	Ulcer (+)	≤ 3 cm	> 3 cm		
		1/2 (50.0)			
SM1		≤ 3 cm	> 3 cm		
		7/61 (11.5)			

SM1 < 500 μm from the muscularis mucosae

Pyo JH. Ann Surg Oncol 2019:26:449

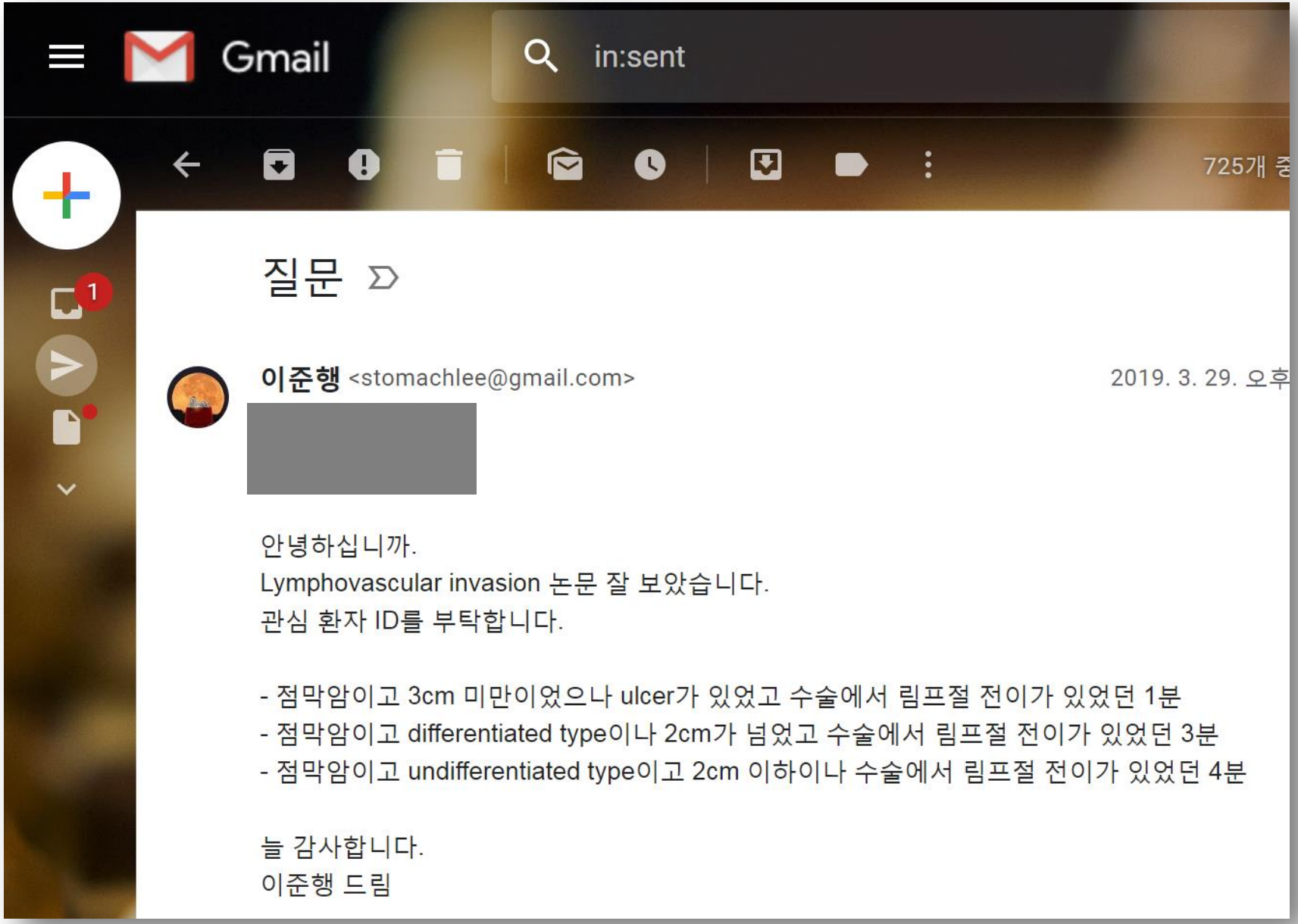
Gmail
in:sent
725개 중
1
질문
이준행 <stomachlee@gmail.com>
2019. 3. 29. 오후
안녕하십니까.
Lymphovascular invasion 논문 잘 보았습니다.
관심 환자 ID를 부탁합니다.
- 점막암이고 3cm 미만이었으나 ulcer가 있었고 수술에서 림프절 전이가 있었던 1분
- 점막암이고 differentiated type이나 2cm가 넘었고 수술에서 림프절 전이가 있었던 3분
- 점막암이고 undifferentiated type이고 2cm 이하이나 수술에서 림프절 전이가 있었던 4분
늘 감사합니다.
이준행 드림

어디에 문제가 있습니까?

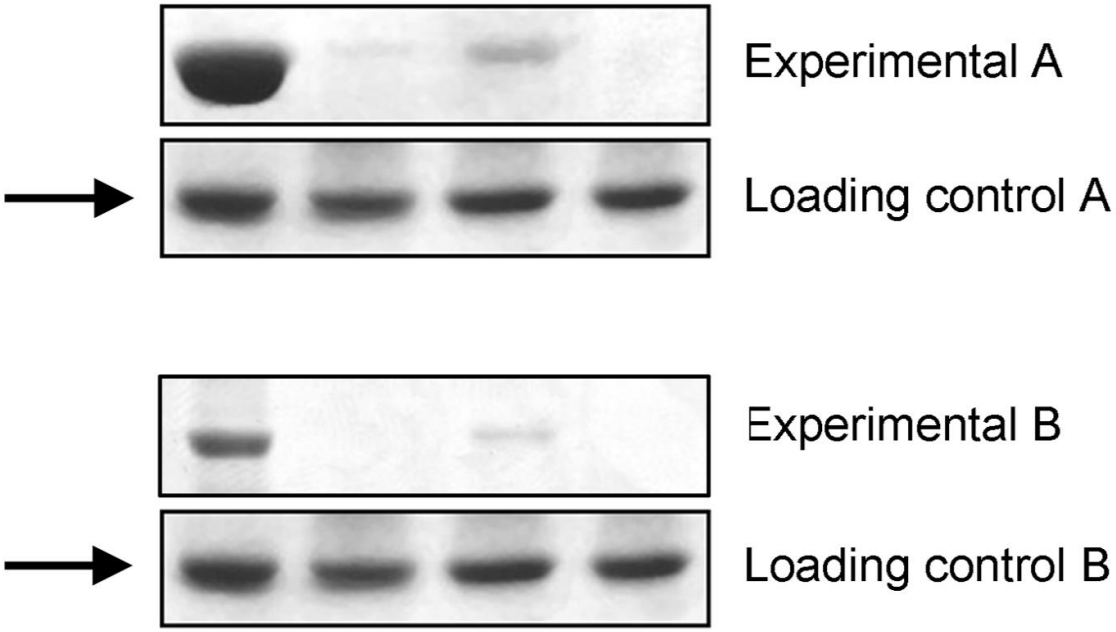

Figure 2. **Gross manipulation of blots.** Example of a duplicated panel (arrows).

J Cell Biol 2004:166:11-15

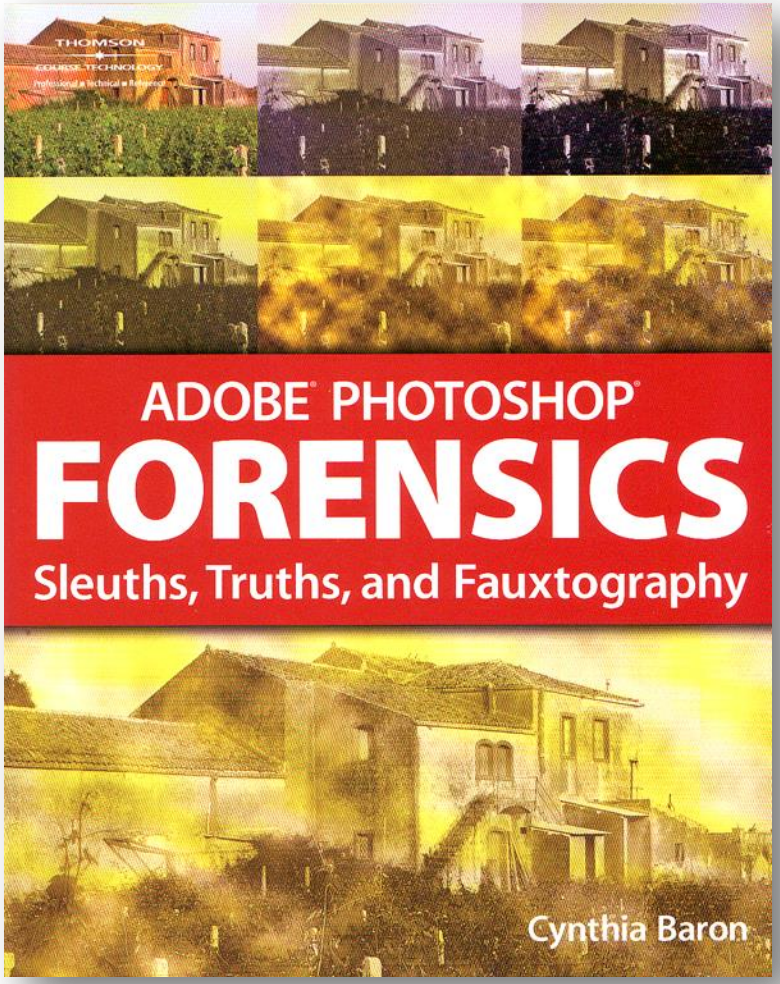
THOMSON
COURSE TECHNOLOGY
ADOBE® PHOTOSHOP®
FORENSICS
Sleuths, Truths, and Fauxtography
Cynthia Baron

Piltdown Man was a clever forgery. Instead, even as other finds around the world pointed consistently to a very different evolutionary path, people were forced to make room for Piltdown's big brain and primate jaw.

Finally, in 1953, anthropologist Joseph Weiner investigated and then documented the details of the hoax. A closer look found that the teeth of a modern ape jaw had been filed down to look like human molars. The skull had probably been dug up from a medieval grave, and all the bones had been stained to make them appear old.

Even after all this time, the forger has not definitively been named. Most people believe the finger points to Charles Dawson himself, particularly after Weiner's research found a pattern of deception in his earlier archeological digs. Yet almost every other man involved in the story has had his turn in the role, and some of them are almost as likely candidates—which doesn't speak well of the level of academic honesty a hundred years ago.

The Neverending Fraud

Outside the scientific community, we don't always realize how serious such fakery can be. But bad science contributes to the misuse of millions of dollars in government and corporate grants. It misrepresents reality to the public, creating panic or prompting bad political and social decisions. It can delay medical cures by misdirecting effort and funding to fantasyland.

And once a bad paper gets published, it lives a kind of half-life in the community. Even if the authors retract a paper (or are asked to retract it, which is much the same thing but considerably more embarrassing), the paper is still searchable online and continues to live in its original form in libraries and labs. Doctoral students looking for citations to bolster their own work may continue to cite it.

The Korean Stem Cell Scandal

The high-profile science fraud cases that do splatter the news media come to light in part because the field they're in is hot. There are dozens of other researchers competing to be the first to make a breakthrough. When someone beats them to it, they do the experiments to see if they get the same results. If they can't, they try to find out why. Ultimately, no fraud can withstand such a concentrated assault. But that process can take a long while—frequently years, like the Piltdown Man fiasco.

In other cases, a single image was divided into two, either to separate two cells on the same slide or to crop one cell into two images (Figures 6-20 and 6-21).

Figure 6-20 These two cells, which were split between the two pages in Figure 6-18, are two halves of the same cell.

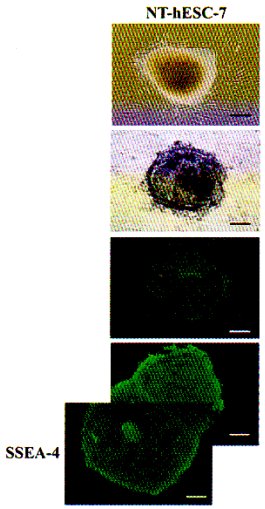

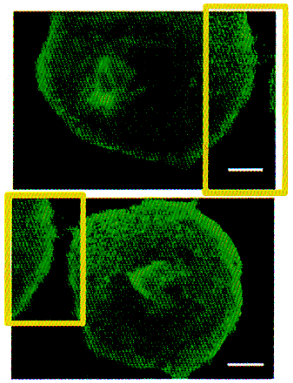

Figure 6-21 The images outlined in yellow are two views of the same two cells.

At first, Hwang claimed that some of the figures had been inserted in the paper by mistake, which was sloppy but an honest mistake. But little by little, it became clear that Hwang and his team had not successfully cloned a single human stem cell.

Having resigned in disgrace and been indicted for fraud and embezzlement in 2006, Hwang has still never admitted to any form of misconduct. He blames his team of researchers for deliberate sabotage and for creating false data on their own. As of June 2007, he was looking for new partners in other countries to continue his research.

Moving Forward

One of the outcomes of the Hwang shocker has been the increased scrutiny given to other papers involving stem cells and cloning research. All of the major scientific journals have published new guidelines on how to prepare figures and have warned that they will reject new papers that don't live up to standards.

Table

성균관대학교 의과대학 삼성서울병원 내과 이준행

Table의 가장 흔한 오류는 무엇일까요?

환자의 성별 분포는 남자 32예(39%), 여자 50예(61%)로 남녀 비가 1:1.56으로 여자가 많았다. 연령 분포는 21세에서 78세로 평균 연령은 51.4세였다. 연령대별 발생 분포는 50대에서 27예(32.9%), 60대에서 17예(20.7%)로 50-60대에 가장 많이 발생하였다(Table 2).

3. 임상증상

임상증상은 상복부 동통이 54예(65.8%)로 가장 많았으며 그 외 소화불량, 오심 또는 구토, 체중 감소 등의 증상이 있었다. 또한, 11예에서는 증상이 없었는데 이 환자들은 정기검사나 다른 이유로 검사 도중 우연히 발견되었다(Table 3).

증상의 지속 기간은 6개월 이하가 48예(58.5%)로 대부분이었으며 이중, 1-3개월이 19예(23.1%)로 가장 많았다. 하지만 5년 이상된 경우도 5예(6.1%)에서 나타났다(Table 4).

4. 술전 진단 방법

술전 진단 방법으로는 위내시경 및 생검을 78예에서, 위십이지장조영술을 14예에서, 내시경적 초음파술을 24예에서, 복부 전산화단층촬영을 17예에서 시행하였다.

5. 종양의 위치

82예 환자의 총 병변 수는 86개로 이중 전정부에 35개(40.7%), 체부에 24개(27.9%), 기저부에 22개(25.6%), 그리고 전 유문부에 4개(4.6%)가 위치하였다. 또한 위암으로 수술을 시행받았던 1예에서 위-공장 문합부에서 발견되었다.

조직학적 분류별 종양의 위치로 용종은 50개였으며 10 mm 이하의 크기가 42개(48.8%)로 가장 많

Table 2. Age and Sex Distribution

Age	Male	Female	Total (%)
21-30	1	4	5 (6.1%)
31-40	8	4	12 (14.6%)
41-50	5	10	15 (18.3%)
51-60	8	19	27 (32.9%)
61-70	7	10	17 (20.7%)
71-	3	3	6 (7.4%)
Total	32 (39.0%)	50 (61.0%)	82 (100%)

Table 3. Symptoms and Signs

Symptom	Number of patients
Epigastric pain	54
Indigestion	32
Nausea	7
Weight loss	3
Asymptomatic	11

Table 4. Duration of Symptoms and Signs

Duration	Number of patients (%)
<1 month	15 (18.3)
1-3 month	19 (23.1)
3-6 month	14 (17.1)
6-12 month	8 (9.8)
12-24 month	5 (6.1)
24-60 month	5 (6.1)
>60 month	5 (6.1)
Asymptomatic	11 (13.4)

우리의 목표: 쉽고 정보가 많은 표

Table 3—*Demographic Characteristics of GERD-Positive and GERD-Negative Patients With the Nodular Bronchiectatic Form of NTM Lung Disease**

Characteristics	GERD Positive (n = 15)	GERD Negative (n = 43)	p Value
Age, yr	56 (43–63.5)	57 (53–66.5)	0.320
Female gender	13 (87)	37 (86)	1.000
Body mass index, kg/m^2	20.0 (18.6–21.7)	20.6 (19.5–22.2)	0.316
Smoking status			
Non-smoker	14 (93)	40 (93)	1.000
Ex-smoker	1 (7)	3 (7)	
Etiology			
M avium complex	5 (33)	22 (51)	0.368
M abscessus	10 (67)	21 (49)	
AFB smear positive	12 (80)	19 (44)	0.033
Involved lobes on HRCT, No.			
Bronchiectasis	4 (3–4)	2 (2–3)	0.008
Bronchiolitis	4 (3–5)	2 (2–4)	0.005
Pulmonary function tests			
FVC, % of predicted	93.0 (83.0–102.0)	87.0 (77.5–93.5)	0.170
FEV_1, % of predicted	92.5 (76.5–107.0)	88.0 (72.5–102.0)	0.508
FEV_1/FVC, ratio	76.0 (67.0–84.0)	74.0 (71.0–80.0)	0.880
Peak expiratory flow, % of predicted	92.0 (80.0–111.5)	96.0 (74.5–99.0)	0.748

*Data are presented as the median (interquartile range) or No. (%). Bronchiolitis was defined as the presence of small centrilobular nodules (< 10 mm in diameter) or branching nodular structures (tree-in-bud pattern) on HRCT.

Table 작성법

– 어떤 도서관 자료에서

<Table 점검표>

① Table의 제목이 소설체처럼 장황하지 않으면서도 충분히 서술적인가?

② 줄과 칸이 깔끔하게 구성되어 있는가? 각 칸의 자료가 제목 아래 가운데에 정렬되어 있는가? 칸 제목들을 묶을만한 공통 요소가 있나? 칸 제목은 이탤릭체 같이 구분되는 글자체로 되어 있는가? 줄 제목에는 단위가 붙어 있는가?

③ 불필요한 자료, 반복되는 연구대상자수 표시, 지나친 정밀함, 의미가 모호한 약자들이 있지 않는가? 이 Table이 꼭 필요한지, 이렇게 자세하게 할 필요가 있는지, 이 단어를 약자로 써야 하는지를 검토해 본다.

④ 본문을 보지 않고도 모든 항목의 의미를 명확히 알 수 있는가?

⑤ 모든 Table을 완성한 후 두 개 이상의 표를 하나로 묶을 수 없는지 체크해 본다

⑥ 모든 Table을 본문에서 언급했는가? 또한 순서대로 언급되었는가?

사례 검토 1

Table 2 Univariate and multivariate analysis of factors associated with metachronous recurrence after curative endoscopic submucosal dissection (ESD) for differentiated-type early gastric cancer.

	Metachronous recurrence[1]		Odds ratio	95%CI	*P* value
	None (n=1259)	Present (n=47)			
Age, mean ± SD, y	61.5 ± 9.7	63.1 ± 8.8	1.015	0.983 – 1.047	0.364
Gender, n (%)					0.427
Male	1004 (79.7)	40 (85.1)			
Female	255 (20.3)	7 (14.9)	0.714	0.311 – 1.640	
Number of lesions, n (%)					0.025
Single	1229 (97.6)	43 (91.5)			
Multiple	30 (2.4)	4 (8.5)	3.691	1.177 – 11.574	
Tumor site, n (%)					0.238
Antrum/angle	994 (79.0)	34 (72.3)			
Body/fundus/cardia	265 (21.0)	13 (27.7)	1.491	0.768 – 2.896	
Tumor shape, n (%)					0.683
Elevated	715 (56.8)	28 (59.6)			
Flat or depressed	544 (43.2)	19 (40.4)	0.882	0.482 – 1.613	
Tumor size, mean ± SD, cm	1.4 ± 0.8	1.3 ± 0.8	0.724	0.409 – 1.280	0.267
Tumor depth (%)					0.516
Mucosa	1194 (94.8)	45 (95.7)			
sm1[2]	65 (5.2)	2 (4.3)	0.556	0.094 – 3.274	
Differentiation, n (%)					0.016
Well differentiated	506 (40.2)	28 (59.6)			
Moderately differentiated	753 (59.8)	19 (40.4)	0.477	0.262 – 0.869	
Indication, n (%)					0.595
Absolute	994 (79.0)	38 (80.9)			
Expanded	265 (21.0)	9 (19.1)	1.406	0.400 – 4.937	

CI, confidence interval; SD, standard deviation.

[1] If patients had multiple tumors including both absolute-indication and expanded-indication early gastric cancer, data from the expanded-indication tumor were used. If patients had multiple tumors including only absolute-indication cancers or only expanded-indication cancers, data from the largest tumor were used.

[2] sm1, submucosal invasion depth < 500 µm from muscularis mucosa layer

Min. Endoscopy 2015

Final accepted manuscript 원고

Table 2. Univariate and multivariate analysis of factors associated with the occurrence of metachronous recurrence after curative endoscopic submucosal dissection for differentiated-type early gastric cancer (EGC)

	No metachronous recurrence* (n = 1259)	Metachronous recurrence* (n = 47)	Odds ratio	95% CI	*P* value
Age (yrs, Mean ± SD)	61.5 ± 9.7	63.1 ± 8.8	1.015	0.983 - 1.047	0.364
Gender (%)					
Male	1004 (79.7)	40 (85.1)			
Female	255 (20.3)	7 (14.9)	0.714	0.311 - 1.640	0.427
Number of lesion (%)					
Single	1229 (97.6)	43 (91.5)			
Multiple	30 (2.4)	4 (8.5)	3.691	1.177 - 11.574	0.025
Tumor site (%)					
Antrum/Angle	994 (79.0)	34 (72.3)			
Body/Fundus/Cardia	265 (21.0)	13 (27.7)	1.491	0.768 - 2.896	0.238
Tumor shape (%)					
Elevated	715 (56.8)	28 (59.6)			
Flat or depressed	544 (43.2)	19 (40.4)	0.882	0.482 - 1.613	0.683
Tumor size (cm, Mean ± SD)	1.4 ± 0.8	1.3 ± 0.8	0.724	0.409 - 1.280	0.267
Tumor depth (%)					
Mucosa	1194 (94.8)	45 (95.7)			
SM1	65 (5.2)	2 (4.3)	0.556	0.094 - 3.274	0.516
Differentiation (%)					
Well differentiated	506 (40.2)	28 (59.6)			
Moderately differentiated	753 (59.8)	19 (40.4)	0.477	0.262 - 0.869	0.016
Indication					
Absolute	994 (79.0)	38 (80.9)			
Expanded	265 (21.0)	9 (19.1)	1.406	0.400 - 4.937	0.595

CI, confidence interval; SD, standard deviation; SM1, submucosal invasion depth < 500 μm from muscularis mucosa layer

*If patients had multiple tumors including both EGC-absolute and EGC-expanded, data of EGC-expanded was used.
If patients had multiple tumors including only EGCs-absolute or only EGCs-expanded, data of the largest tumor was used.

Excel을 이용하여 표를 만든 후 옮긴 예

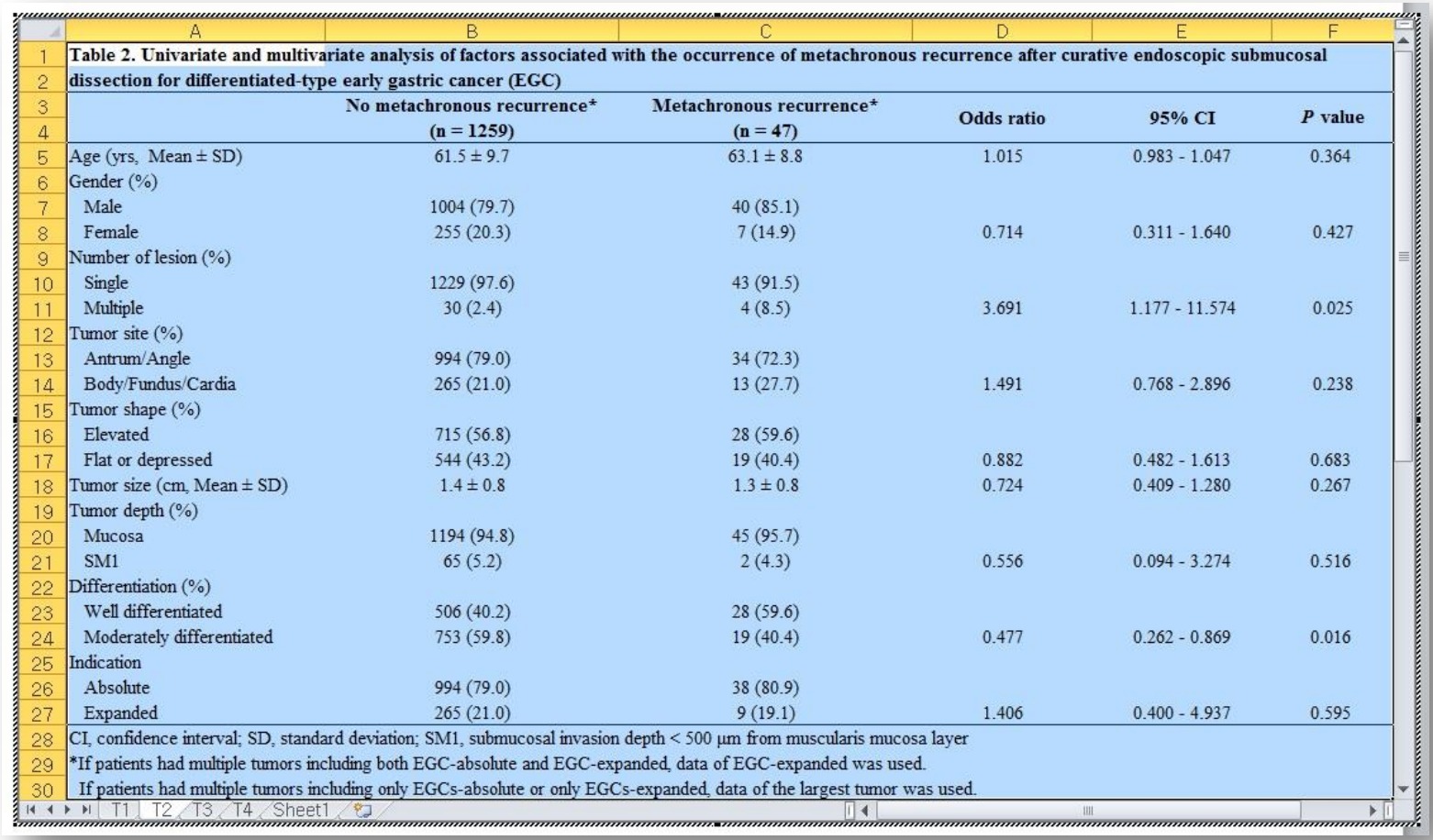

	A	B	C	D	E	F
1	**Table 2. Univariate and multivariate analysis of factors associated with the occurrence of metachronous recurrence after curative endoscopic submucosal**					
2	**dissection for differentiated-type early gastric cancer (EGC)**					
3		**No metachronous recurrence***	**Metachronous recurrence***	**Odds ratio**	**95% CI**	***P* value**
4		**(n = 1259)**	**(n = 47)**			
5	Age (yrs, Mean ± SD)	61.5 ± 9.7	63.1 ± 8.8	1.015	0.983 - 1.047	0.364
6	Gender (%)					
7	Male	1004 (79.7)	40 (85.1)			
8	Female	255 (20.3)	7 (14.9)	0.714	0.311 - 1.640	0.427
9	Number of lesion (%)					
10	Single	1229 (97.6)	43 (91.5)			
11	Multiple	30 (2.4)	4 (8.5)	3.691	1.177 - 11.574	0.025
12	Tumor site (%)					
13	Antrum/Angle	994 (79.0)	34 (72.3)			
14	Body/Fundus/Cardia	265 (21.0)	13 (27.7)	1.491	0.768 - 2.896	0.238
15	Tumor shape (%)					
16	Elevated	715 (56.8)	28 (59.6)			
17	Flat or depressed	544 (43.2)	19 (40.4)	0.882	0.482 - 1.613	0.683
18	Tumor size (cm, Mean ± SD)	1.4 ± 0.8	1.3 ± 0.8	0.724	0.409 - 1.280	0.267
19	Tumor depth (%)					
20	Mucosa	1194 (94.8)	45 (95.7)			
21	SM1	65 (5.2)	2 (4.3)	0.556	0.094 - 3.274	0.516
22	Differentiation (%)					
23	Well differentiated	506 (40.2)	28 (59.6)			
24	Moderately differentiated	753 (59.8)	19 (40.4)	0.477	0.262 - 0.869	0.016
25	Indication					
26	Absolute	994 (79.0)	38 (80.9)			
27	Expanded	265 (21.0)	9 (19.1)	1.406	0.400 - 4.937	0.595
28	CI, confidence interval; SD, standard deviation; SM1, submucosal invasion depth < 500 μm from muscularis mucosa layer					
29	*If patients had multiple tumors including both EGC-absolute and EGC-expanded, data of EGC-expanded was used.					
30	If patients had multiple tumors including only EGCs-absolute or only EGCs-expanded, data of the largest tumor was used.					

T1 T2 T3 T4 Sheet1

사례 검토 2

- 가장 중요한 자료는 main manuscript에 넣고…

Table 1. Association Between Receipt of Gastric Cancer Screening and Cause of Mortality: Number of Pairs and Proportions of the Screened Case Subjects and Matched Controls, as Well as ORs and 95% CIs Compared With Never-Screened Individuals

	All-cause mortality					GC-specific mortality					All-cause mortality except from GC				
		Screened, %					Screened, %					Screened, %			
	Pairs, n	Case	Control	OR	95% CI	Pairs, n	Case	Control	OR	95% CI	Pairs, n	Case	Control	OR	95% CI
Overall	54,418	25.7	28.9	0.83	0.81–0.85	44,095	24.7	28.8	0.79	0.77–0.81	10,323	29.9	29.4	1.03	0.98–1.08
Year of entry															
2002	31,111	26.1	29.4	0.83	0.81–0.86	25,157	25.2	29.3	0.79	0.76–0.81	5954	30.3	29.5	1.04	0.97–1.11
2003	23,307	25.1	28.2	0.83	0.80–0.86	18,938	24.1	28.0	0.79	0.76–0.82	4369	29.4	29.3	1.01	0.93–1.09
Sex															
Male	37,739	26.7	29.8	0.84	0.82–0.86	29,783	25.4	29.6	0.79	0.77–0.81	7956	31.4	30.6	1.05	0.99–1.11
Female	16,679	23.5	26.9	0.81	0.78–0.84	14,312	23.3	27.1	0.79	0.75–0.83	2367	24.6	25.5	0.95	0.85–1.06
Age group, *y*															
40-44	3396	19.8	24.1	0.76	0.69–0.84	3100	20.1	24.4	0.77	0.69–0.85	296	16.6	20.9	0.74	0.52–1.05
45–49	3324	20.8	27.3	0.67	0.61–0.74	2969	20.7	27.4	0.67	0.60–0.74	355	21.1	27.1	0.71	0.53–0.94
50–54	5074	24.4	31.8	0.67	0.62–0.72	4309	23.0	31.9	0.61	0.57–0.67	765	32.3	31.8	1.02	0.86–1.22
55–59	4510	28.4	35.3	0.70	0.65–0.76	3746	27.6	35.4	0.67	0.61–0.73	764	32.2	34.8	0.88	0.74–1.05
60–64	9538	31.8	37.0	0.77	0.73–0.81	7486	30.5	36.8	0.73	0.69–0.77	2052	36.2	37.7	0.93	0.84–1.04
65–69	8411	31.4	35.0	0.83	0.79–0.88	6469	30.3	35.1	0.78	0.73–0.83	1942	35.0	34.5	1.02	0.92–1.14
70–74	10,695	26.9	27.5	0.96	0.92–1.01	8320	26.1	27.5	0.92	0.87–0.97	2375	29.7	27.6	1.13	1.01–1.25
75–79	5212	20.2	18.6	1.13	1.04–1.22	4230	19.3	18.2	1.09	1.00–1.19	982	24.0	20.2	1.29	1.08–1.55
80–84	3557	12.8	10.5	1.28	1.14–1.44	2908	12.5	10.5	1.23	1.08–1.40	649	14.3	10.3	1.53	1.17–2.01
≥85	701	7.1	4.1	1.82	1.28–2.59	558	7.2	4.2	1.80	1.22–2.67	143	7.0	3.9	1.91	0.87–4.19
Socioeconomic status															
NHI, high	16,104	26.4	29.2	0.85	0.82–0.89	12,637	25.7	29.7	0.80	0.76–0.84	3467	28.7	27.5	1.07	0.98–1.17
NHI, middle	15,656	18.2	21.2	0.80	0.76–0.84	13,098	17.5	20.9	0.78	0.74–0.82	2558	21.4	23.0	0.89	0.80–1.00
NHI, low	18,243	30.0	34.0	0.82	0.79–0.85	14,876	28.6	33.7	0.77	0.74–0.80	3367	36.0	34.9	1.05	0.97–1.15
MAP	4415	32.3	33.9	0.92	0.85–0.99	3484	31.5	33.9	0.88	0.81–0.96	931	35.5	34.2	1.06	0.91–1.24

NOTE. Analyses were conducted for 1-to-4 matched case–control sets using conditional logistic regression.
GC, gastric cancer; MAP, Medical Aid Program; NHI, National Health Insurance

Jun JK. Gastroenterology 2017;152:1319–1328

사례 검토 2

- 필요하지만 너무 복잡한 내용은 supplement로 돌릴 수 있다.

Supplementary Table 2. Comparison of International Mortality to Incidence Rate Ratios

Population	Incidence					Mortality					
	Quality[b]	Numbers	Crude rate	ASR (W)	Cumulative risk[c]	Quality[b]	Numbers	Crude rate	ASR (W)	Cumulative risk[c]	M/I ratio[a]
World		951,594	13.5	12.1	1.39		723,027	10.2	8.9	0.97	0.74
Very high human development		256,260	22.2	10.9	1.28		143,276	12.4	5.5	0.58	0.50
High human development		141,013	13.5	11.7	1.40		117,795	11.3	9.5	1.12	0.81
Medium human development		518,999	14.6	14.4	1.61		428,671	12.1	11.8	1.24	0.82
Low human development		35,117	2.7	4.6	0.55		33,132	2.5	4.4	0.52	0.96
Africa		23,806	2.2	3.8	0.44		21,801	2.0	3.5	0.41	0.92
Eastern Africa		8036	2.3	4.5	0.54		7568	2.1	4.3	0.51	0.96
Burundi	G6	184	2.1	4.0	0.50	G6	177	2.0	3.9	0.49	0.98
Comoros	G6	4	0.5	1.1	0.13	G6	4	0.5	1.1	0.13	1.00
Djibouti	G6	15	1.6	2.7	0.35	G6	15	1.6	2.7	0.35	1.00
Eritrea	G6	60	1.1	2.4	0.29	G6	58	1.0	2.4	0.28	1.00
Ethiopia	E6	1478	1.7	3.0	0.36	E6	1428	1.7	3.0	0.35	1.00
France, La Reunion	D2	102	11.8	10.0	1.24	D2	73	8.4	6.7	0.79	0.67
Kenya	E6	1811	4.2	9.5	1.15	E6	1675	3.9	8.9	1.06	0.94
Madagascar	G6	543	2.5	4.7	0.58	G6	513	2.3	4.5	0.55	0.96
Malawi	C6	203	1.3	2.7	0.31	C6	188	1.2	2.5	0.29	0.93
Mauritius	D2	121	9.2	8.0	0.97	D2	112	8.5	7.4	0.85	0.93
Mozambique	E6	101	0.4	0.9	0.11	E6	94	0.4	0.8	0.11	0.89
Rwanda	F6	474	4.2	8.2	0.92	F6	458	4.1	8.0	0.88	0.98
Somalia	G6	296	3.0	6.3	0.76	G6	278	2.8	6.1	0.72	0.97
South Sudan	G6	290	2.7	5.0	0.60	G6	276	2.5	4.8	0.58	0.96
Tanzania	E6	752	1.6	3.1	0.37	E6	708	1.5	2.9	0.35	0.94
Uganda	C6	720	2.0	5.1	0.65	C6	666	1.9	4.8	0.61	0.94
Zambia	E6	276	2.0	4.4	0.53	E6	263	1.9	4.2	0.50	0.95
Zimbabwe	C6	600	4.6	8.0	0.93	C6	577	4.4	7.5	0.85	0.94
Middle Africa		2764	2.1	4.0	0.47		2666	2.0	4.0	0.46	1.00
Angola	G6	351	1.7	3.8	0.44	G6	328	1.6	3.7	0.42	0.97
Cameroon	E6	277	1.4	2.4	0.27	E6	256	1.3	2.2	0.26	0.92
Central African Republic	G6	60	1.3	2.3	0.29	G6	60	1.3	2.3	0.29	1.00
Chad	G6	122	1.0	2.0	0.24	G6	118	1.0	2.0	0.24	1.00
Democratic Republic of Congo	G6	1854	2.7	5.4	0.62	G6	1809	2.6	5.4	0.61	1.00
Republic of Congo	E6	63	1.5	2.7	0.37	E6	59	1.4	2.5	0.37	0.93
Equatorial Guinea	G6	12	1.6	2.3	0.27	G6	12	1.6	2.3	0.27	1.00
Gabon	F6	25	1.6	2.4	0.30	F6	23	1.5	2.2	0.28	0.92
Northern Africa		5704	2.7	3.4	0.41		5038	2.4	3.1	0.36	0.91
Algeria	C6	1717	4.7	6.0	0.71	C6	1474	4.0	5.2	0.61	0.87
Egypt	C3	1789	2.1	2.5	0.30	C3	1584	1.9	2.3	0.26	0.92
Libya	C6	164	2.5	3.6	0.47	C6	134	2.1	3.0	0.38	0.83
Morocco	E6	1176	3.6	4.0	0.47	E6	1069	3.3	3.7	0.43	0.93
Sudan	F6	363	1.0	1.8	0.22	F6	351	0.9	1.8	0.21	1.00
Tunisia	C6	470	4.4	4.2	0.49	C6	401	3.7	3.6	0.41	0.86
Western Sahara	G6	25	4.4	6.5	0.70	G6	25	4.4	6.5	0.70	1.00

Jun JK. Gastroenterology 2017;152:1319–1328

좋지 못한 제목의 예와 개선안

좋지 못한 제목	개선된 제목
Characteristics of subjects	Characteristics of the 54 men enrolled in the trial
Comparison of active treatment with diuretic therapy compared with placebo in 122 men	Effects of treatment of hypertension and placebo groups
Predictors of quality of life	Factors associated with differences in quality of life: multivariate models
Independent ($p<0.05$) predictors of quality of life using logistic regression following stepwise selection procedures, using the criteria of reference 6	↑

Browner. Publishing and presenting clinical research (번역본 90쪽)

Figure

성균관대학교 의과대학 삼성서울병원 내과 이준행

Topic 1

해상도란 무엇인가?

성균관대학교 의과대학 삼성서울병원 내과 이준행

논문의 그림은 4 가지 종류가 있다

- Statistical graphs, charts, and simple diagrams
- Photographic images (color photos, radiographs, ultrasound images, CT scans, MRI scans, electron micrographs, and photomicrographs)
- Illustrations
- Videos

→ 4 형태에 모두 **해상도**라는 개념이 들어가야 한다.

해상도란 무엇인가?

- 해상도(解像度)는 어느 일정한 단위 안에서 얼마나 더 자세하게 그 내용을 표현하는가를 나타내는 용어이다.
- 일정한 물리적 길이 단위인 1인치(25.4mm) 안에 표현되는 화소(pixel)의 수를 말한다. 단위로 dpi(dots per inch)가 쓰인다. 예를 들어, 72 dpi라고 하면 1인치 안에 72개의 점이 들어간다는 뜻이다.

http://ko.wikipedia.org/

http://www.ibiblio.org/wm/paint/auth/monet/paris/

출력시 크기가 같다면 pixel의 수가 많을수록 해상도가 높다 (높은 DPI 값)

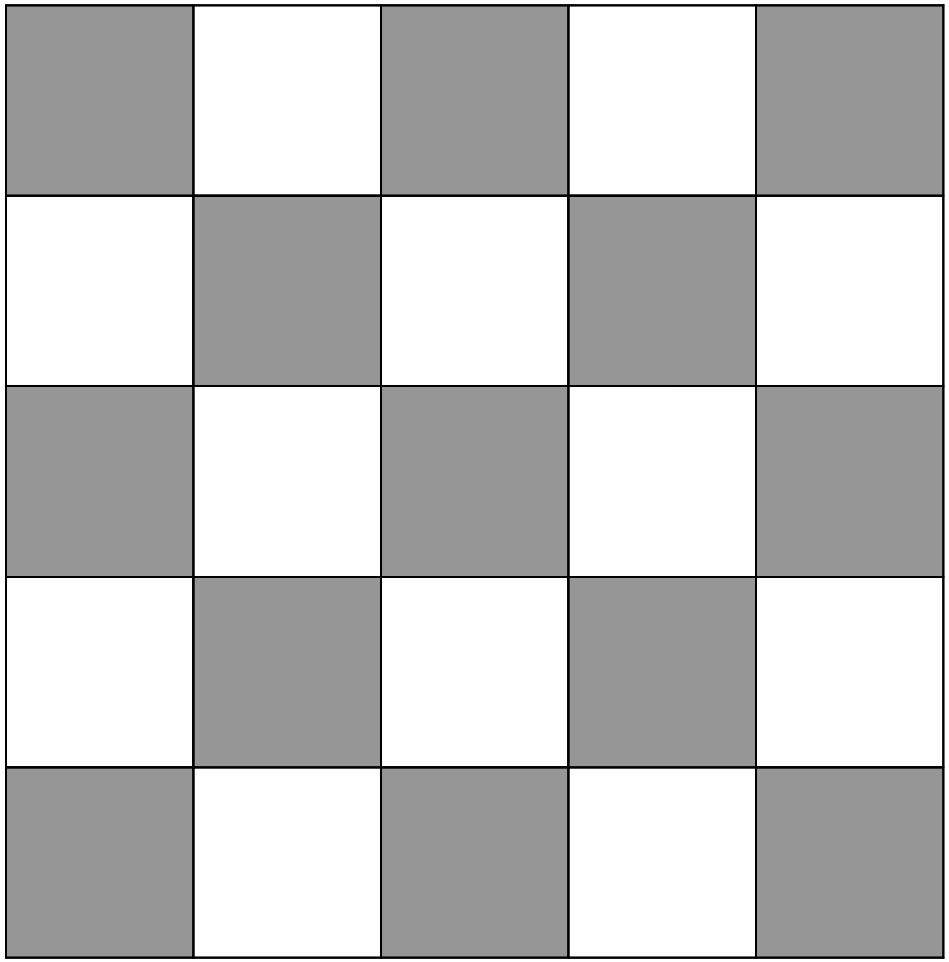

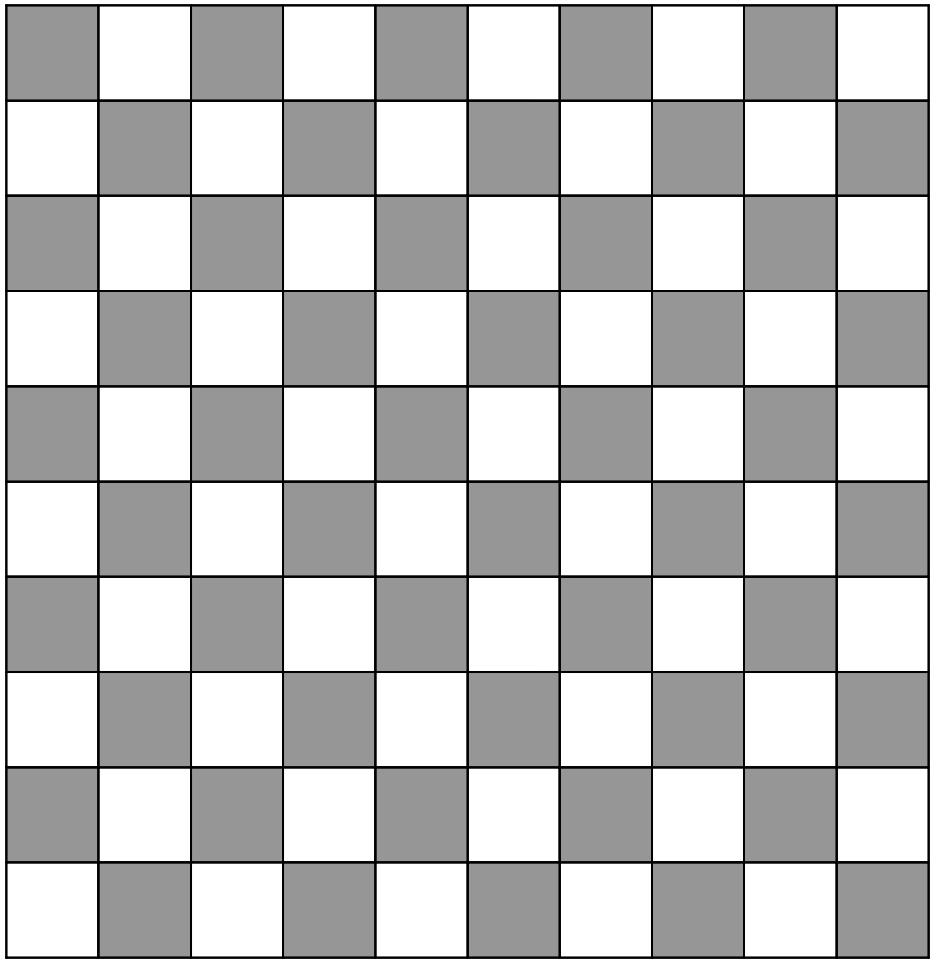

DPI = Dots / Inch

Digital image에서 DPI는 무슨 의미가 있는가?

- A digitally stored image has ***no inherent physical dimensions***, measured in inches or centimetres.

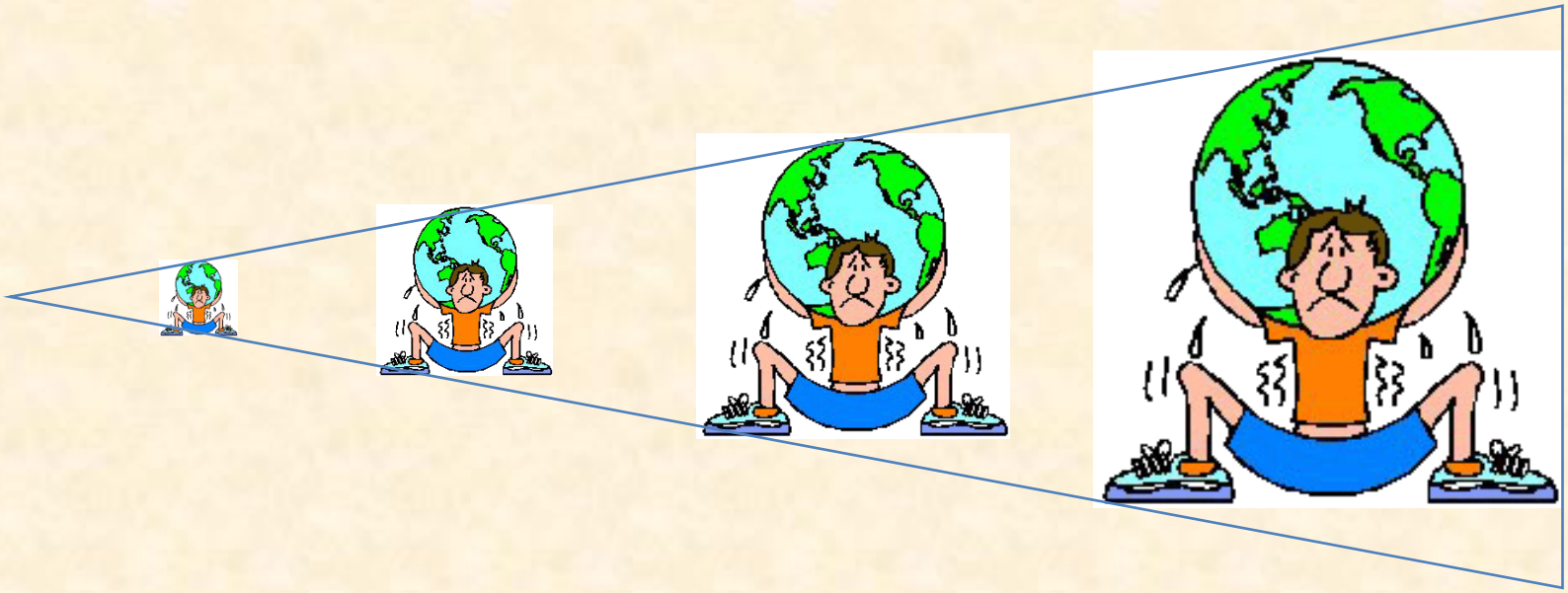

http://en.wikipedia.org/wiki/Dots_per_inch

DPI는 출력을 전제로...

- sungkyunkwan.jpg
- 85,109 byte
- 890 x 890 = 792,100 pixels
- Resolution: dots per inch (dpi)

출력을 하지 않는

한 아무런 의미가

없는 숫자이다

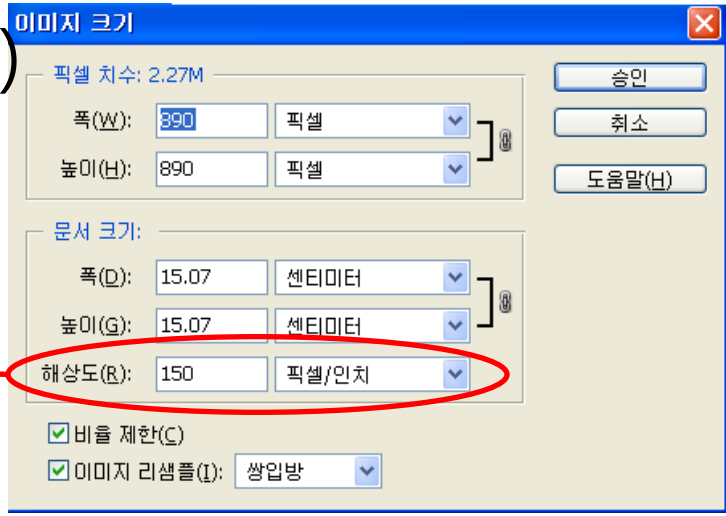

Information amount in a bitmap image

- Determined by the number of pixels
- Size (inches) x resolution (dpi) = pixel numbers

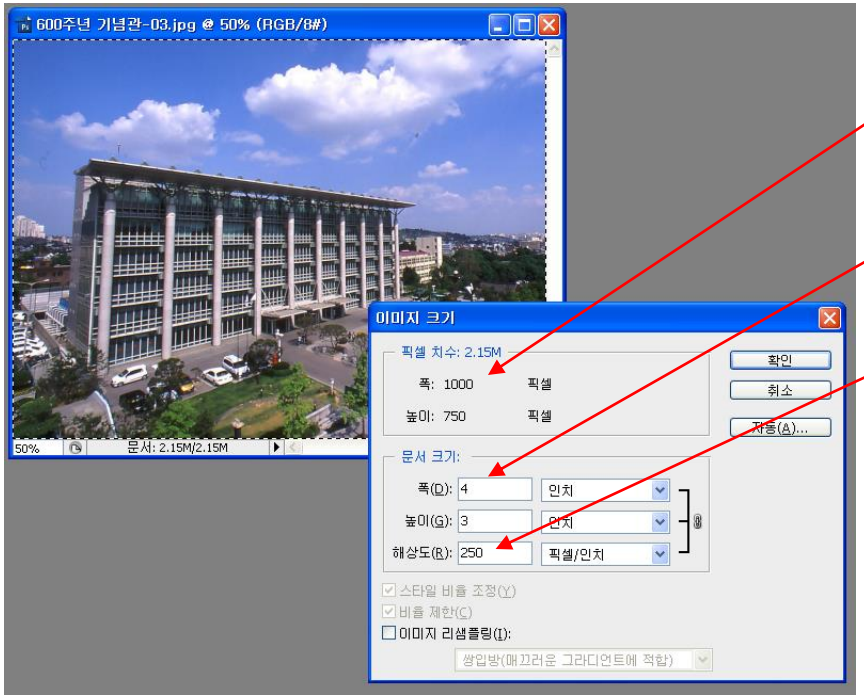

Width 1000 pixels

= 4 inches x 250 pixel/inch

Digital image에서는 pixel 수가 많을수록 정보량이 많다 (높은 해상도)

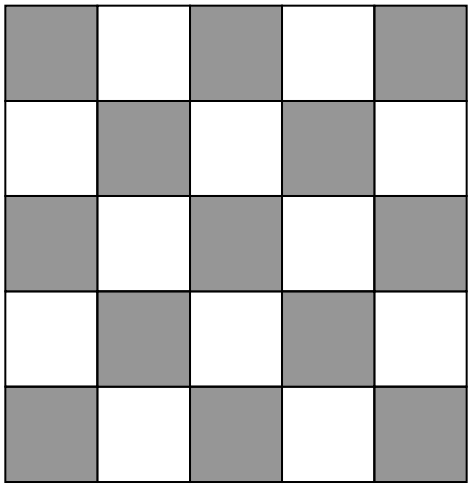

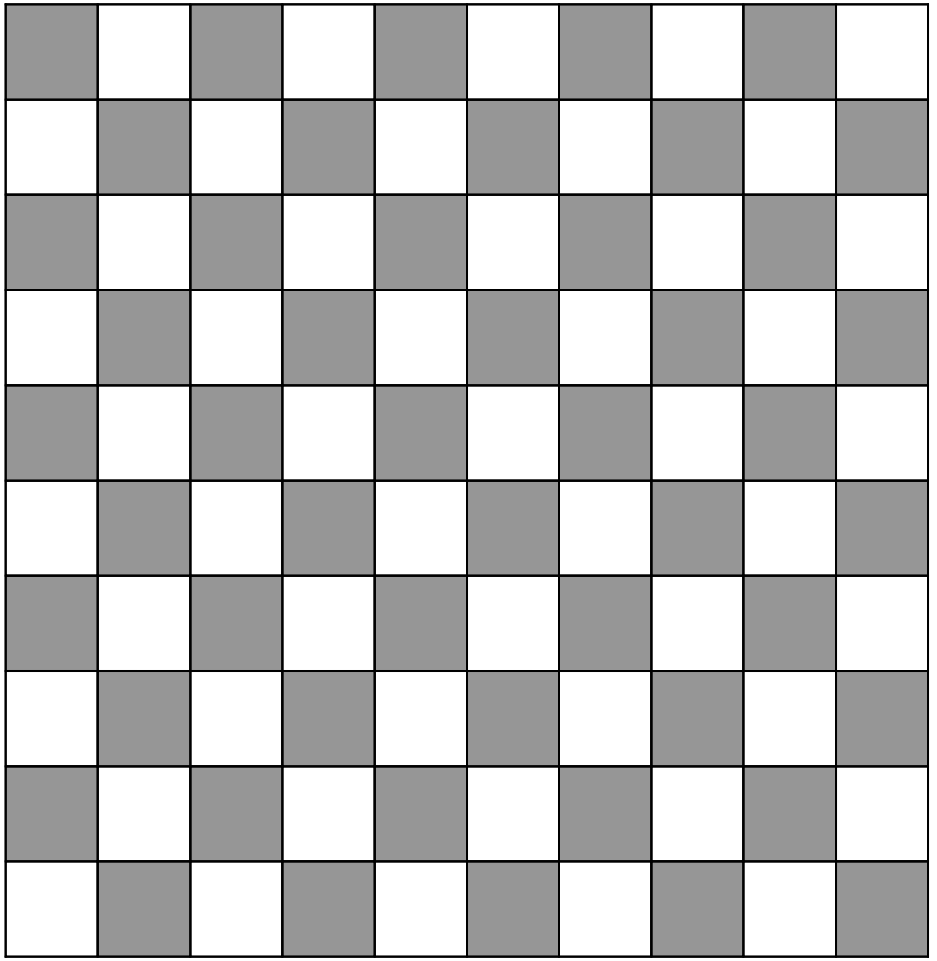

Pixel 수가 많다고 항상 고해상도는 아니다

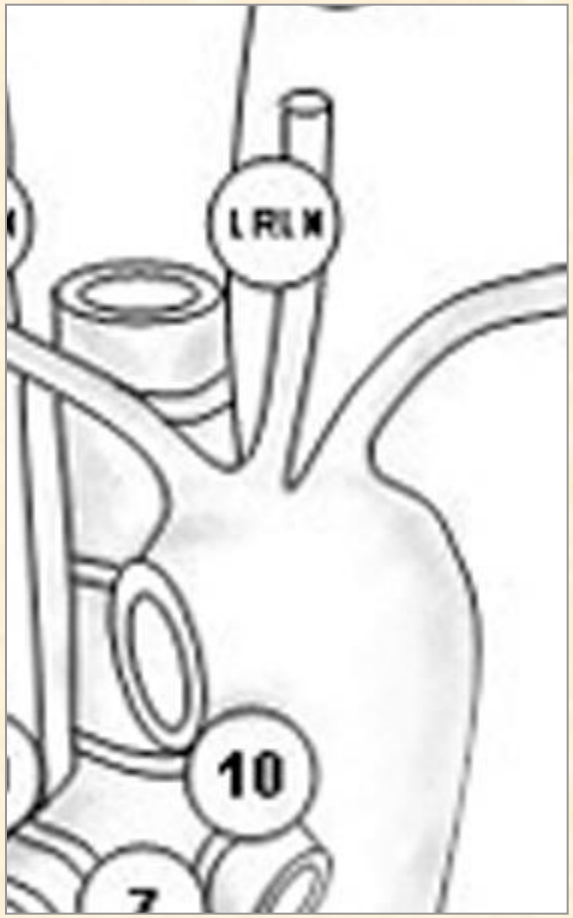

1.14 inch, 300 dpi

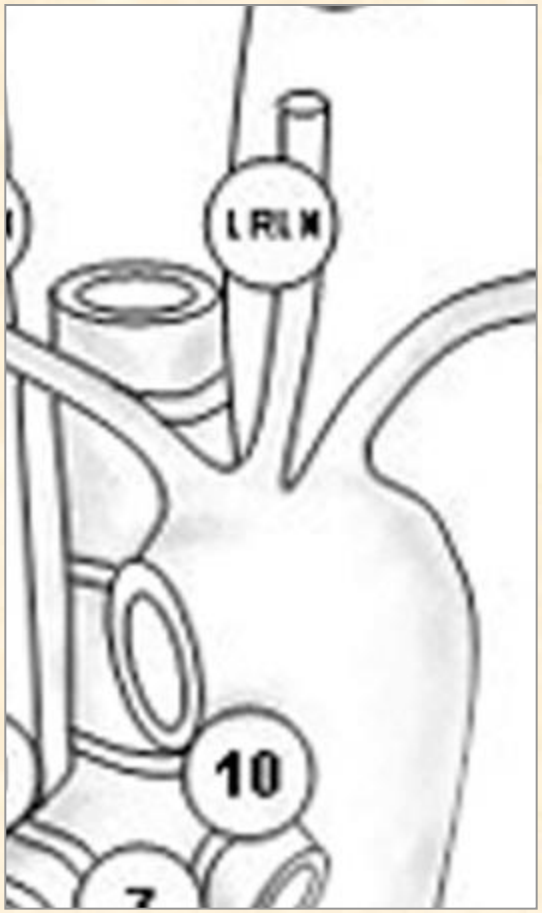

4 inch, 900 dpi

한번 줄인 pixel 수는 되돌이킬 수 없다

- 억지로 pixel 수를 늘려도 정보의 양은 늘지 않는다

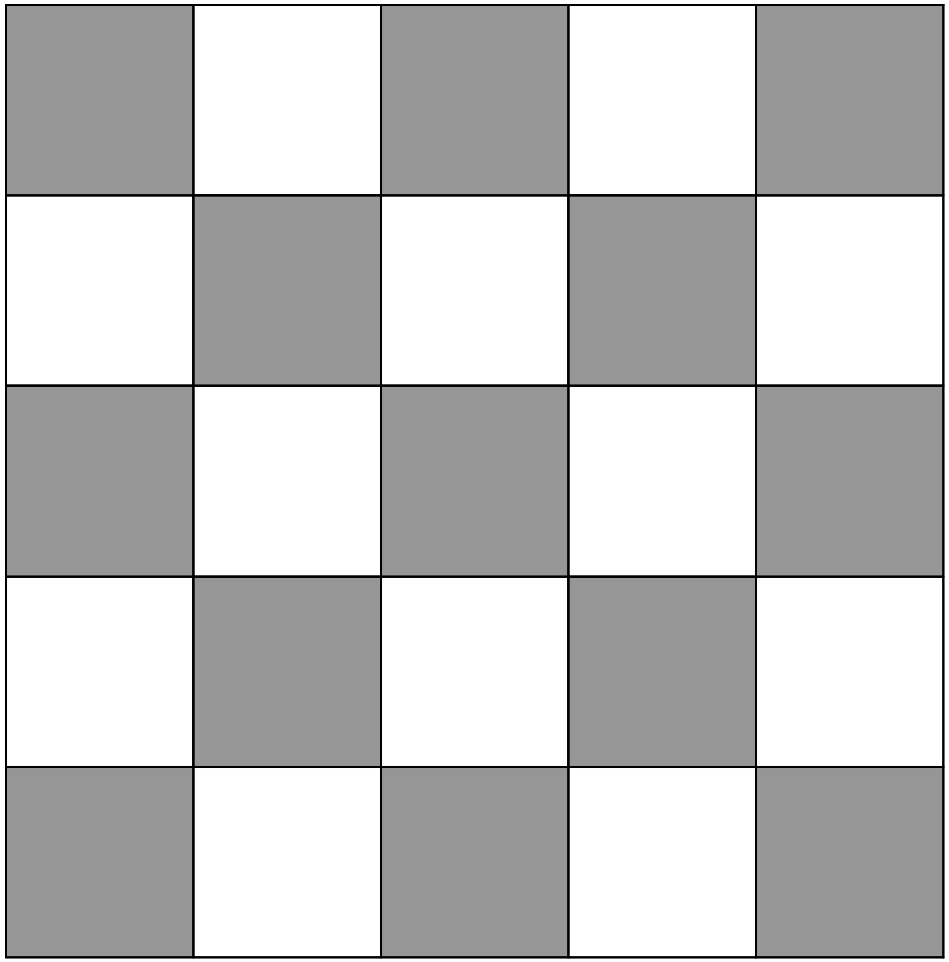

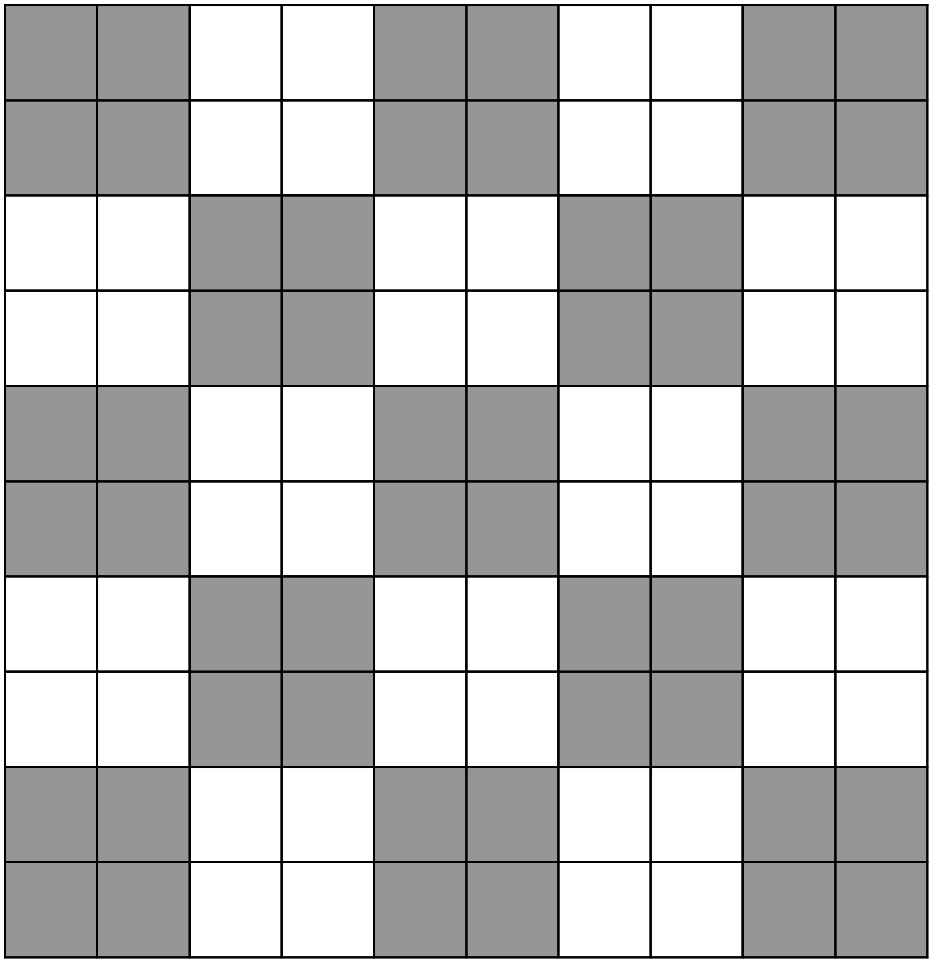

Population bottleneck

- an important concept from evolutionary biology

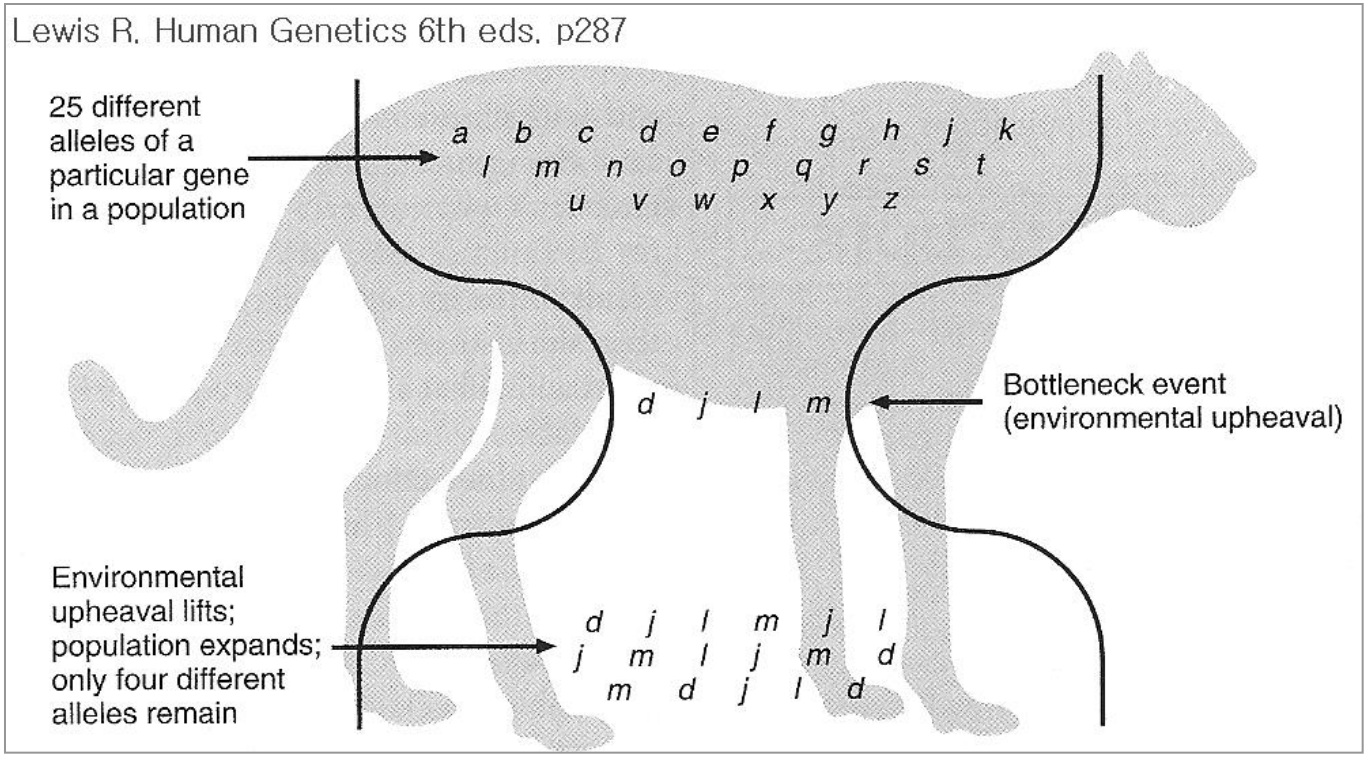

Lewis R. Human Genetics 6th eds. p287

요약 - 해상도

- 디지털 이미지의 정보는 pixel의 수로 결정된다.
- 이미지의 정보양을 증가시킬 방법은 없다.
- 이미지의 변형은 항상 해상도의 저하를 동반한다. 원본이미지를 확실하게 보관하자.

- 질문: 그래픽 이미지에는 항상 해상도가 있나요?

Topic 2

Vector image란 무엇인가?

성균관대학교 의과대학 삼성서울병원 내과 이준행

Digital camera로 찍은 image는 전형적인 bitmap image다.
확대를 하지 않으면 매우 자연스럽게 보인다.

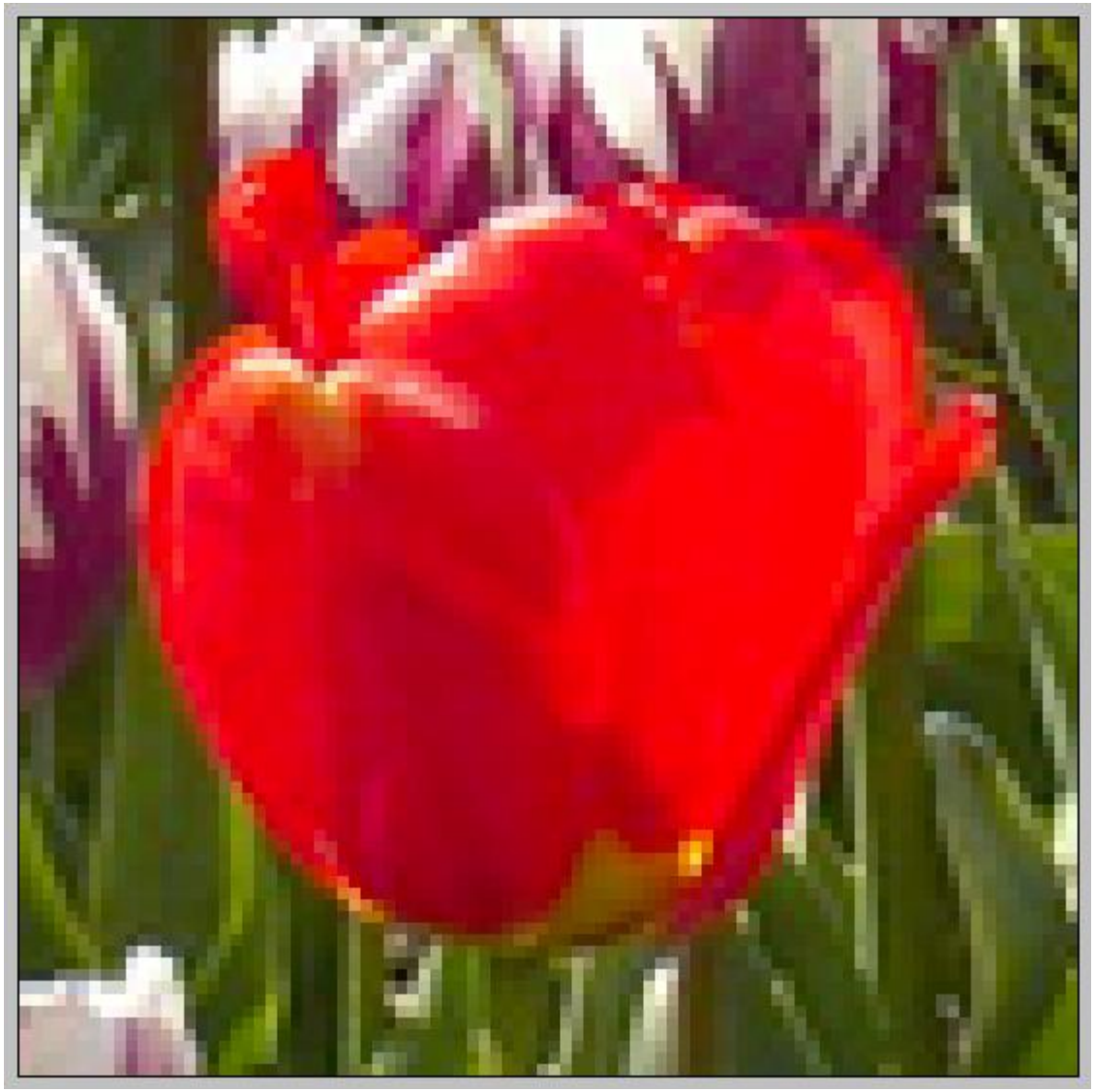

Pixel이 보이도록 크게 확대하면 격자구조를 볼 수 있다.

선을 그리는 두 가지 방법

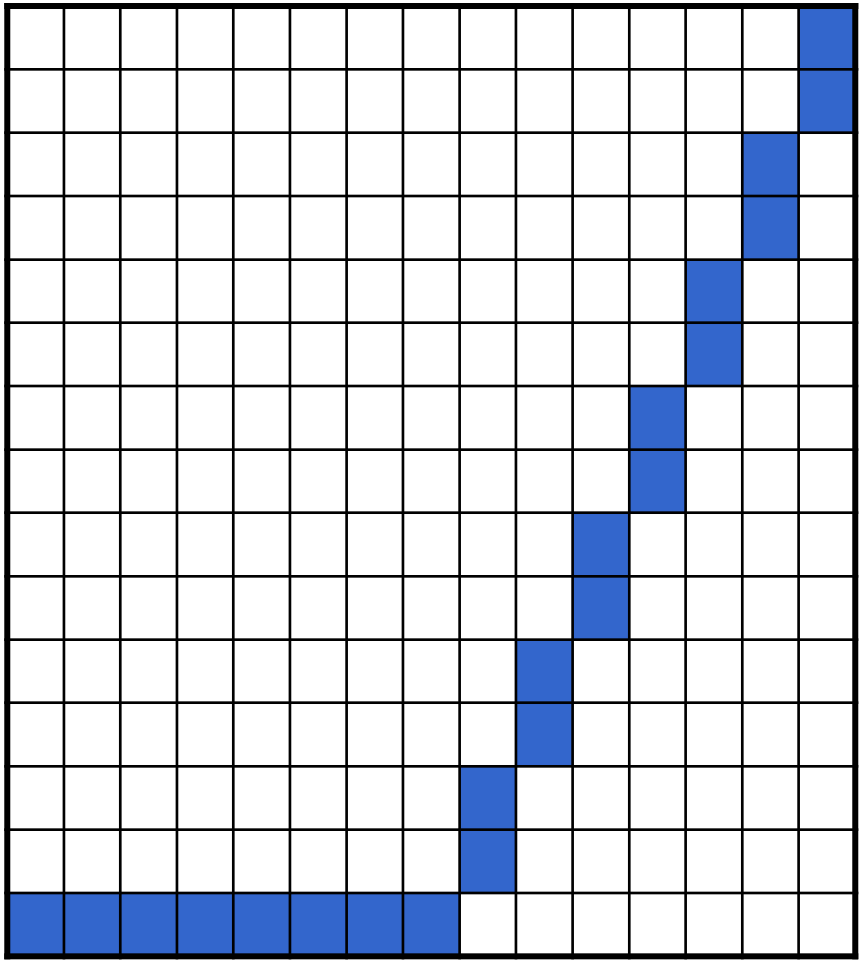

Bitmap (=rastor) image

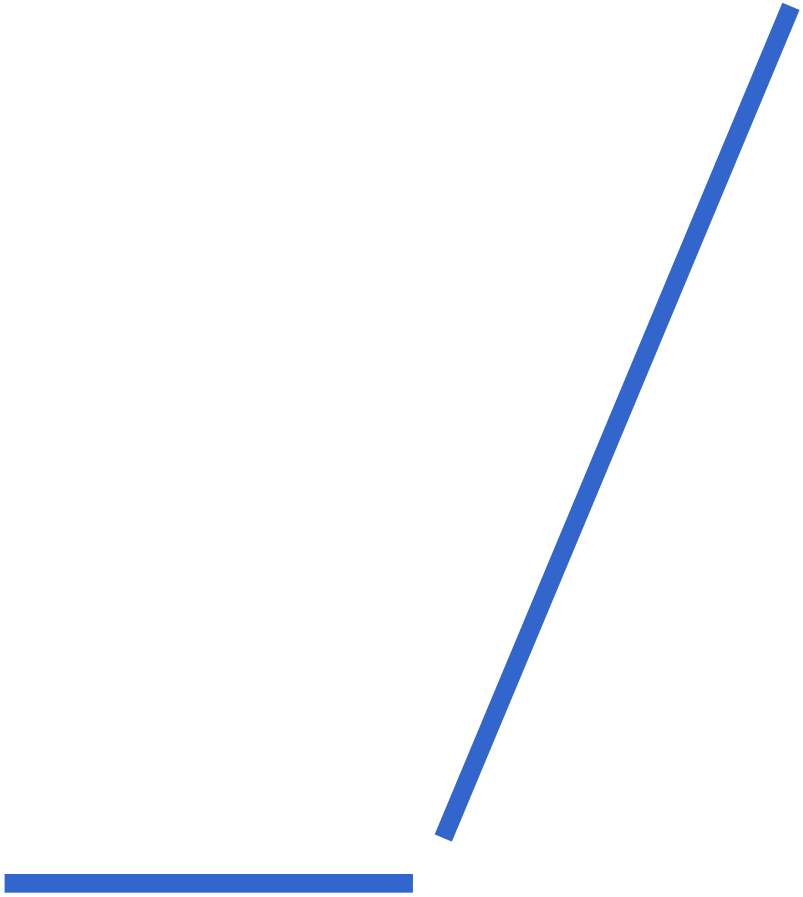

Vector image

Raster image (=bitmap image)

- A "raster" is a grid-like organization of image elements.
- Standard raster format: TIFF
- Raster image file has all the information for every pixel (picture element).

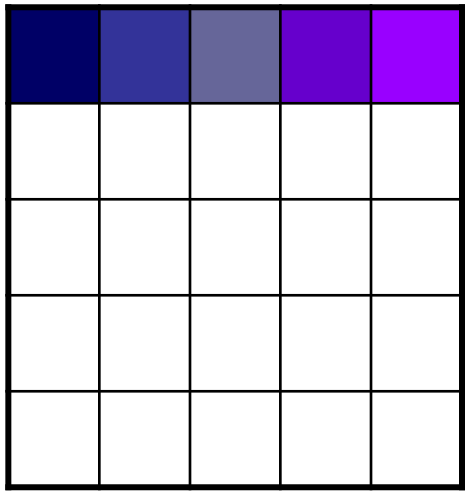

Is my image a vector file?

To ensure that your image is a vector drawing please conduct the following test:

1 In the document zoom in to the diagram 500% or more.

2 Check if lines such as curves have lost any quality, are appearing pixelated (made up of small squares rather than clear

3 If they are same file mentione check that

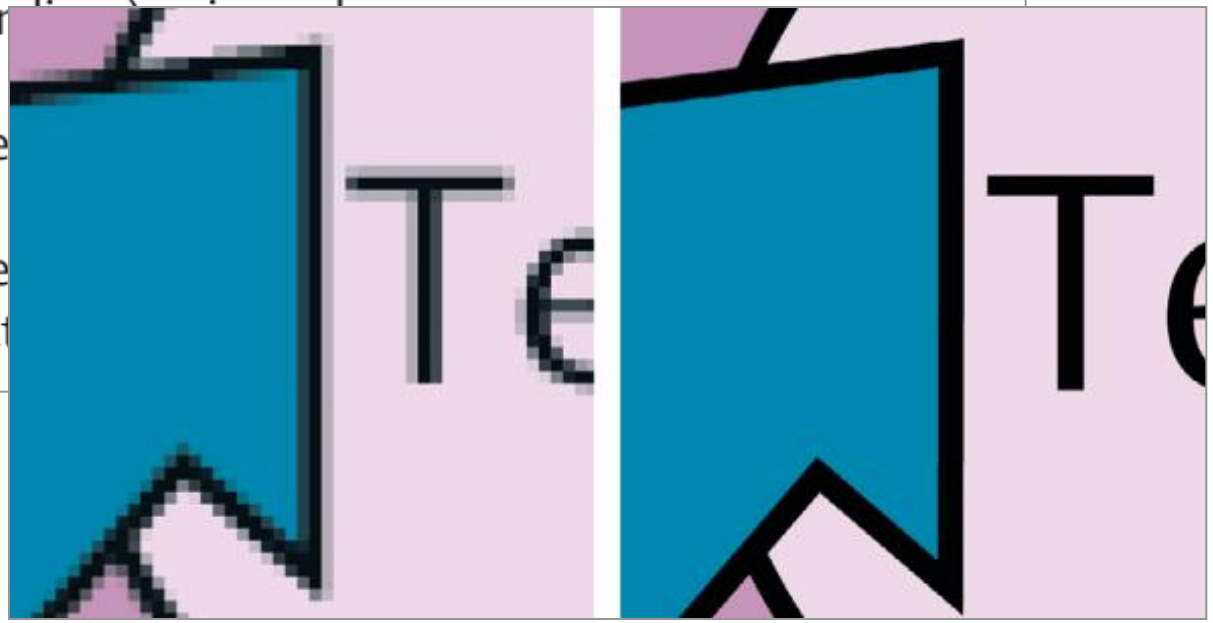

http://www.thelancet.com/webfiles/images/clusters/thelancet/EESartwork.pdf

우리가 흔히 사용하는 format은 대부분 bitmap (=rastor) image file format이다

File Format	Pertinent Application
DICOM	PACS
JPEG	PowerPoint, web-based display
TIFF	Print output, journal publication
PSD	Print output, when arrows or labels are necessary
GIF	Web-based display
EPS	Vector graphics
PDF	Distribution, web-based or otherwise
PICT	Some Macintosh applications use this format though it is largely replaced by the other formats
PNG	New format, may replace JPEG eventually

Note.—PICT = PICTure; PNG = portable networks graphics; PSD = PhotoShop document.

LaBerge. J Vasc Interv Radiol 2003;14:1223-1229

Some journals may requires vector drawings

Accepted file types

- For graphs and diagrams we prefer to accept vector drawings. These files would ideally be created in a program such as Adobe Illustrator or Corel Draw and saved as an encapsulated postscript (**.eps**) or portable document format (**.pdf**) files for uploading on-line.

- Other accepted vector files are Corel Draw (**.cdt**) and Adobe Illustrator (**.ai**). Please email these directly to the article editor as these formats are not supported for uploading.

http://www.thelancet.com/webfiles/images/clusters/thelancet/EESartwork.pdf

Selecting programs for vector images

- 우리가 사용하는 프로그램/도구는 대부분 bitmap임

- Bitmap (=raster) image
  - Photoshop
  - Cameras
  - Scanners
- Vector image
  - **Adobe illustrator**
  - Corel draw

Making a vector file in Prism

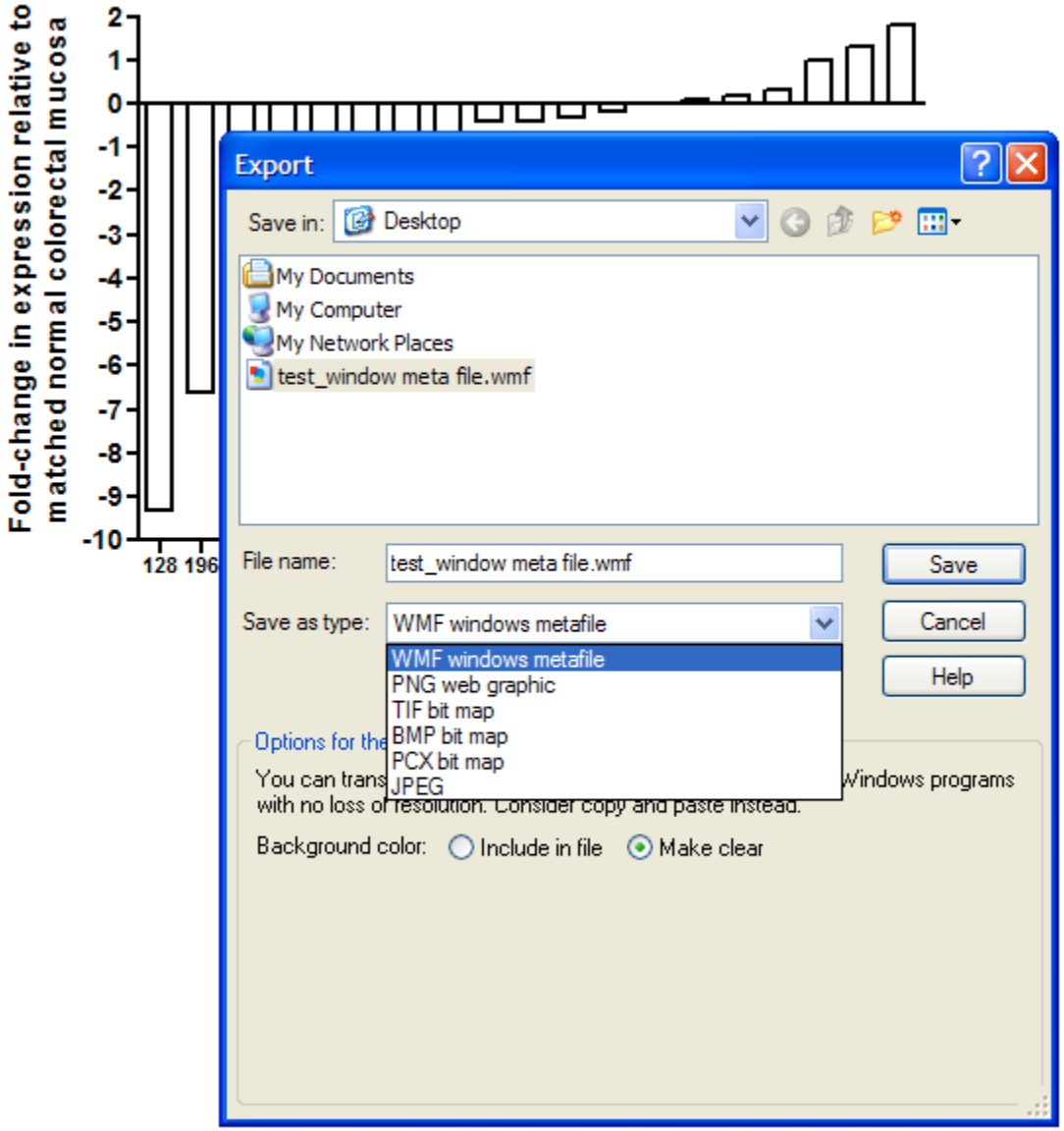

Insertion of the WMF file

- File size: 5,158 bytes

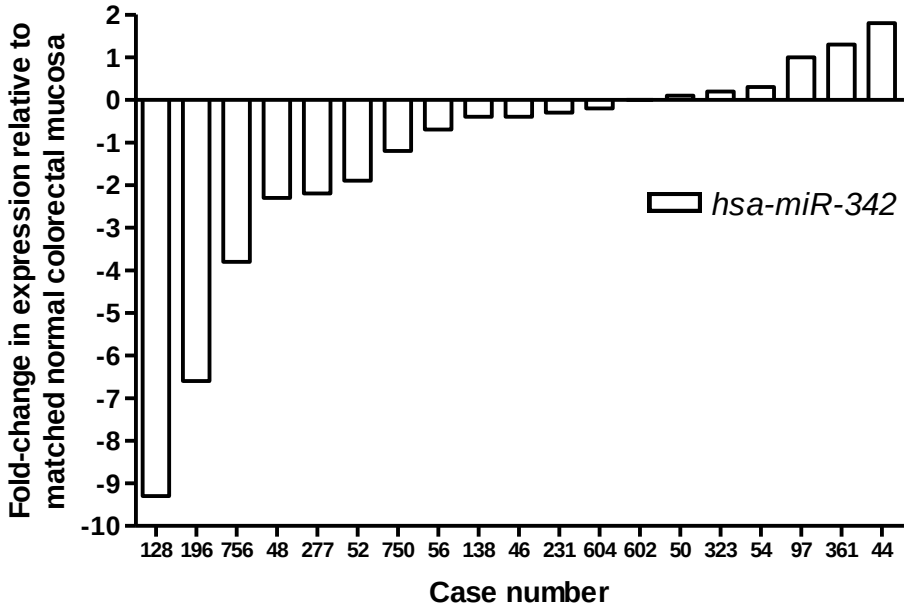

Windows Metafile (WMF) is a vector graphics format which also allows the inclusion of raster graphics.

X10 enlargement of the inserted WMF file

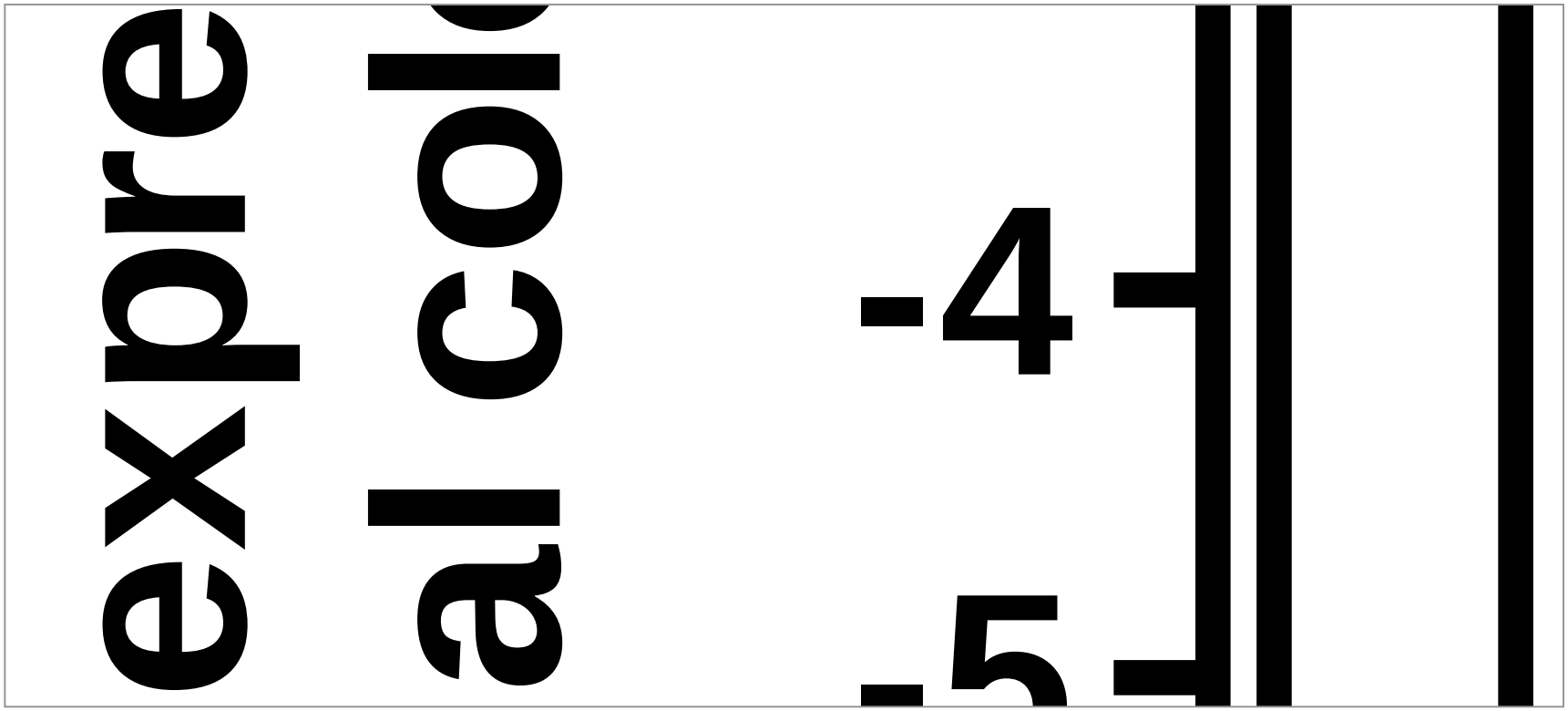

X100 enlargement of the inserted WMF file

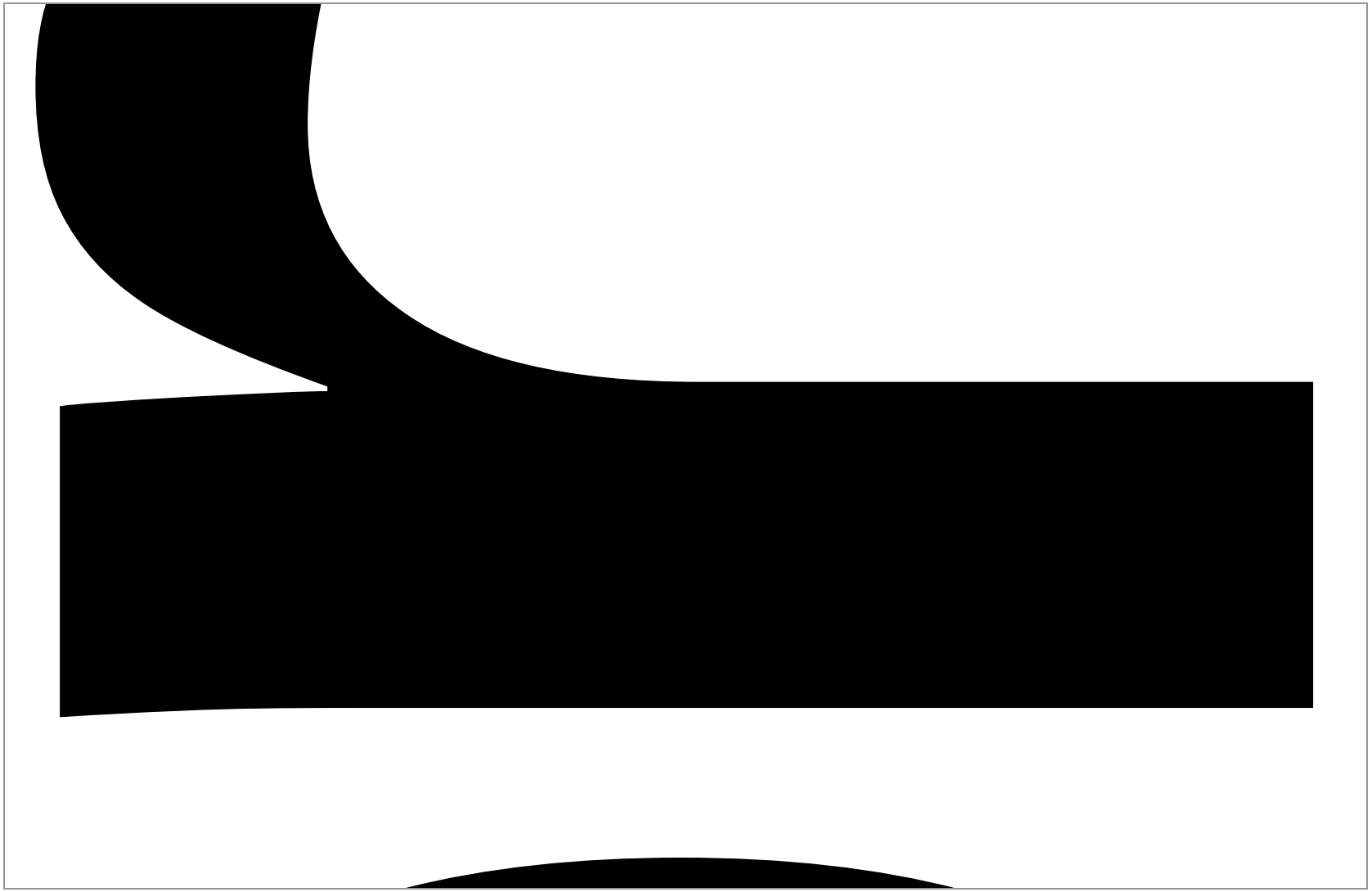

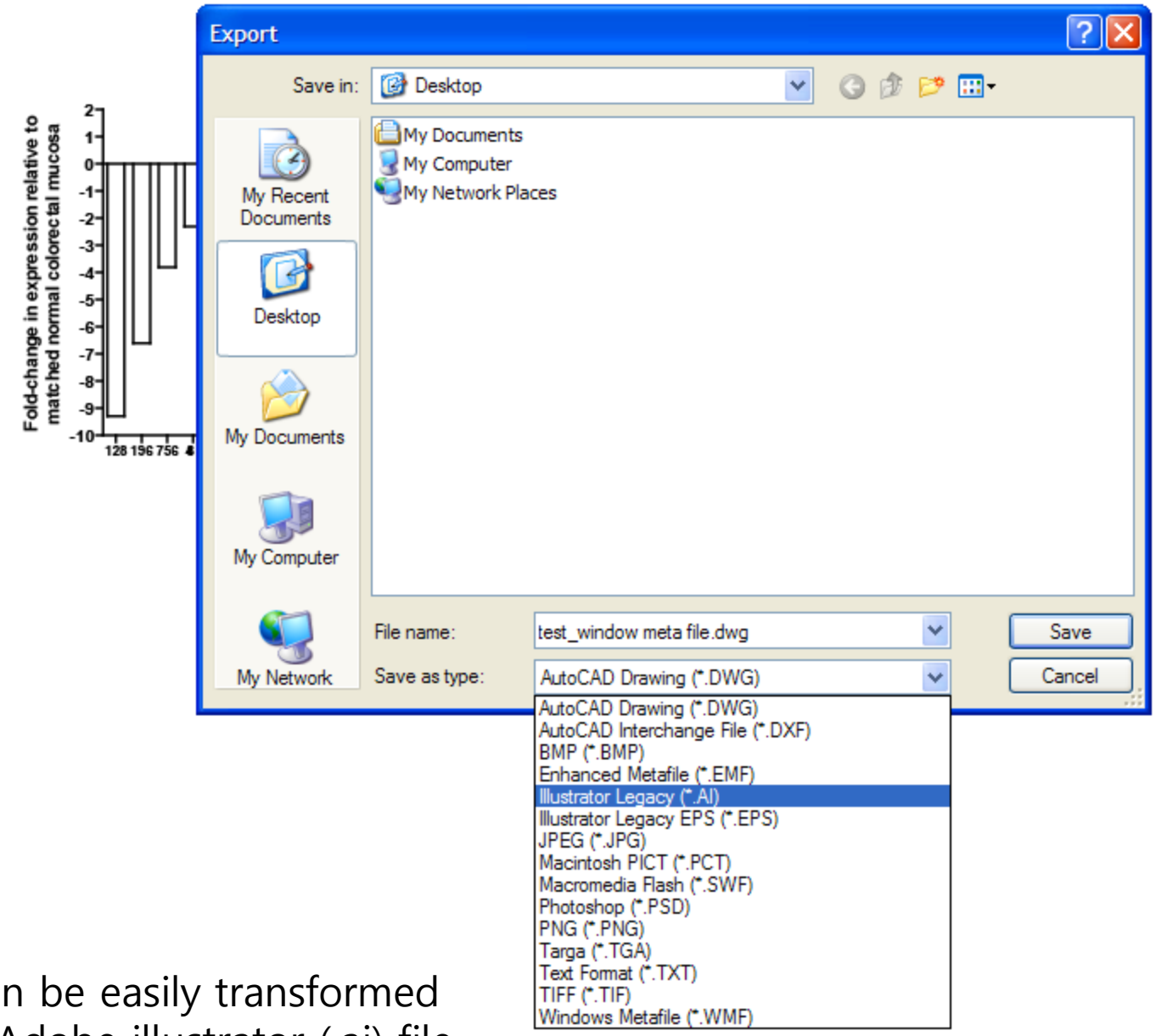

WMF can be easily transformed into an Adobe illustrator (.ai) file.

PowerPoint에서 구현하는 vector

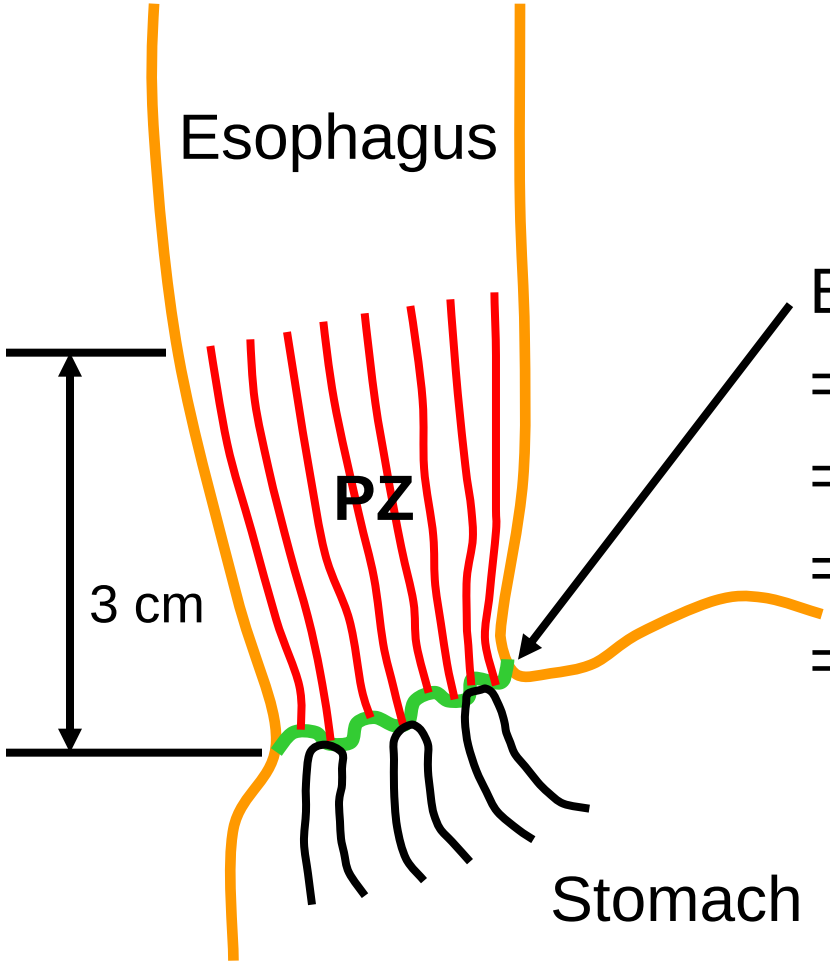

Esophagogastric junction (EGJ)
= Proximal margin of gastric folds
= Distal end of palisade zone
= Pinchcock action (PCA)
= Squamocolumnar junction

요약: vector image

- 선을 그리는 방법은 두 가지: Rastor와 vector
- Vector에서는 확대하여도 격자구조가 발생하지 않는다.
- 최고의 해상도를 얻기 위해서는 vector program을 이용하여 figure를 작성한 후 마지막에 필요한 해상도의 bitmap 파일로 변경하는 것이 좋다.

Topic 3

논문 제출을 위한 적절한 해상도?

성균관대학교 의과대학 삼성서울병원 내과 이준행

출판을 위한 해상도 선정 원칙

- Color: 300 dpi
- Gray scale: 300 - 600 dpi [required for photos, without text]
- Combination art (combo): 600 - 900 dpi [required for photos and text]
- Line art (monochrome 1-bit image): 900 - 1200 dpi [B&W text only]

DPI = Dots / Inch

최종 편집된 페이지에서 어떤 크기?

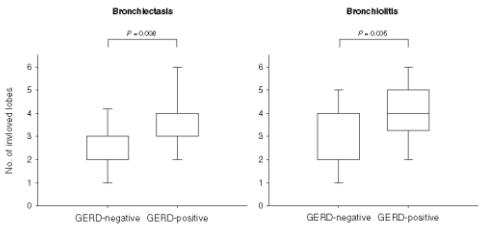

FIGURE 1. Box-and-whiskers graph of the quantitative imaging analysis showing the number of involved lobes with bronchiectasis and bronchiolitis. Bronchiolitis is defined as the presence of centrilobular small nodules (< 10 mm in diameter) or branching nodular structures (tree-in-bud pattern) on HRCT. The ends of the boxes indicate the 25th and 75th percentiles, and the lines in the bars indicate the median value. The 10th and 90th percentiles are indicated with whiskers. In the patients without GERD, the median numbers of involved lobes with bronchiectasis and bronchiolitis are both 2. In the patients with GERD, the median numbers of involved lobes with bronchiectasis and bronchiolitis are both 4. Bronchiectasis and bronchiolitis were observed in more lobes in pateints with GERD than in patients without GERD (p = 0.008 and p = 0.009, respectively).

In addition, patients with GERD were more likely to have AFB-positive sputum smear results in comparison with patients without GERD. These findings suggest that further studies to investigate the nature of the association between GERD and NTM lung disease are needed. If GERD is causative, its treatment may be critical. If GERD is secondary to more advanced lung disease, its treatment may be less important in managing the lung disease.

Our study had some limitations. First, this study did not include a control group. However, our principal goal was to investigate the prevalence of GERD in patients with the nodular bronchiectatic form of NTM lung disease, and ours is the only study to use 24-h pH monitoring to determine this.

Second, a significant proportion (34 of 92 patients, 37%) of screened patients did not perform 24-h esophageal pH monitoring. Then, the study group did not accurately reflect total population of patients with NTM lung disease. In particular, the study group had a significantly higher proportion of patients with *M abscessus* infection than the total group. This is very significant because it has been shown that patients with *M abscessus* infection have a higher rate of gastroesophageal abnormalities.

Third, we used accepted criteria used by gastroenterologists for the diagnosis of GERD, but these may not apply for a person to be susceptible to NTM infection by possible aspiration. For example, it is not known if someone has to have a pH
4 for > 4% of the study time to place NTM in his or her lungs. Also, the patients were only studied for 24 h, which does not exclude that aspiration may have occurred at other times not studied.

Although we showed that GERD is prevalent in patients with NTM lung disease, the nature of this relationship remains uncertain. Our study was not designed to investigate a possible causal association between GERD and NTM lung disease. Our data are consistent with GERD causing or contributing to the development or progression of NTM lung disease via recurrent exposure of the pulmonary parenchyma to the acidity of the refluxed gastric contents. Alternatively, GERD might be a secondary phenomenon. Patients with NTM lung disease might be at increased risk for abnormal reflux because of the increased pressure gradient across the diaphragm during frequent coughing and changes in pulmonary mechanics.

In addition, non-acid reflux as well as acid reflux may be present in patients with NTM lung disease. The measurement of acid reflux using esophageal pH monitoring is just a marker for possible aspiration but may not be related to the pathogenesis of NTM infection. In fact, it is possible that the increased use of acid suppressants with a resultant aspiration of relative alkaline pH into the esophagus may actually make the environment more favorable to NTM infection and the relative alkaline pH exacerbate further aspiration.

In conclusion, our study showed that patients with the nodular bronchiectatic form of NTM lung disease have a high prevalence of GERD. However, most patients with NTM lung disease and GERD lacked the typical symptoms of heartburn and regur-

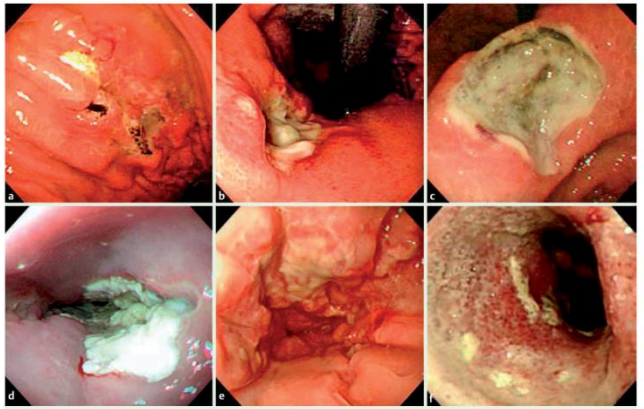

Figure 1 Endoscopic appearances of primary upper gastrointestinal NK-/T-cell lymphoma. **a** Superficial/erosive type (patient 1): several superficial erosions of various sizes in a continuous focal pattern in the body of the stomach. **b** Ulcerative type (patient 2): a round 1.5-cm well defined deep ulcer in the body of the stomach. **c** Ulcerative type (patient 3): round 2-cm well defined deep ulcer at the angle of the stomach. **d** Ulcerative type (patient 4): a long irregular 4-cm well defined deep ulcer in the mid esophagus. **e** Ulceroinfiltrative type (patient 5): diffuse ill defined ulcers of various sizes in a continuous pattern in the lower esophagus. **f** Ulceroinfiltrative type (patient 6): diffuse ill defined ulcers of various sizes in a continuous pattern in the second portion of the duodenum.

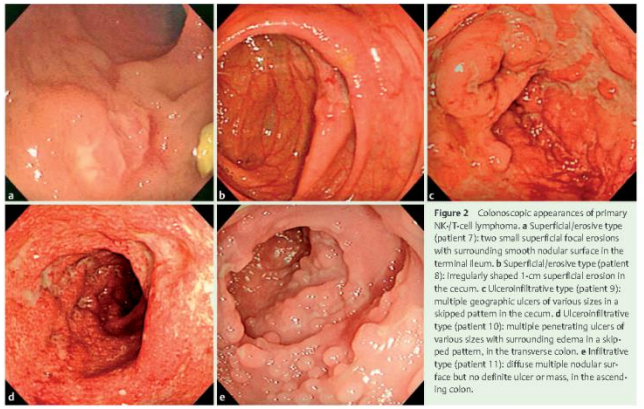

Figure 2 Colonoscopic appearances of primary NK-/T-cell lymphoma. **a** Superficial/erosive type (patient 7): two small superficial focal erosions with surrounding smooth nodular surface in the terminal ileum. **b** Superficial/erosive type (patient 8): irregularly shaped 1-cm superficial erosion in the cecum. **c** Ulceroinfiltrative type (patient 9): multiple geographic ulcers of various sizes in a skipped pattern in the cecum. **d** Ulceroinfiltrative type (patient 10): multiple penetrating ulcers of various sizes with surrounding edema in a skipped pattern, in the transverse colon. **e** Infiltrative type (patient 11): diffuse multiple nodular surface but no definite ulcer or mass, in the ascending colon.

매우 불친절한 *Science* 투고규정

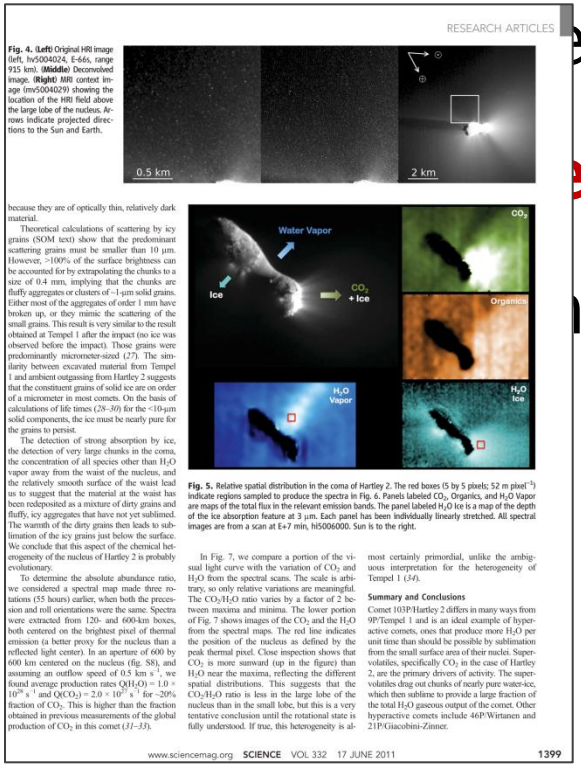

RESEARCH ARTICLES

Fig. 4. (Left) Original HRI image (left, hv5004024, E-66s, range 915 km). **(Middle)** Deconvolved image. **(Right)** MRI context image (mv5004029) showing the location of the HRI field above the large lobe of the nucleus. Arrows indicate projected directions to the Sun and Earth.

because they are of optically thin, relatively dark material.

Theoretical calculations of scattering by icy grains (SOM text) show that the predominant scattering grains must be smaller than 10 μm. However, 100% of the surface brightness can be accounted for by extrapolating the chunks to a size of 0.4 mm, implying that the chunks are fluffy aggregates or clusters of ~1-μm solid grains. Either most of the aggregates of order 1 mm have broken up, or they mimic the scattering of the small grains. This result is very similar to the result obtained at Tempel 1 after the impact (no ice was observed before the impact). Those grains were predominantly micrometer-sized (*27*). The similarity between excavated material from Tempel 1 and ambient outgassing from Hartley 2 suggests that the constituent grains of solid ice are on order of a micrometer in most comets. On the basis of calculations of life times (*28*–*30*) for the <10-μm solid components, the ice must be nearly pure for the grains to persist.

The detection of strong absorption by ice, the detection of very large chunks in the coma, the concentration of all species other than H_2O vapor away from the waist of the nucleus, and the relatively smooth surface of the waist lead us to suggest that the material at the waist has been redeposited as a mixture of dirty grains and fluffy, icy aggregates that have not yet sublimed. The warmth of the dirty grains then leads to sublimation of the icy grains just below the surface. We conclude that this aspect of the chemical heterogeneity of the nucleus of Hartley 2 is probably evolutionary.

To determine the absolute abundance ratio, we considered a spectral map made three rotations (55 hours) earlier, when both the precession and roll orientations were the same. Spectra were extracted from 120- and 600-km boxes, both centered on the brightest pixel of thermal emission (a better proxy for the nucleus than a reflected light center). In an aperture of 600 by 600 km centered on the nucleus (fig. S8), and assuming an outflow speed of 0.5 km s^{-1}, we found average production rates $Q(H_2O) = 1.0 \times 10^{28}$ s^{-1} and $Q(CO_2) = 2.0 \times 10^{27}$ s^{-1} for ~20% fraction of CO_2. This is higher than the fraction obtained in previous measurements of the global production of CO_2 in this comet (*31*–*33*).

Fig. 5. Relative spatial distribution in the coma of Hartley 2. The red boxes (5 by 5 pixels; 52 m $pixel^{-1}$) indicate regions sampled to produce the spectra in Fig. 6. Panels labeled CO_2, Organics, and H_2O Vapor are maps of the total flux in the relevant emission bands. The panel labeled H_2O Ice is a map of the depth of the ice absorption feature at 3 μm. Each panel has been individually linearly stretched. All spectral images are from a scan at E+7 min, hi5006000. Sun is to the right.

In Fig. 7, we compare a portion of the visual light curve with the variation of CO_2 and H_2O from the spectral scans. The scale is arbitrary, so only relative variations are meaningful. The CO_2/H_2O ratio varies by a factor of 2 between maxima and minima. The lower portion of Fig. 7 shows images of the CO_2 and the H_2O from the spectral maps. The red line indicates the position of the nucleus as defined by the peak thermal pixel. Close inspection shows that CO_2 is more sunward (up in the figure) than H_2O near the maxima, reflecting the different spatial distributions. This suggests that the CO_2/H_2O ratio is less in the large lobe of the nucleus than in the small lobe, but this is a very tentative conclusion until the rotational state is fully understood. If true, this heterogeneity is almost certainly primordial, unlike the ambiguous interpretation for the heterogeneity of Tempel 1 (*34*).

Summary and Conclusions

Comet 103P/Hartley 2 differs in many ways from 9P/Tempel 1 and is an ideal example of hyperactive comets, ones that produce more H_2O per unit time than should be possible by sublimation from the small surface area of their nuclei. Supervolatiles, specifically CO_2 in the case of Hartley 2, are the primary drivers of activity. The supervolatiles drag out chunks of nearly pure water-ice, which then sublime to provide a large fraction of the total H_2O gaseous output of the comet. Other hyperactive comets include 46P/Wirtanen and 21P/Giacobini-Zinner.

RESEARCH ARTICLES

O-Glycosylated Cell Wall Proteins Are Essential in Root Hair Growth

Silvia M. Velasquez,[1] Martiniano M. Ricardi,[1] Javier Gloazzo Dorosz,[1] Paula V. Fernandez,[2] Alejandro D. Nadra,[3] Laercio Pol-Fachin,[4] Jack Egelund,[5] Sascha Gille,[6] Jesper Harholt,[7] Marina Ciancia,[2] Hugo Verli,[4] Markus Pauly,[6] Antony Bacic,[8] Carl Erik Olsen,[9] Peter Ulvskov,[9] Bent Larsen Petersen,[9] Chris Somerville,[6] Norberto D. Iusem,[1,10] Jose M. Estevez[1]*

Root hairs are single cells that develop by tip growth and are specialized in the absorption of nutrients. Their cell walls are composed of polysaccharides and hydroxyproline-rich glycoproteins (HRGPs) that include extensins (EXTs) and arabinogalactan-proteins (AGPs). Proline hydroxylation, an early posttranslational modification of HRGPs that is catalyzed by prolyl 4-hydroxylases (P4Hs), defines the subsequent O-glycosylation sites in EXTs (which are mainly arabinosylated) and AGPs (which are mainly arabinogalactosylated). We explored the biological function of P4Hs, arabinosyltransferases, and EXTs in root hair cell growth. Biochemical inhibition or genetic disruption resulted in the blockage of polarized growth in root hairs and reduced arabinosylation of EXTs. Our results demonstrate that correct O-glycosylation on EXTs is essential for cell-wall self-assembly and, hence, root hair elongation in *Arabidopsis thaliana*.

Plant cell walls are complex and dynamic structures composed mostly of high-molecular-weight polysaccharides and highly glycosylated proteins (*1*, *2*). During plant growth, cells may expand up to 200 times their original length. During this process, the cell wall maintains its thickness through the addition of newly synthesized polysaccharides and proteins. Therefore, walls must possess sufficient tensile strength to withstand enormous turgor pressures (the driving force for growth) and involves controlled chemical modifications of wall constituents and wall networks. Approximately 1 to 2% of the *Arabidopsis* genome represents genes encoding putative enzymes that catalyze such modifications (*2*). Although the catalytic activity of the encoded protein is inferred from the predicted peptide sequence, the precise enzymatic function and biological role of many of these putative cell wall–modifying genes are unknown (*1*, *2*).

Cell walls contain abundant hydroxyproline-rich glycoproteins (HRGPs), a superfamily that encompasses extensins (EXTs) (*3*, *4*), proline-rich proteins (PRPs) (*4*), and arabinogalactan-proteins (AGPs) (*4*, *5*). These proteins undergo extensive posttranslational modification, which includes the modification of proline (Pro) residues to hydroxyproline (Hyp) by membrane-bound prolyl 4-hydroxylases (P4H2) (*6*). Nascent HRGPs are O-glycosylated (with arabinose and/or galactose) by glycosyltransferases (GTs) in the Golgi and endoplasmic reticulum (ER) (*7*–*11*) and are cross-linked into the wall by peroxidases through alternate Tyr residues to form a covalent network (*12*, *13*).

Root hair growth and proline hydroxylation. To study the function of HRGPs, we focused on root hairs because they represent a single cell type that plays an important role in nutrient absorption, and the growth morphology is easily

[1]Instituto de Fisiología, Biología Molecular y Neurociencias–Consejo Nacional de Investigaciones Científicas y Técnicas (IFIByNE-CONICET), Facultad de Ciencias Exactas y Naturales, Universidad de Buenos Aires, Buenos Aires C1428EGA, Argentina. [2]Cátedra de Química de Biomoléculas, Departamento de Biología Aplicada y Alimentos (Centro de Investigaciones en Hidratos de Carbono–CONICET), Facultad de Agronomía, Universidad de Buenos Aires, Buenos Aires CD1417DSE, Argentina. [3]Departamento de Química Biológica, Facultad de Ciencias Exactas y Naturales, Universidad de Buenos Aires, Buenos Aires C1428EGA, Argentina. [4]Programa de Pos-Graduação em Biologia Celular e Molecular, Centro de Biotecnologia, 91500-979, and Faculdade de Farmácia, Universidade Federal do Rio Grande do Sul, 90610-000, Brazil. [5]Department of Plant Biology and Biotechnology, Faculty of Life Sciences, University of Copenhagen, Copenhagen 1871, Denmark. [6]Energy Biosciences Institute, University of California, Berkeley, Berkeley, CA 94720, USA. [7]Department of Plant Biology and Biotechnology, Faculty of Life Sciences, University of Copenhagen, Copenhagen 1871, Denmark. [8]Plant Cell Biology Research Centre, School of Botany, University of Melbourne, Melbourne VIC 3010, Australia. [9]Department of Natural Sciences, Bioorganic Chemistry, Faculty of Life Sciences, University of Copenhagen, 1871, Denmark. [10]Departamento de Fisiología, Biología Molecular y Celular, Laboratorio de Fisiología y Biología Molecular (UFBM), Facultad de Ciencias Exactas y Naturales, Universidad de Buenos Aires, Buenos Aires C1428EGA, Argentina.

*To whom correspondence should be addressed. E-mail: jestevez@fbmc.fcen.uba.ar

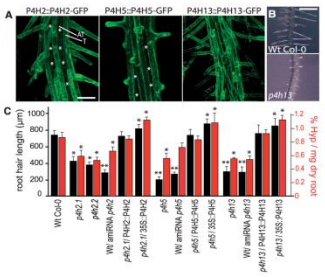

Fig. 1. *Arabidopsis* root hair growth is modulated by P4Hs. **(A)** Localization of GFP-tagged P4H2, P4H5, and P4H13 enzymes. GFP-tagged P4H2 and P4H5 are expressed in trichoblast cells (T), and GFP-tagged P4H13 is expressed in both trichoblast and atrichoblast (AT) root cells. Absence of GFP signal is indicated by asterisks. Scale bar, 200 μm. **(B)** Shorter root hairs in *p4h13* mutant. Scale bar, 800 μm. **(C)** Root hair length (black bars) and Hyp content (red bars) in roots of WT Col-0 (WT), *p4h* insertional mutants, silenced [artificial microRNA (amiRNA)], and rescued mutants. Complementation of each *p4h* mutant was achieved by the corresponding WT P4H driven by either its own endogenous promoter or the 35S promoter. *P* values of one-way analysis of variance (ANOVA) test, $*P < 0.01$, $**P < 0.001$.

RESEARCH ARTICLES

observed with light microscopy. A link between P4Hs, glycosylation, and root hair phenotype was first suggested by results from an in vivo biochemical experiment that analyzed roots from plants carrying a green fluorescent protein (GFP)–tagged HRGP transgene (LeAGP1-GFP) (*14*) that were treated with either ethyl-3,4-dihydroxybenzoate (EDHB), which binds to the active site of AtP4Hs (fig. S1) (*15*), or α,α-dipyridyl (DP), which chelates the cofactor Fe^{2+} (*16*, *17*). This treatment caused an up to 50% inhibition of root hair growth at 48 to 219 nM (fig. S2) and the accumulation of the non-glycosylated ~42 kD form of LeAGP1-GFP rather than the fully O-glycosylated 150-to-200-kD form (fig. S2) (*14*).

We then characterized different members of the AtP4H family with distinct expression patterns, particularly those expressed in a tissue-specific manner in roots such as AtP4H2 and AtP4H5, which are expressed mainly in the root hair morphogenic zone (fig. S3 and table S1) (*18*, *19*), as well as AtP4H13, which is also expressed in roots (Fig. 1A). Cell-type expression analysis showed that GFP-tagged P4H2 and P4H5 are present only in trichoblast cells, whereas P4H13 is expressed in both trichoblast and atrichoblast cells (Fig. 1A). Subcellular localization of all three P4Hs was confined to the apical zone of emerging root hairs but was distributed throughout the cell in elongated root hairs (Fig. 2). At the subcellular level, all three P4Hs colocalized with an ER marker. P4H2 and P4H5 partially colocalized with a Golgi marker (fig. S4). To clarify the role of these P4Hs in developing root hairs, we used plants with transferred DNA (T-DNA) insertions (knockout lines) in each of these three AtP4H genes (fig. S5). We observed that the P4H-deficient lines displayed shorter-than-normal root hair length (Fig. 1B, fig. S5, and table S2), which mimicked the pharmacological inhibition of P4Hs that was previously reported (fig. S2). In addition, the *p4h2* mutant showed reduced root hair density. All three mutants lacked normal AtP4H transcripts, with the exception of *p4h2.1* (fig. S5) and showed reduced Hyp content in root cell walls in roots (Fig. 1C). Similar results were obtained by silencing normal AtP4H gene expression with complementary microRNA (Fig. 1C and fig. S5). Therefore, we concluded that the normal elongation of root hair cells requires Pro hydroxylation, performed by AtP4H enzymes, and the subsequent O-glycosylation of HRGPs, which is a consequence of Pro hydroxylation (*20*).

In support of the conclusions derived from *p4h* mutants, GFP-tagged P4Hs driven by either their own promoter (Fig. 1C and fig. S5) or the strong 35SCaMV constitutive promoter (Fig. 1C and table S2) restored root hair length, morphological phenotypes, and cell wall Hyp content to wild-type (WT) levels. Overexpression of P4Hs in a WT genetic background (fig. S6) doubled root hair length (Fig. 1D and fig. S6) and increased root hair density (fig. S7).

Given the overlapping substrate specificity of P4Hs (*6*), we explored the potential genetic interactions among P4Hs by observing the root hair phenotype that was displayed by double mutants (fig. S7). The *p4h2-p4h5* double mutant phenotype was similar to that of the single mutant *p4h5*, suggesting a functional overlap between P4H2 and P4H5. In contrast, the double mutant *p4h2-p4h13* line had shorter root hairs and exhibited a lower Hyp content in the cell walls than that of the respective single *p4h* mutant (fig. S7), suggesting subtle differences in substrate specificity for each of these P4Hs. To address the target specificity of P4H5, we performed a yeast two-hybrid screen using P4H5 as bait and identified LRX3, a root-specific leucine-rich-repeat extensin (At4g13340) and proteins containing polyproline II repeats (*25*) as targets of P4H5 (table S3). We calculated the interaction of each P4H (P4H2, P4H5, and P4H13) with the ($SP)_3$ and PAPAPSPT peptides that are present in AGPs or a polyproline repeat that is usually present in EXTs and PRPs [fig. S8, table S4, and supporting online material (SOM) text S1]. The modeling showed that these P4Hs have a high affinity of P4Hs for polyproline-like (EXT-PRP–type) substrates (fig. S8). Other biochemical studies have also demonstrated a greater hydroxylation activity on consecutive Pro residues compared with that on nonadjacent residues (*6*).

O-linked glycans in extensins. Having established the importance of P4Hs in posttranslational modifications of the EXT peptide backbone and considering that O-glycosylation is relevant in protein function either directly or indirectly through changes in polypeptide conformation, we explored O-glycosylation, mainly O-arabinosylation, in the context of EXT structure. Using genome-wide expression analysis, we determined that glycosyltransferases (GTs) RRA3 (reduced residual arabinose 3; At1g19360) and XEG113 (At2g35610) (fig. S9), both members of the GT family 77 (GT 77) of the Carbohydrate Active enZYme database (CAZY; www.cazy.org), were coexpressed with P4H2 and P4H5. RRA3 was 70 and 82% identical to the putative membrane-bound type-II arabinosyltransferases RRA1 and RRA2, respectively, which are implicated in EXT glycosylation (fig. S9) (*8*, *9*). The impaired root hairs that were exhibited by *rra1-rra3* mutants were similar to those of *p4h2*, *p4h5*, and *p4h13* mutants (Fig. 3A). In addition, *rra1-rra3* mutants had reduced EXT epitope content in their root cell walls (fig. S10). Another GT77 family member, XEG113 (At2g35610), which is a putative arabinosyltransferase, has also been reported to glycosylate EXTs (*10*). The *xeg113-2*

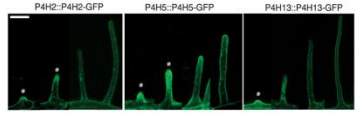

Fig. 2. Expression of GFP-tagged P4H2, P4H5, and P4H13 under the control of their respective endogenous promoters at different stages of root hair development. Scale bar, 200 μm.

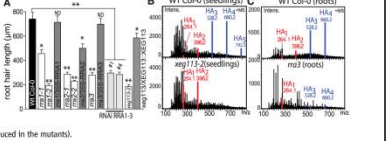

Fig. 3. EXT-associated arabinosyltransferases. **(A)** Root hair length (mean ± SEM) in *rra1-3*/*xeg113-2* mutants and their complemented lines. *P* values from one-way ANOVA test, $*P < 0.01$, $**P < 0.001$. **(B** and **C)** Mass-spectra of EXT O-glycans (Hyp-arabinosides, HA1-HA5) analyzed with ESI-MS on WT or mutant (B) seedlings and (C) roots. Hyp-arabinosides were detected as follows: HA5, $Hyp\text{-}(Ara)_5$; HA4, $Hyp\text{-}(Ara)_4$; HA3, $Hyp\text{-}(Ara)_3$; HA2, $Hyp\text{-}(Ara)_2$; and HA1, $Hyp\text{-}(Ara)_1$. Ions important for the interpretation of the results are highlighted in red (moieties containing up to two arabinose residues) or in blue (moieties containing three to five arabinose units, which are lacking or notably reduced in the mutants).

매우 친절한 *Lancet*

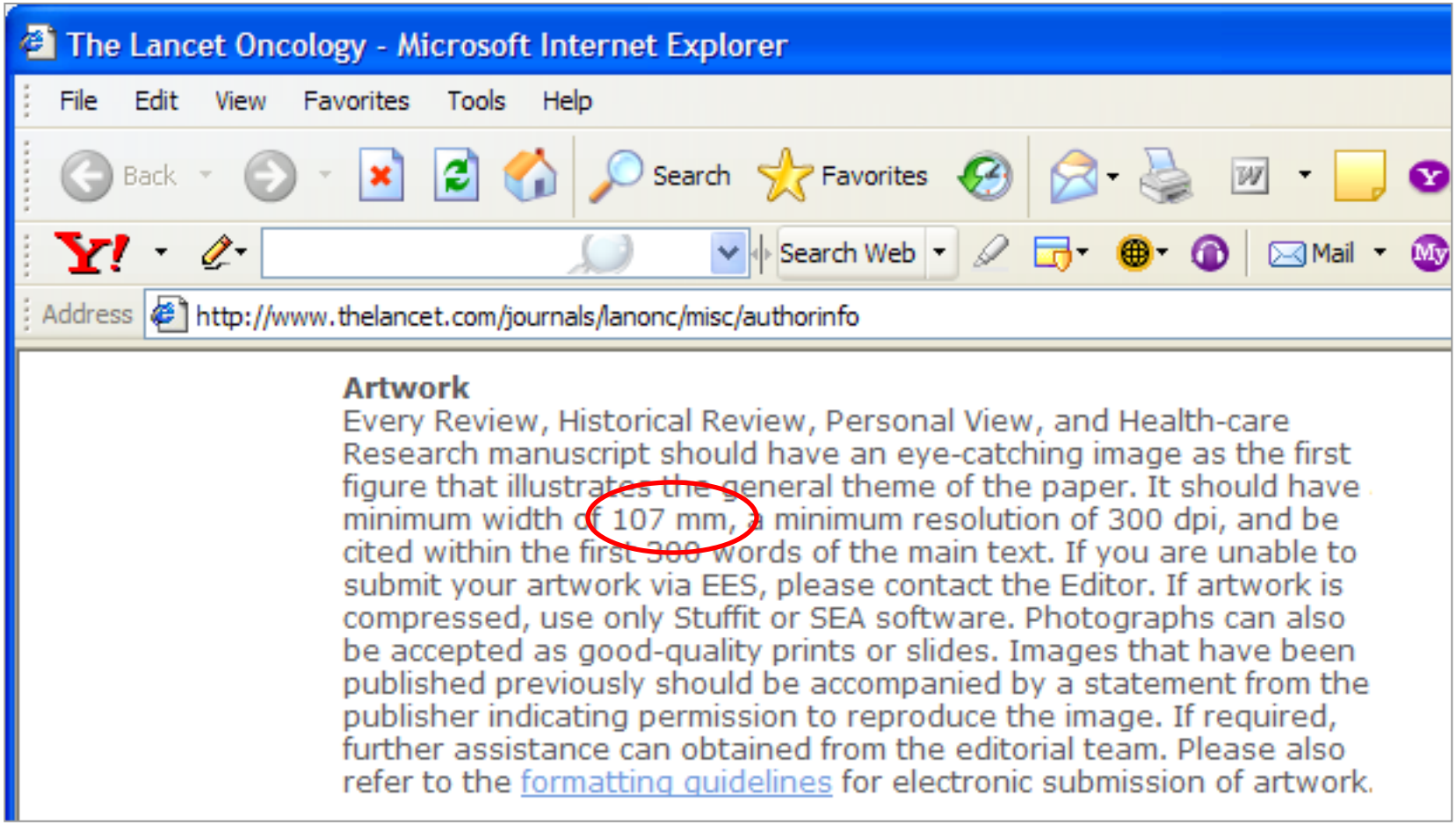

http://www.thelancet.com/journals/lanonc/misc/authorinfo

One column is usually 3.5 inch or less

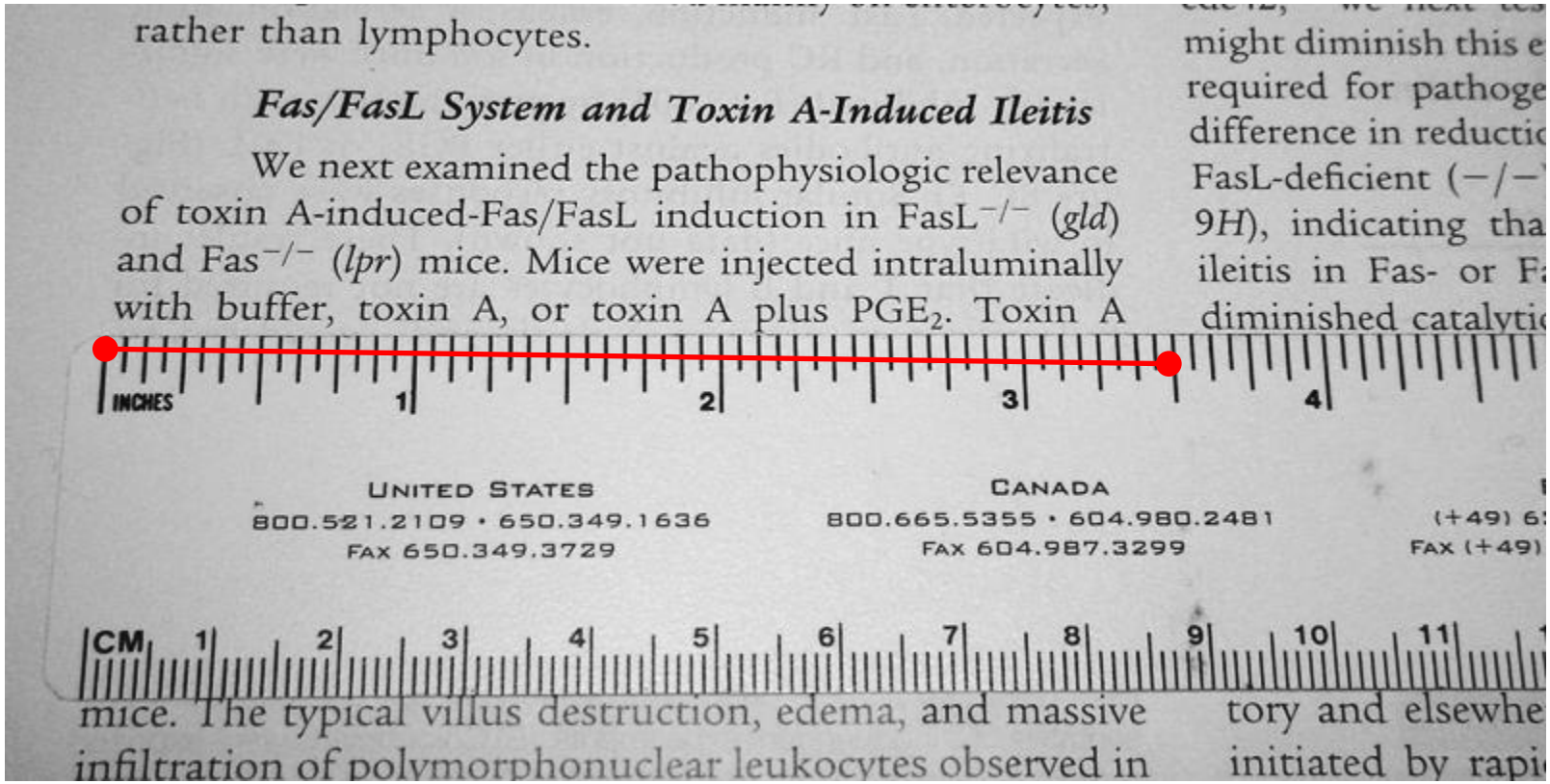

4 inch, 900 dpi로 작업을 하면 대부분의 경우에 문제가 없다

Kim. Gastroenterology 2007;133:875-886

요약: 논문 제출을 위한 이미지

- 논문에 제출할 그림은 대표적인 line art이다.
- 가능하면 vector형식의 image program을 사용하여 그림을 만드는 것이 좋다.
  예) 그림은 Adobe Illustrator, Graph는 Prism
- 마지막 단계에서 “TIFF 형식, size 4 inch, resolution 900 dpi, 색상 흑백” 선택

Topic 4

Powerpoint file을 TIFF로 바꾸기

성균관대학교 의과대학 삼성서울병원 내과 이준행

PowerPoint에서 손쉽게 TIFF로 만들기

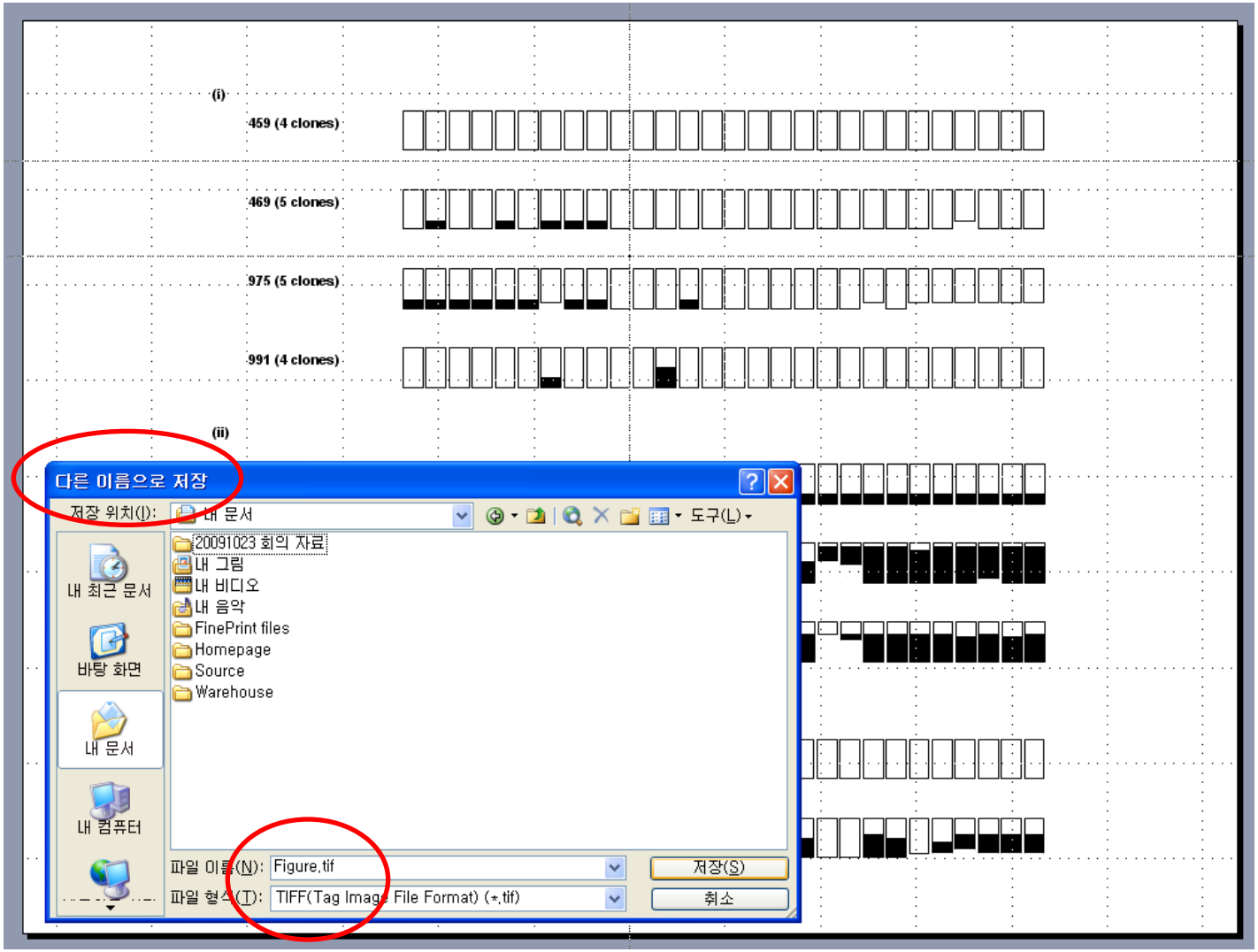

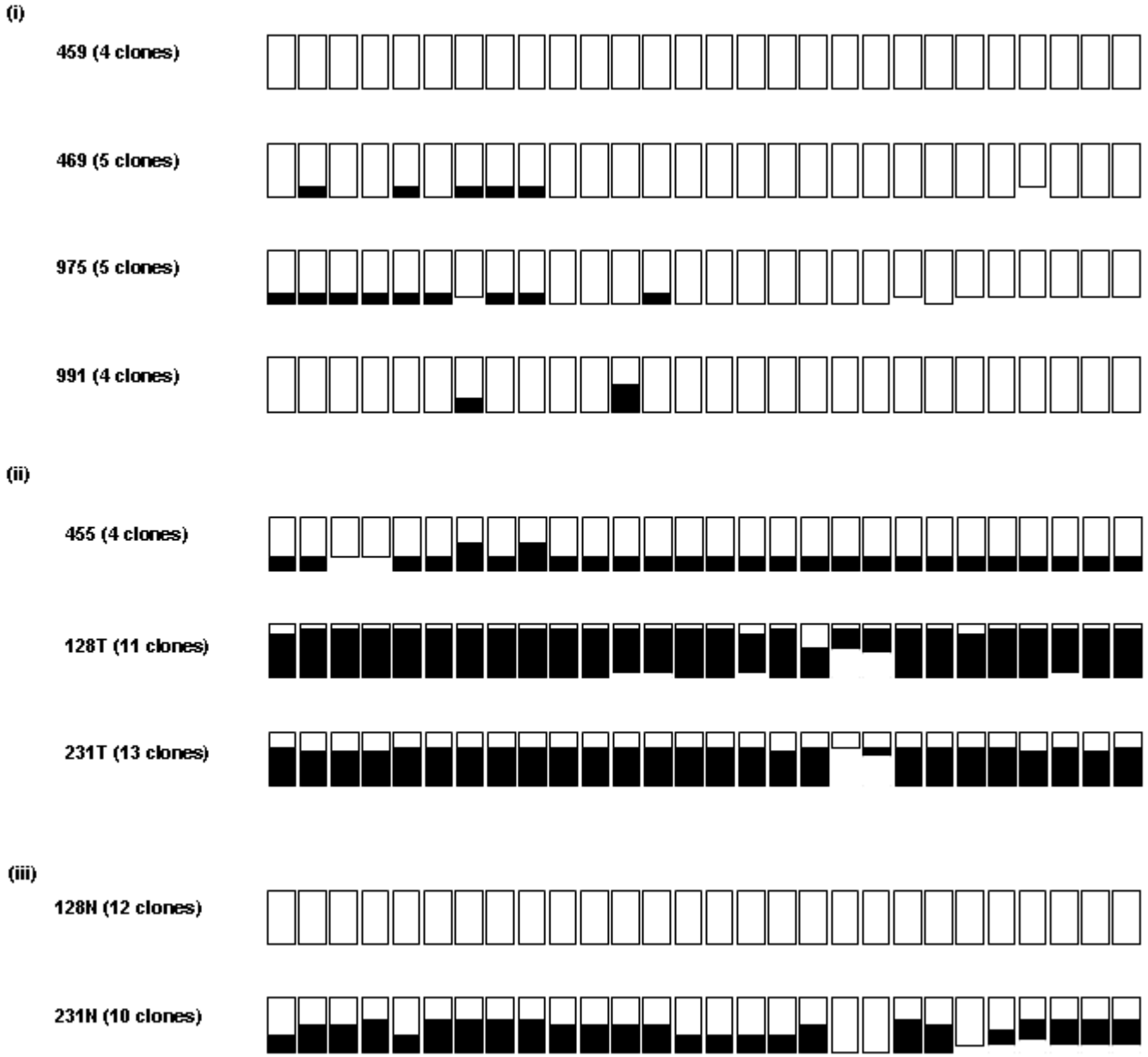
(i)
459 (4 clones)
469 (5 clones)
975 (5 clones)
991 (4 clones)
(ii)
455 (4 clones)
128T (11 clones)
231T (13 clones)
(iii)
128N (12 clones)
231N (10 clones)

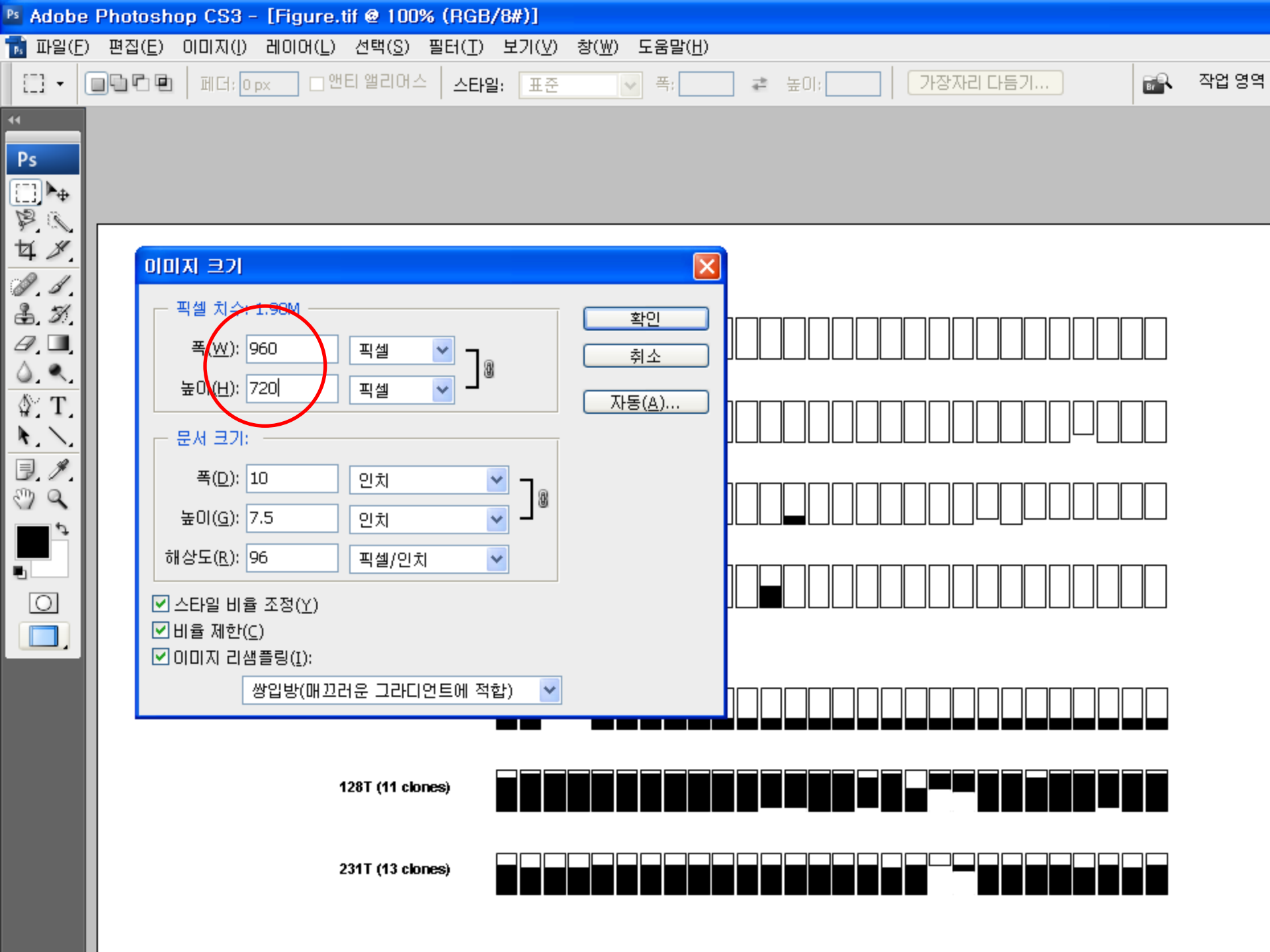
Adobe Photoshop CS3 - [Figure.tif @ 100% (RGB/8#)]
파일(F) 편집(E) 이미지(I) 레이어(L) 선택(S) 필터(T) 보기(V) 창(W) 도움말(H)
이미지 크기
픽셀 치수: 1.98M
폭(W): 960 픽셀
높이(H): 720 픽셀
문서 크기:
폭(D): 10 인치
높이(G): 7.5 인치
해상도(R): 96 픽셀/인치
스타일 비율 조정(Y)
비율 제한(C)
이미지 리샘플링(I):
쌍입방(매끄러운 그라디언트에 적합)
확인
취소
자동(A)...
128T (11 clones)
231T (13 clones)

PowerPoint 이미지를 고해상도 TIFF 파일로 바꾸는 방법

- Adobe Acrobat를 사용하는 방법
- Powerpoint를 사용하는 방법

Acrobat 혹은 Powerpoint를 이용하여 PDF 파일로 변환

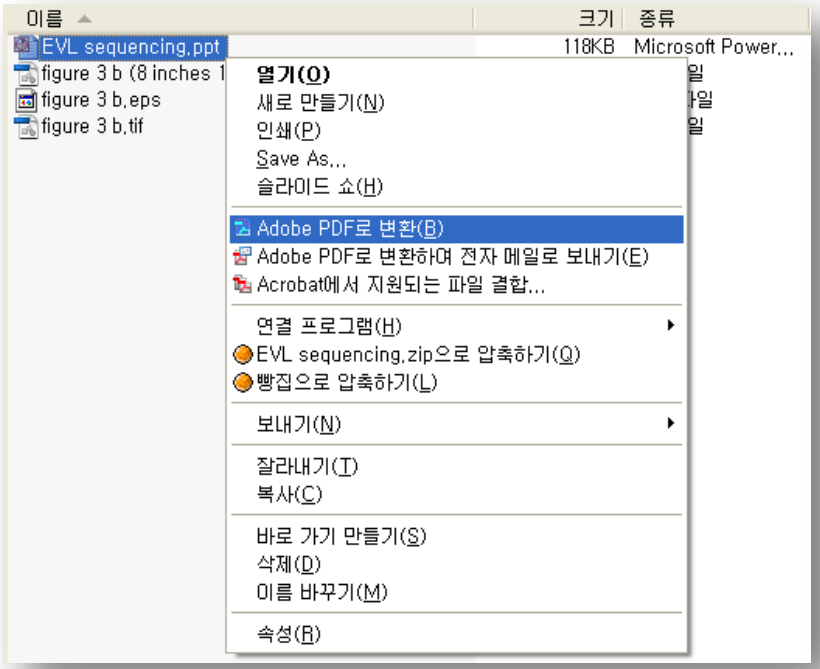

Acrobat

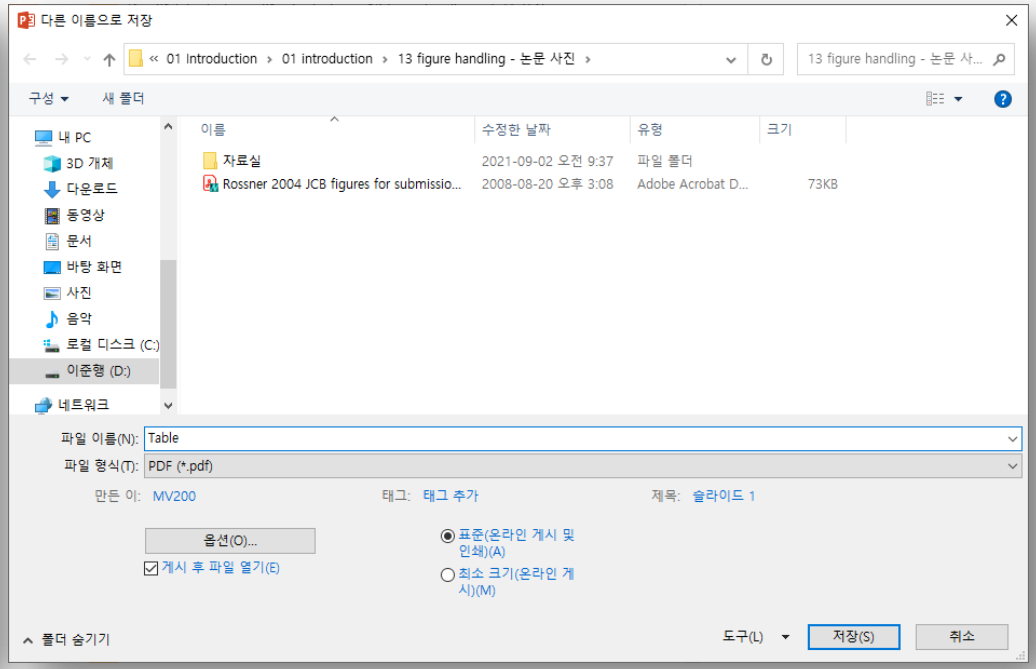

PowerPoint

PDF 파일을 Photoshop으로 불러온다

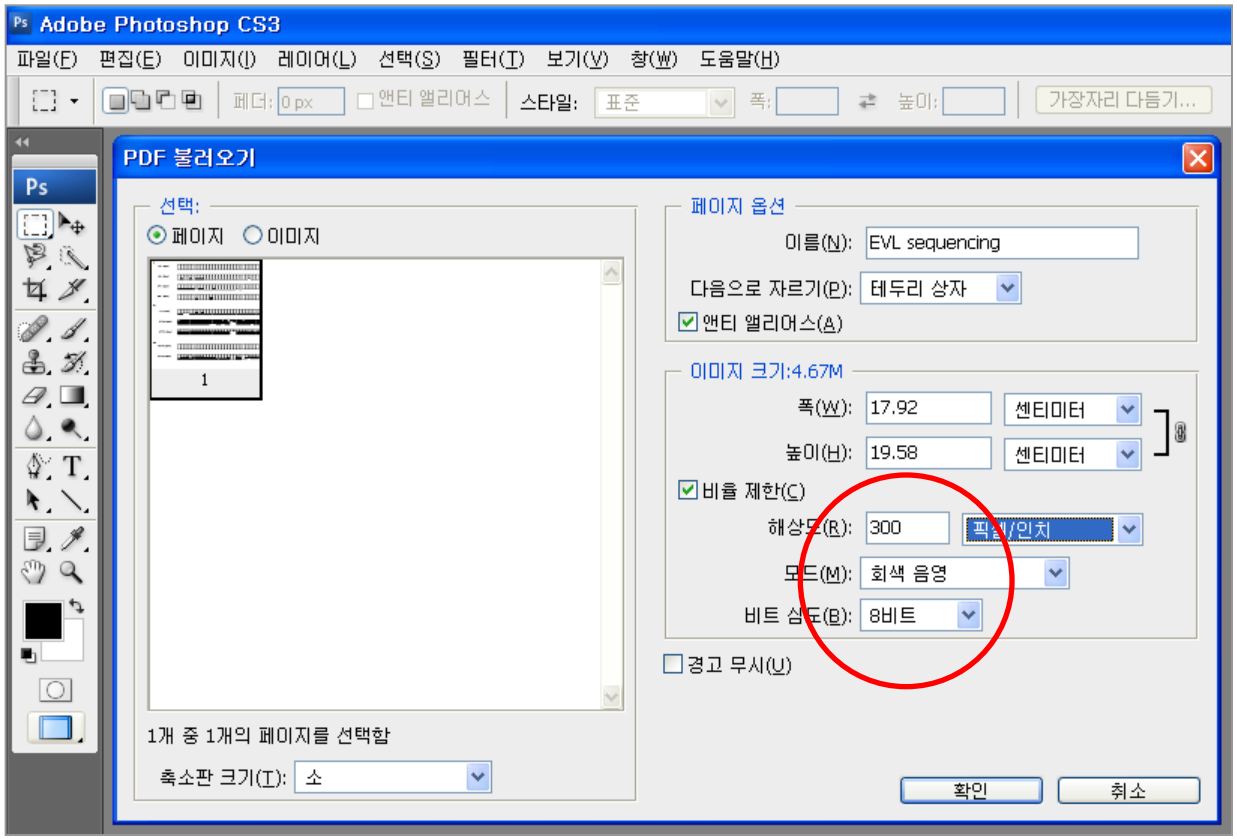

Photoshop에서 TIFF 파일로 저장한다

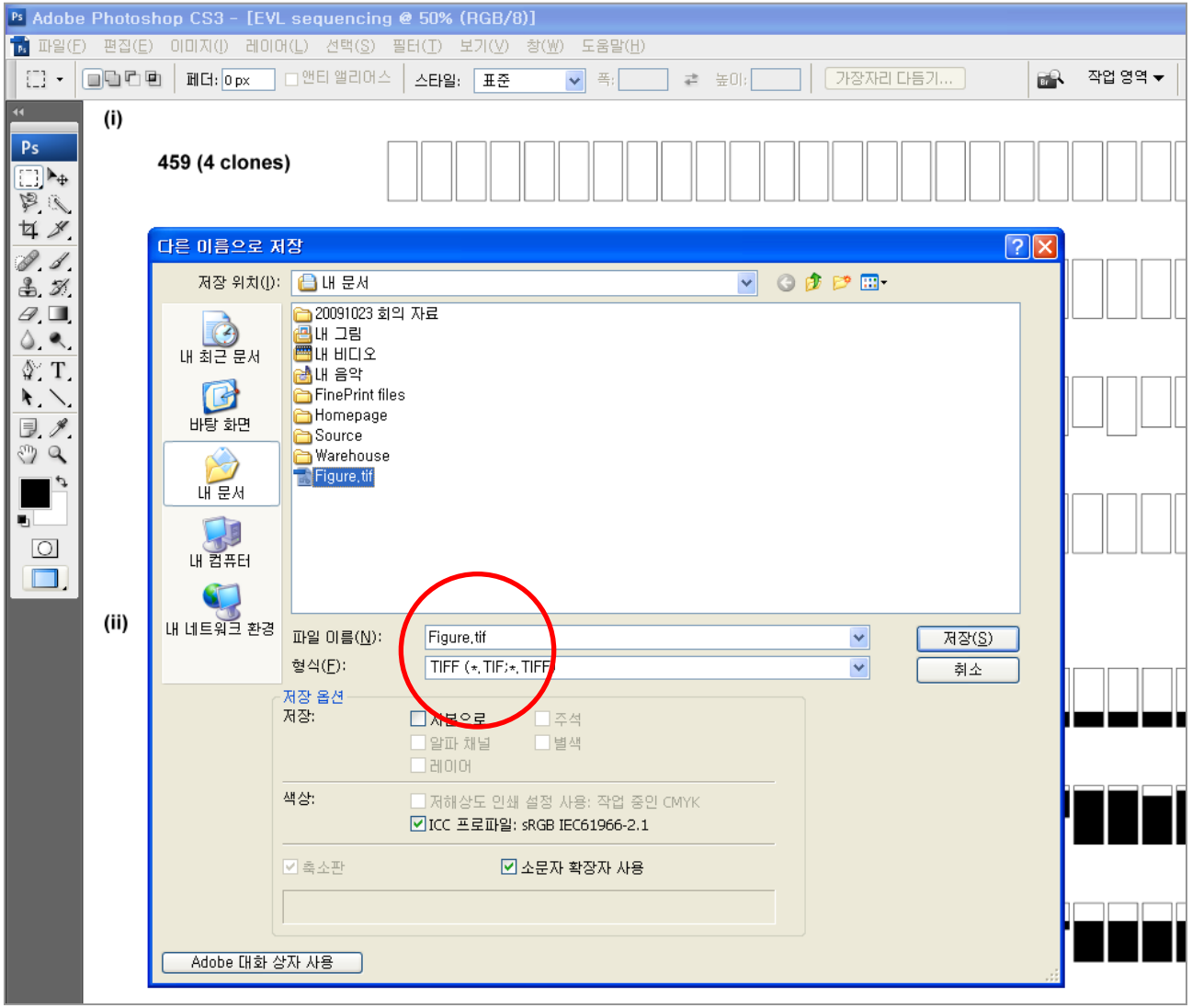

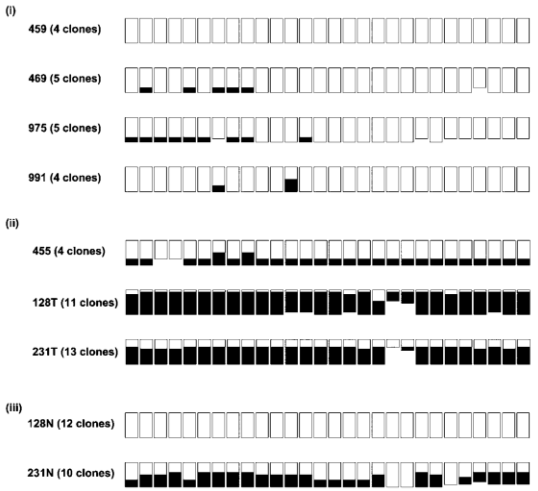

Figure 3 *EVL*/*hsa-miR-342* locus CpG methylation in colorectal carcinogenesis: evidence for a 'field defect' of *EVL*/*hsa-miR-342* locus CpG methylation in colorectal cancer. Bisulfite genomic sequencing results are shown for the *EVL*/*hsa-miR-342* CpG island from (i) normal colorectal mucosa from four individuals without cancer, (ii) colorectal cancer tissue from three individuals and (iii) normal appearing colorectal mucosa from two patients with concurrent colorectal cancer. The numbers in the left column represent patient identifiers. The number of clones sequenced from each patient sample is indicated in parentheses. Matched tumor (T) and normal (N) colorectal mucosa were analysed from patients no. 128 and no. 231 with results shown in (ii) and (iii). Each bar represents one CpG dinucleotide and the proportion of methylated CpGs is indicated by black shading. The height of the bar is representative of the number of informative clones at a given CpG site.

identify genes that are (a) overexpressed in colorectal cancer based on results from three relevant gene expression profiling studies (Alon *et al*., 1999; Notterman *et al*., 2001; Zou *et al*., 2002) and (b) PicTar-predicted targets of *hsa-miR-342*. Eleven genes satisfied these criteria and are presented in Supplementary Table S3.

Discussion

In this study, we confirmed that silencing of *hsa-miR-342* is a common event in colorectal cancer and provided evidence for coordinate epigenetic silencing of an intronic microRNA and its host gene in human cancer. Given that roughly half of microRNA genes are located in introns (Rodriguez *et al*., 2004; Kim and Kim, 2007; Saini *et al*., 2007), we suggest that this mode of coordinate silencing may represent a more general mechanism of microRNA suppression in human cancer.

Our data also suggest that methylation of the *EVL*/*hsa-miR-342* locus is an early event in colorectal carcinogenesis, given that it is detectable in 67% of adenomas, as well as in 56% of histologically normal colorectal mucosal specimens from patients with concurrent colorectal cancer. Based on these observations, we propose that the methylated DNA corresponding to the *EVL*/*hsa-miR-342* locus may merit further investigation as a biomarker for non-invasive disease detection or risk prediction for colorectal cancer, especially in light of its apparent specificity for colorectal cancer.

With respect to carcinogenesis, the data suggest a model in which the aberrant methylation of *EVL*/*hsa-miR-342* precedes histologically apparent neoplastic alterations in the colon and leads to an early expansion of precancerous progenitor cells carrying methylated CpG islands at the *EVL*/*hsa-miR-342* locus. The presence of methylation of *EVL*/*hsa-miR-342* in normal appearing colorectal mucosa may reflect an acquired, early epigenetic change in the pathogenesis of colorectal cancer. Alternatively, it could also be the consequence of clonal expansion of rare, normal colorectal epithelial cells that carry a methylated *EVL*/*hsa-miR-342* locus as a part of their normal physiological state (Ohm and Baylin, 2007; Widschwendter *et al*., 2007).

Given that *EVL* and *hsa-miR-342* are coordinately silenced, we cannot determine *a priori* whether suppression of *EVL*, *hsa-miR-342* or both is the relevant event in colorectal carcinogenesis. EVL is a member of the Ena/VASP protein family, which are actin-associated proteins involved in a variety of processes related to

PowerPoint 파일 → 고해상도 TIFF 요약

- PowerPoint file (vector image)를 직접 TIFF로 변환하면 960x720 px의 저해상도 TIFF로 바뀐다.
- PDF 파일(vector image)로 변환한다.
- Photoshop을 이용하여 PDF 파일을 고해상도 rastor 이미지로 불러온다.
- TIFF 형식으로 저장한다.

요약

- 모든 Table은 정확하게 만들어야 한다. 오타 주의.
- 모든 이미지는 필요에 따라 적절한 해상도로 만들어져야 한다. 가능하면 vector graphic이 좋다.